KINEMATICS OF SURF ZONE BREAKING WAVES: MEASUREMENT AND ANALYSIS

James Joseph Galvin

NAVAL POSTGRADUATE SCHOOL
Monterey, California

THESIS

KINEMATICS OF SURF ZONE BREAKING WAVES:
MEASUREMENT AND ANALYSIS

by

James Joseph Galvin

September 1975

Thesis Advisor: E. B. Thornton

Approved for public release; distribution unlimited.

UNCLASSIFIED

SECURITY CLASSIFICATION OF THIS PAGE (When Data Entered)

REPORT DOCUMENTATION PAGE		READ INSTRUCTIONS BEFORE COMPLETING FORM
1. REPORT NUMBER	2. GOVT ACCESSION NO.	3. RECIPIENT'S CATALOG NUMBER
4. TITLE (and Subtitle) Kinematics of Surf Zone Breaking Waves: Measurement and Analysis		5. TYPE OF REPORT & PERIOD COVERED Master's Thesis; September 1975 6. PERFORMING ORG. REPORT NUMBER
7. AUTHOR(s) James Joseph Galvin		8. CONTRACT OR GRANT NUMBER(s)
9. PERFORMING ORGANIZATION NAME AND ADDRESS Naval Postgraduate School Monterey, California 93940		10. PROGRAM ELEMENT, PROJECT, TASK AREA & WORK UNIT NUMBERS
11. CONTROLLING OFFICE NAME AND ADDRESS Naval Postgraduate School Monterey, California 93940		12. REPORT DATE September 1975 13. NUMBER OF PAGES 96
14. MONITORING AGENCY NAME & ADDRESS(if different from Controlling Office) Naval Postgraduate School Monterey, California 93940		15. SECURITY CLASS. (of this report) Unclassified 15a. DECLASSIFICATION/DOWNGRADING SCHEDULE

16. DISTRIBUTION STATEMENT (of this Report)

Approved for public release; distribution unlimited

17. DISTRIBUTION STATEMENT (of the abstract entered in Block 20, if different from Report)

18. SUPPLEMENTARY NOTES

19. KEY WORDS (Continue on reverse side if necessary and identify by block number)

Breaking Waves
Surf Zone
Waves

20. ABSTRACT (Continue on reverse side if necessary and identify by block number)

Simultaneous measurements of water surface fluctuations and horizontal water particle velocities in a line perpendicular to the direction of wave approach extending across the surf zone were taken in varying surf conditions at two locations. The spectral velocities calculated using linear theory as a transfer function underestimated measured values by 79-86% at the peak of the spectrum. The coherence

DD FORM 1 JAN 73 1473 EDITION OF 1 NOV 65 IS OBSOLETE
S/N 0102-014-6601 |
(Page 1)

UNCLASSIFIED

SECURITY CLASSIFICATION OF THIS PAGE (When Data Entered)

values were generally low indicating non-linear and turbulent conditions. Strong harmonics in the spectra of the waves and water particle velocities further suggest a non-linear system. The theoretical phases computed using linear theory did not accurately predict the observed phases. In general breaking waves can be characterized as a strongly non-linear wave phenomenon. Measured frequency distributions were compared with both Gaussian and Gram-Charlier distributions by using the chi-square goodness-of-fit test. Qualitatively, the Gram-Charlier distribution gave the better fit to the flow velocity data.

Kinematics of Surf Zone Breaking Waves: Measurement and Analysis

by

James Joseph Galvin
Lieutenant Commander, United States Navy
B.S., United States Naval Academy, 1966

Submitted in partial fulfillment of the
requirements for the degree of

MASTER OF SCIENCE IN OCEANOGRAPHY

from the

NAVAL POSTGRADUATE SCHOOL
September 1975

ABSTRACT

Simultaneous measurements of water surface fluctuations and horizontal water particle velocities in a line perpendicular to the direction of wave approach extending across the surf zone were taken in varying surf conditions at two locations. The spectral velocities calculated using linear theory as a transfer function underestimated measured values by 79-86% at the peak of the spectrum. The coherence values were generally low indicating non-linear and turbulent conditions. Strong harmonics in the spectra of the waves and water particle velocities further suggest a non-linear system. The theoretical phases computed using linear theory did not accurately predict the observed phases. In general breaking waves can be characterized as a strongly non-linear wave phenomenon. Measured frequency distributions were compared with both Gaussian and Gram-Charlier distributions by using the chi-square goodness-of-fit test. Qualitatively, the Gram-Charlier distribution gave the better fit to the flow velocity data.

ACKNOWLEDGEMENTS

I am deeply indebted to Dr. Edward B. Thornton for his knowledge and assistance.

I also received much aid and rapid response to requests for assistance from Mr. Robert Smith of the Research Administration Department. Petty Officer First Class Donald Antonacci, USN, of the Machine Facility, Petty Officer Second Class, John Fanning, USN, of the Oceanography Department, Ms. Sharon Raney of the W. R. Church Computer Center, and the Computer Center "night crew": Mr. Edwin Donnellan, Mrs. Kristina Butler and Mr. Mannas Anderson.

I am also very deeply thankful to my wife, Barbara, for her encouragement and understanding, and my sons, Michael and J. J., for being patient while waiting for Daddy to come home from school to play.

For my Mother and Father

TABLE OF CONTENTS

LIST OF TABLES

LIST OF DRAWINGS

I. INTRODUCTION

Wave theories developed for deep water waves can be applied with some degree of certainty, and can be tested in laboratory and field situations. These theories generally hold until such time that the shoaling process begins, and with somewhat lesser accuracy, throughout the shoaling process up to the point of near breaking. At the breaker point, however, there is a transition from ordered to turbulent motion and the description of wave kinematics becomes more difficult. The most forthright approach to the problem of describing the kinematics of surf zone breaking waves is through direct measurements. Advances in instrument design have led to simple, sturdy, measuring devices with rapid response time which can sense the small scale as well as the large scale features.

The study of the kinematics of breaking waves in the surf zone has progressed slowly due both to the problems encountered in making direct field measurements and the difficulty in modeling the surf zone in the laboratory. Breaking waves were measured in the laboratory in early work by Iverson (1953) using photographic techniques. The length of the channel limited the wave type to plunging and surging breakers. Adeyemo (1970) made similar laboratory measurements using hydrogen bubble and photographic methods. Gaughan and Komar (1975) applied the theory of

wave propagation in water of gradually varying depth, as developed by Biesel, to determine the dependence of breaker type on the beach slope tangent and the deep water wave steepness.

Inman and Nasu (1956) made field measurements of water particle velocity by measuring the drag force under the wave in order to infer particle velocities. Miller and Ziegler (1964) used both acoustic and electromagnetic current meters to determine the particle motion in the surf zone. Walker (1969) made studies using propeller-type flow meters. Wood (1973) measured waves and currents in the surf zone using movies of dye movement and capacitance wave gauges. Führböter and Büsching (1974) utilized a two-component current meter and two pressure-type wave meters to measure simultaneous orbital velocities and water levels. Thornton (1968), Steer (1972), Thornton and Richardson (1973) and Bub (1974) used pressure meters, capacitance wave gauges and electromagnetic current meters to measure surface profiles and particle velocities; the work presented here is an extension of these studies.

The objective of this research is to study the kinematics of water particles in breaking waves within the surf zone. Simultaneous measurements were made of the instantaneous wave profile and the horizontal water particle velocities at fixed locations in the surf zone. Estimates of the probability density functions and power

spectra of the wave heights and particle velocities are made. The applicability of using linear wave theory as a spectral transfer function in computing velocity spectral components from the power spectrum of the waves is measured. The computed velocity spectra are compared with actually measured velocity spectra. Theoretical phase spectra between wave gauges are calculated and compared to measured phase spectra.

II. MEASUREMENTS

A. EXPERIMENT SITES

The experimental sites are in the vicinity of Monterey, California. The beaches here are some of the first intensively studied to gain an understanding of amphibious warfare techniques and are described by Bascom (1964). It was desired to measure the various types of breaking waves in the study including spilling, plunging and surging breakers. The manner in which waves break depends very much on the characteristics of the beach and near-shore bottom slope (Table I). Plunging and spilling breakers occur most frequently at the Del Monte Beach site within Monterey Bay. The waves at this location are generally severely directionally filtered and refracted by the geometry of the bay and impinge almost perpendicular to the shore with a resulting simplification in the wave description. A second experimental site was Carmel River Beach, five miles to the south, where the beach is very steep and very often has surging type breakers. Again here, the beach is within an embayment and the waves impinge almost perpendicular to the shore. A typical beach profile and instrument location for Del Monte Beach is shown in Figure 1. Del Monte Beach profiles for 4 - 10 March 1975 are given in Appendix A. Figure 2 shows the beach profile and instrument location at Carmel River Beach on 29 May 1975. A beach

TABLE I. BEACH AND WAVE CHARACTERISTICS

Location	Del Monte Beach	Carmel River Beach
Date	4 - 10 March 1975	29 May 1975
Beach Slope	Figure 1 and Appendix A	7.2:1 (Figure 2)
Sand Type	Quartz feldspar	Quartz feldspar
Sand Median Diameter	300 μ	410 μ
Breaker Type	Plunging and spilling	Surging and spilling
Wave Period	10.9 to 16.4 seconds	12.8 seconds
Wave Height	Up to 1 meter	Up to 2 meters

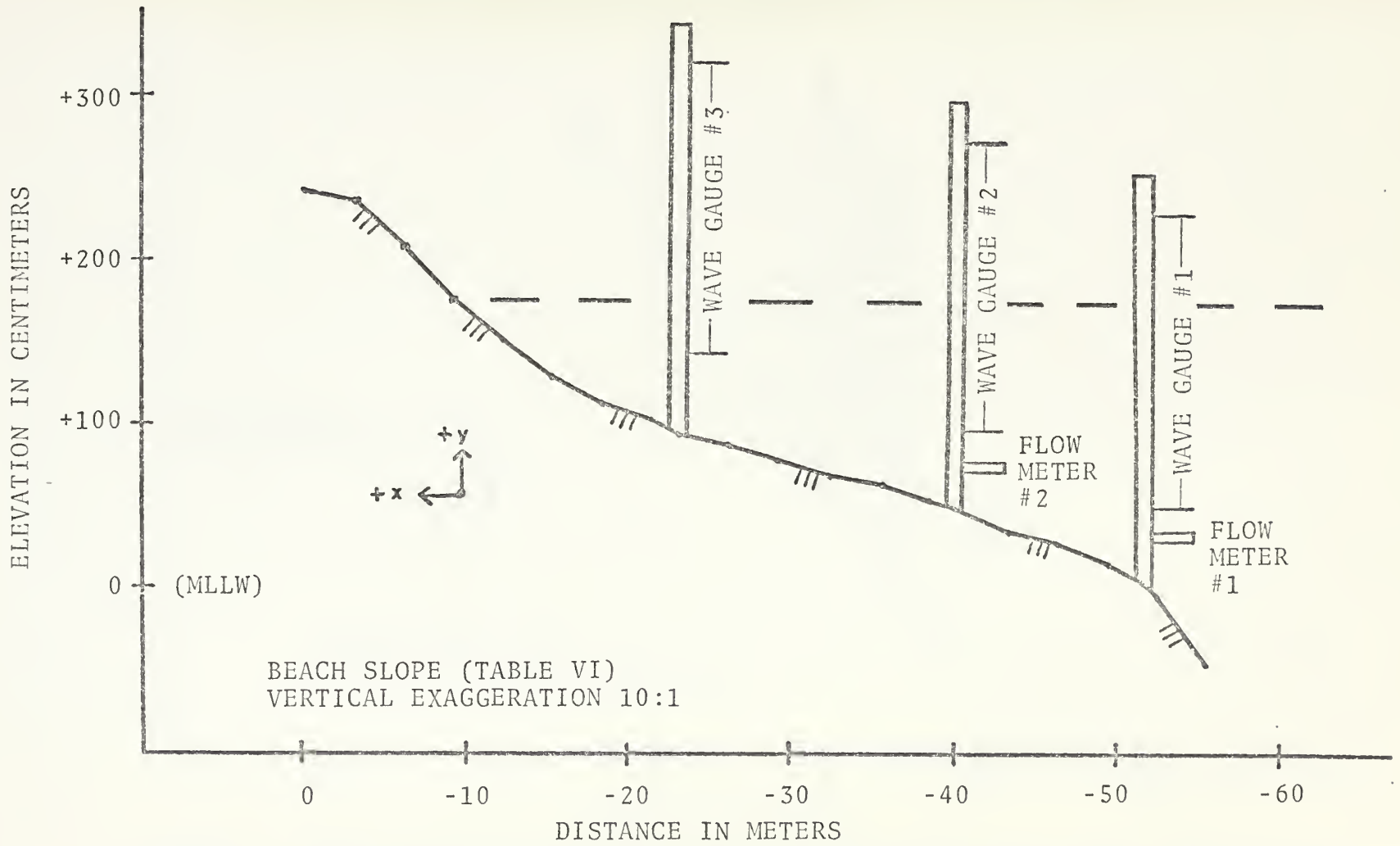

FIGURE 1. Typical Beach Profile and Instrument Location at Del Monte Beach 4 - 10 March 1975

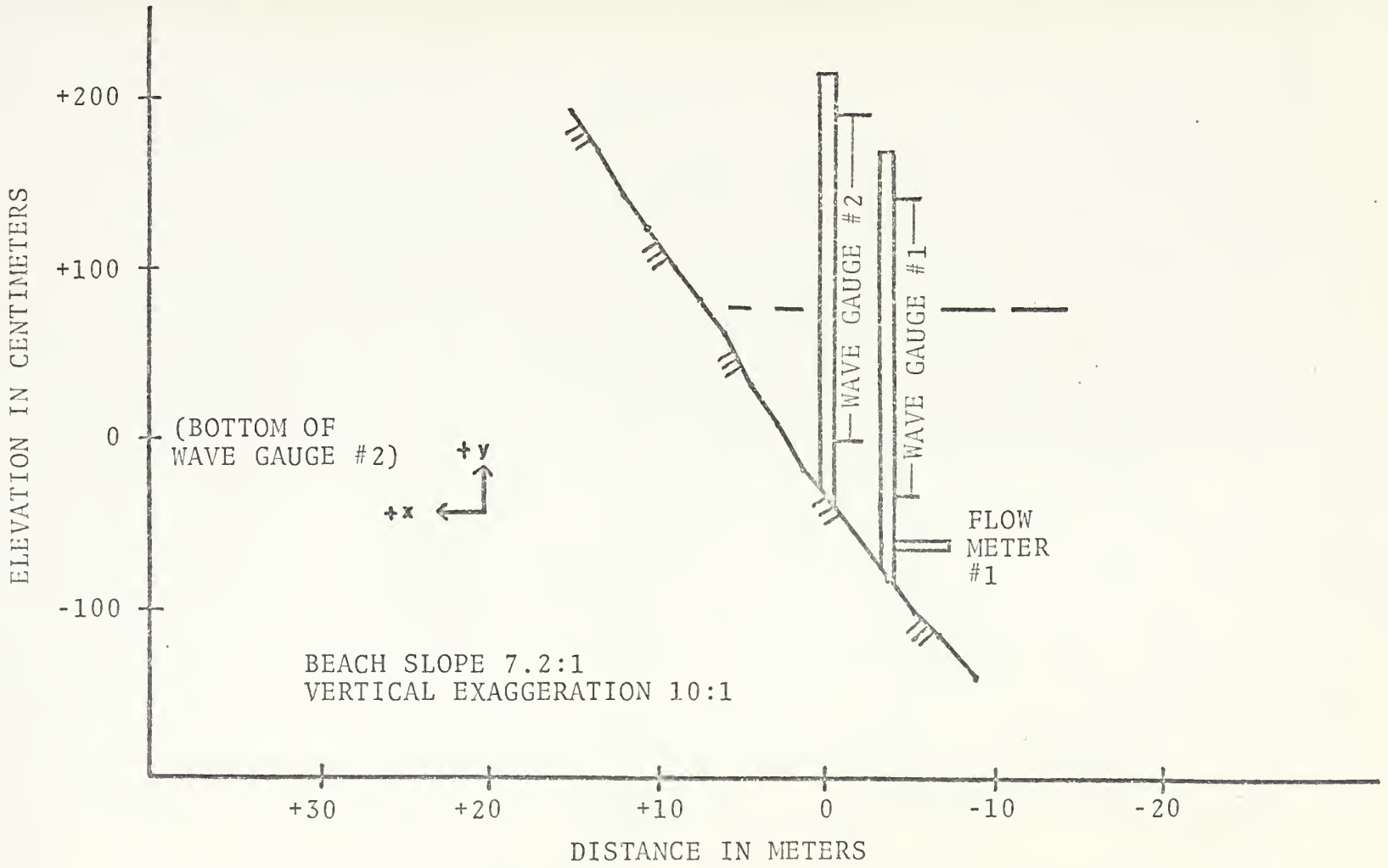

FIGURE 2. Beach Profile and Instrument Location at Carmel River Beach
29 May 1975

profile taken the following day was identical to Figure 2.

B. INSTRUMENTATION

Many problems were encountered in the initial attempt in February 1975 to measure the desired parameters. The first wave gauges were manufactured from 1.0 cm diameter stripped RG-11 coaxial cable as was done by Bub (1974). Large masses of kelp torn loose by high waves, flotsom and the pounding surf easily broke these cables. Scouring around the base-plates of the instrument towers and the blade-type anchors caused the towers to topple. The construction of the wave gauges was modified to a three-eighths inch outside diameter stainless steel rod, covered with a one-sixteenth inch wall thickness teflon tubing fitted tightly over the rod; these wave gauges withstood the severe forces in the surf well. Steel pipe extensions each 0.6 m in length were added under the tower base plates and resulted in stable platforms. An extension was built for the top of the anchors; with this device, the anchors were sledge-hammered deeper into the beach so that the top of each anchor was approximately 15 cm below the sand. The extension was then removed and scouring was minimized.

Measurements at Del Monte Beach were made using two electromagnetic flow meters and three capacitance wave gauges. One flow meter and two wave gauges were used at Carmel River Beach. The instruments were mounted on the

towers within the surf zone. All equipment was calibrated in the laboratory prior to the experiments.

The electronics package for each of the 2.5 m capacitance wave gauges was constructed using the design of McGoldrick (1969). The capacitance wave gauge operates on the principle that a change of capacitor plate dimensions changes the circuitry voltage output. The rod and the sea water act as plates and the teflon insulation as the dielectric. As the wave elevation fluctuates, the capacitance of the circuit changes and the voltage output responds linearly. These water surface fluctuations were sensed by a transistorized circuit operated by self-contained batteries. The electronics package was housed in a watertight brass case which was mounted on the tower. This enabled the connecting leads to be less than 30 cm, thereby minimizing wire-to-wire capacitance. Accuracy was estimated to be ±0.005 m. The calibration plots are shown in Appendix B. Minor modifications to the wave gauges immediately following the Del Monte Beach measurements are the cause for the different calibration graphs in Appendix B.

The two flow meters were Marsh-McBirney Model 721 Electromagnetic Current Meters. The flow meter operation is based on Faraday's principle of electromagnetic induction. Each probe measures water velocity in two orthogonal directions. The flow meters were calibrated with an

oscillating platform attached to an eccentric arm driven by a variable speed motor using the method of Thornton and Krapohl (1974). Measurement accuracy was determined to be ±0.005 m/sec during calibration. The flow meter calibration plots are shown in Appendix C.

In the field the instruments were attached to 6.3 cm outside diameter steel pipes which were 3.6 m high with a 1.0 m base plate and the 0.6 m steel pipe extensions. The towers were placed on a line perpendicular to the predominant wave direction and were erected during low tide when the beach was easily accessible. The measurements were then conducted at high tide. The tidal range in the Monterey area is typically two meters. The towers were supported by steel guy wires fastened to the anchors. Several types of anchors were tried and the blade anchor worked quite satisfactorily in the relatively coarse sand. The wave gauges were attached to the towers with locally fabricated micarta clamps. A 1.6 cm steel stiffening rod was added to the arrangement in order to reduce wave gauge vibration following breaker impact. The flow meters were positioned directly under the wave gauges with the axes aligned horizontally (+X, shoreward) and vertically (+Y, upward). A carpenter's level was used to establish axis alignment with an estimated error of ±2 degrees. A typical tower and sensor arrangement is shown in Figure 3.

All signals were cabled ashore and recorded on a Vidar Corporation 32-channel digital data acquisition system.

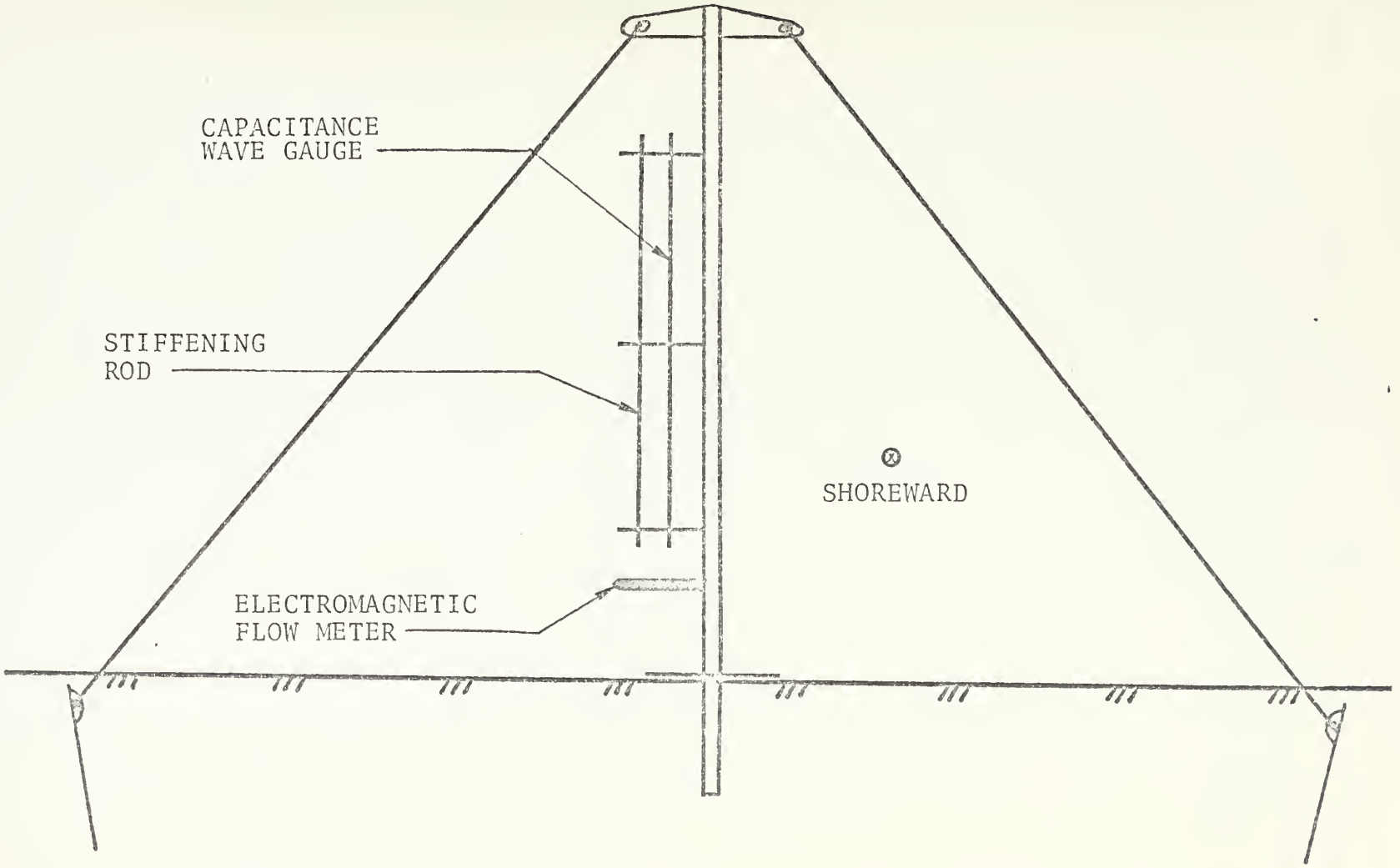

FIGURE 3. Schematic of Typical Instrument Tower with Sensors

A Sangamo model 3500 14-channel FM tape recorder was utilized as a secondary recording system. A Brush 8-channel strip chart recorder was used to monitor the instrumentation performance during recording and as a means to select the appropriate data sections to be analyzed.

III. ANALYSIS OF DATA

Record lengths of 30 minutes from each data set were analyzed. The details of the analysis system including calibration factors are given in Appendices D and E. A mean value was calculated for all data sets and the data was linearly detrended to exclude the rise and fall of the tide. The variance, standard deviation and average period were calculated. The average period was determined by calculating the time between zero upcrossings. However, perturbations caused by secondary gravity waves "riding" the primary gravity waves, capillary waves and minor instrument noises increased zero upcrossing occurrences and caused the calculated average periods to be lower than visually observed. Probability density functions for each data set were calculated and graphically compared with Gaussian and Gram-Charlier distributions.

For each signal an auto-covariance function was calculated and smoothed with a Parzen window. A Fourier transform was then applied to the smoothed auto-covariance function and the power spectrum determined. A cross-covariance function between data sets was computed, smoothed with a Parzen window, a Fourier transform applied, and the cross-spectrum computed. The coherence and phase were then calculated. To compare waves and flow velocity, the wave profile spectrum was converted to a theoretical velocity

spectrum for comparison with the measured flow velocity spectrum. The two power spectra, the coherence and the phase were then plotted. In comparing two wave profiles, theoretical celerities were calculated using linear theory and its shallow water approximation which were then converted to phases and plotted for comparison with the measured phase difference.

Aliasing testing was performed on all spectra. Nyquist frequencies of 1.25 and 0.98 Hz were determined optimal for Del Monte Beach and Carmel River Beach data sets, respectively. The frequency bands of 0.0 to 1.25 and 0.98 Hz include the region of gravity waves (0.033 to 1.0 Hz).

The maximum lag time in calculating the covariance functions was taken as five percent of the record giving a spectral bandwidth resolution of 0.00556 Hz and results in 40 degrees of freedom for each spectral estimate. The 80 percent confidence limits for 40 degrees of freedom using a chi-square distribution are found to be between 0.73 and 1.30 of the measured power spectral estimates.

IV. RESULTS

A. QUALITATIVE DESCRIPTION

A number of similarities of wave form can be observed for various types of breakers occurring on different beaches around the world. Figures 4 and 5 are typical analog records of waves and horizontal velocities beneath the waves obtained from Del Monte and Carmel River Beaches, respectively. In general, there is a quick drawdown of water just before the breaking wave arrives, followed by a steep, almost vertical leading edge, and a sloping profile toward the trailing edge. On the trailing edge of the wave secondary waves are often noted. These are harmonics of the primary wave frequency and are indicative of very non-linear waves. At Del Monte Beach the waves break as plunging and spilling breakers giving a generally saw-toothed shape; the plunging or spilling occurs rapidly at the crest and moves down the wave. The surging breakers occurring at Carmel River Beach rise and fall off more gradually.

B. PROBABILITY DENSITY FUNCTIONS

1. Gaussian and Gram-Charlier Frequency Distributions

Frequency distributions were computed for each measured quantity for all runs and compared with Gaussian and Gram-Charlier distributions. The chi-square

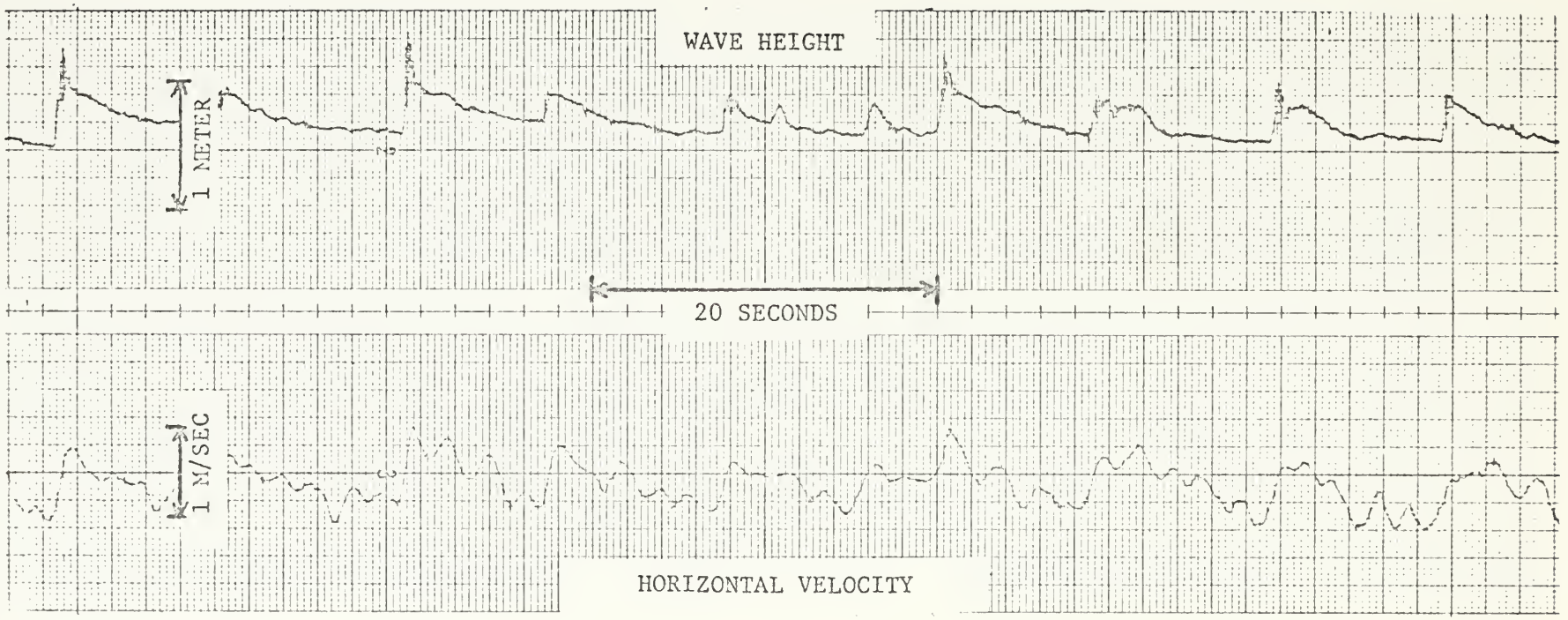

FIGURE 4. Typical Analog Record of Waves and Horizontal Velocities beneath the Waves from Del Monte Beach

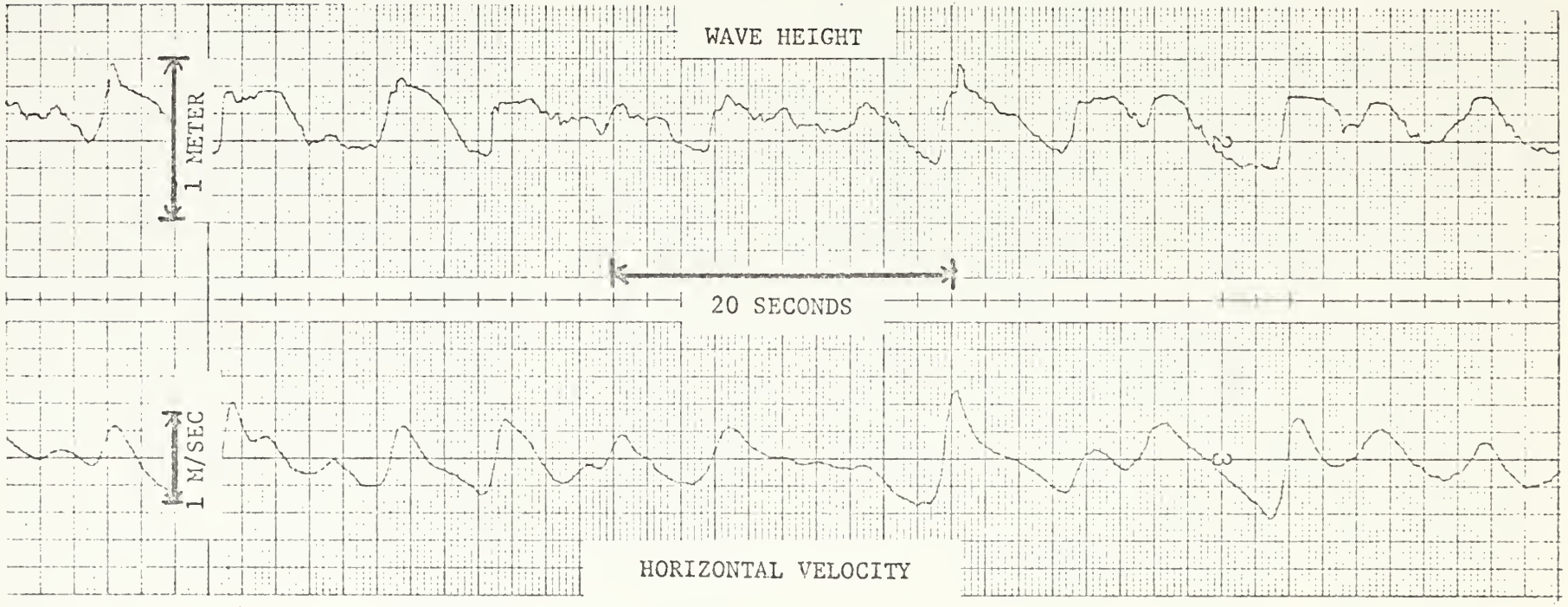

FIGURE 5. Typical Analog Record of Waves and Horizontal Velocities beneath the Waves from Carmel River Beach

goodness-of-fit test was computed using both theoretical distributions. The variance, standard deviation, skewness and kurtosis were also computed for all data sets and are summarized in Table II. The closer the chi-square fit parameter is to zero, the better the fit.

In deep water,the sea surface has approximately a Gaussian distribution which results in a skewness of zero and a kurtosis of 3. However, non-linearities introduce skewness and kurtosis values that deviate from Gaussian and result in a distribution more closely approximated by the Gram-Charlier. These non-linearities are evident in the frequency distribution of Wave Gauge #2 on 4 March as shown in Figure 6, and result in bi-modal or tri-modal distributions. Figure 7 is the graph of distributions computed for the particle velocity at Flow Meter #2 on the same date. The latter has a uni-modal distribution. Appendix F contains distributions computed for all other data sets.

The distributions for all flow velocities are either uni-modal or have less pronounced secondary peaks compared to the distributions of wave heights. As noted in Table II, this results in nearly equal fit parameters for both Gaussian and Gram-Charlier distributions, although the latter values are smaller, and therefore give the better fit in ten of eleven cases. The exception is Flow Meter #2 on 8 March. Additionally, the fit parameters for velocity components are much closer to zero than are the values computed for

TABLE II. COMPUTED STATISTICS

Date	Instrument	Variance	Standard Deviation	Skewness	Kurtosis	Chi-Square Parameter	
						Gaussian	Gram-Charlier
4 March	WG #1	0.04785	0.21874	0.66376	2.79968	889.22	411.78
	FM #1	0.92758	0.96311	-0.33711	3.11333	208.53	85.39
	WG #2	0.02565	0.16015	0.89559	3.32280	1869.72	878.92
	FM #2	0.69224	0.83201	0.27365	3.56087	109.40	98.25
5 March	WG #1	0.02224	0.14913	3.95435	35.51553	2835.35	16553.91
	FM #1	0.36620	0.60514	0.17582	2.94380	92.32	64.57
	WG #2	0.02723	0.16500	0.80306	6.75049	476.30	1644.48
	FM #2	0.44022	0.66349	-0.19583	2.99947	85.19	54.05
6 March	WG #1	0.00497	0.07048	1.49806	14.19603	1005.73	51495.15
	FM #1	0.31536	0.56157	0.10989	3.02128	74.09	66.76
	WG #2	0.01610	0.12689	0.67987	4.94608	177.90	417.24
	FM #2	0.18305	0.42785	-0.07223	3.04810	40.64	38.85
	WG #3	0.01681	0.12964	-0.01734	3.31015	307.37	342.30
8 March	WG #1	0.01487	0.12193	0.97593	8.33973	312.00	18702.37
	FM #1	0.17958	0.42376	0.08748	2.56320	138.24	102.29
	WG #2	0.01801	0.13419	0.59795	3.30346	405.10	191.87
	FM #2	0.34490	0.58728	0.03939	4.44019	306.13	506.93
9 March	WG #1	0.02001	0.14144	0.47342	4.16410	358.92	382.09
	FM #1	0.27789	0.52716	0.07738	3.48368	83.80	62.49
	WG #2	0.01322	0.11498	0.76923	3.13506	1220.76	614.27
	FM #2	0.35601	0.59666	0.17642	3.35326	118.56	89.49
29 May	WG #1	0.03960	0.19900	0.55278	5.67411	1488.50	1184.35
	FM #1	0.48143	0.69385	-0.23986	4.59134	96.48	90.70
	WG #2	0.00924	0.09612	0.64436	3.73892	386.52	246.91

Variance for the wave heights is given in meters squared; variance for the horizontal velocity components is given in meters squared per second squared.

Standard deviation for the wave heights is given in meters; standard deviation for the horizontal velocity components is given in meters per second.

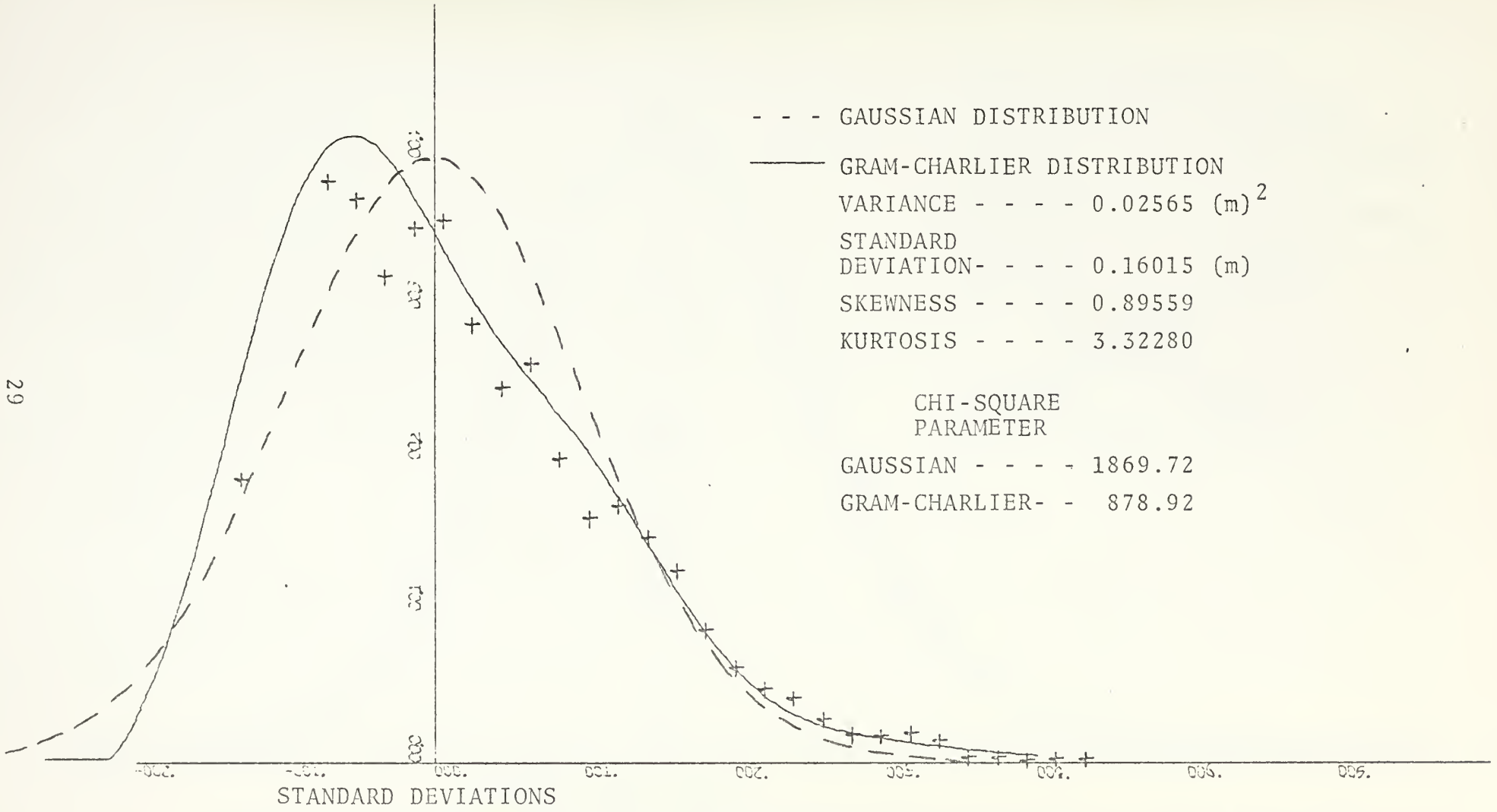

FIGURE 6. Frequency Distribution of the Sea Surface Elevation at Wave Gauge #2 on 4 March 1975

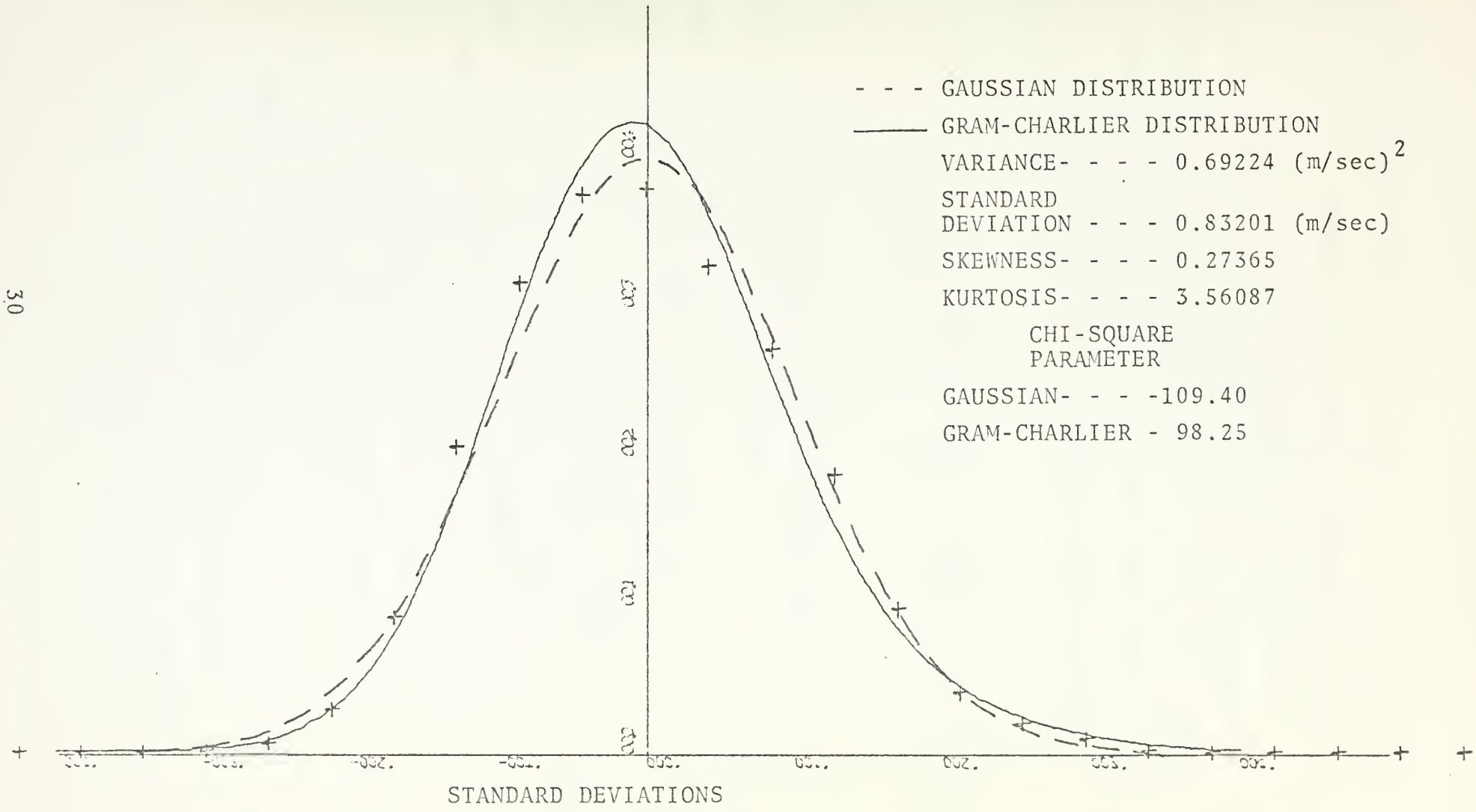

FIGURE 7. Frequency Distribution of the Horizontal Velocity at Flow Meter #2 on 4 March 1975

wave components. This is to be expected since the flow meters do not experience the surface irregularities to the same degree as do the wave gauges. In seven of thirteen fit parameter calculations for wave components, the Gaussian distribution provided the better fit. This is a result of using a truncated form of the Gram-Charlier in calculating the probability density function, P_{GC}, given by

$$P_{GC}(\xi) = P_G(\xi)\left[1.0 + \frac{m_3}{6} H_3 + \frac{m_4}{24} H_4 + \frac{m_3^2}{72} H_6 + ...\right] \quad (1)$$

where

P_G = Gaussian probability density function,

m_3 = skewness of the data record,

m_4 = the kurtosis minus 3,

H_n = Hermite polynomials of degree n.

Higher order moments could be included in equation (1) to possibly improve the fit, but would necessitate analyzing longer record lengths in order to maintain confidence. Stationary problems would be encountered in the longer records, thus producing other errors. Hence, the poor fit is a deficiency of the Gram-Charlier distribution in surf zone applications.

2. Skewness and Kurtosis

The physical geometry of the waves, which characteristically have narrow, steep crests and wide, shallow troughs in the surf zone produce a positive

skewness, indicating a greater amount of time below, rather than above, the mean water level. This is true except at Wave Gauge #3 on 6 March. (See Table II and Appendix F.) Data from this wave gauge was analyzed on this date only, because visual observations noted that most waves were actually breaking on this gauge, rather than on Wave Gauges #1 and #2 as was otherwise the case.

It should follow that the wave induced particle velocities would have probability density functions similar to the waves. However, of the eleven horizontal velocity data records, four did not have positive skewness. These deviations occurred at Flow Meter #1 on 4 March and 29 May and Flow Meter #2 on 5 and 6 March. Reflected waves were originally thought to be a feasible explanation for the negative skewness. If this were so, Flow Meter #2 on 4 March and 29 May would also expect to have negative values. This was not the case. The reason for the large skewness and kurtosis values for Wave Gauge #1 on 5, 6 and 8 March is not known. Similar anomalous results have been found in deeper water outside the surf zone by Thornton and Krapohl (1974).

Kurtosis indicates the peakedness of each parameter. Just prior to breaking the waves achieve the greatest degree of peakedness and should have the highest kurtosis value at this time. Visual observations noted that most waves were breaking at Wave Gauge #1 on 4 March and 29 May, at Wave Gauge #2 on 5 March and on

Wave Gauge #3 on 6 March. It should be expected that the kurtosis values would be greatest at these given gauges for the respective dates. With the exception of 29 May, this did not turn out to be true. The wide surf zone caused by varying breakers heights on 8 and 9 March make evaluation of kurtosis values difficult on these dates.

C. COMPARISONS OF THEORETICAL AND MEASURED POWER SPECTRA

The theoretical velocity spectra generated from the wave spectra and the measured velocity spectra were examined in order to determine the applicability of linear (Airy) wave theory in the breaker zone. Thornton and Richardson (1974) measured waves with maximum heights of 1 m and showed that the application of a linear theory transfer function to the surface profile spectrum resulted in a calculation of the horizontal water particle velocity that underpredicted measured wave-induced horizontal velocity spectral components by about 50 percent. The coherence values between waves and horizontal velocity were high, ranging above 0.75 for an approximate frequency range of 0.075 to 0.60 Hz. The phase angle computations showed the calculated velocity components leading the measured velocity components by an average of 20 degrees. Bub (1974) took measurements in mild surf resulting in theoretical horizontal velocity values 13 percent lower than measured velocity. Coherence values varied from 0.5 to nearly 1.0 over a frequency range of 0.10 to 0.65 Hz. An approximate zero degree phase was observed out to 1.0 Hz.

For this study wave heights of approximately 1 m were typically observed at Del Monte Beach and up to 2 m were recorded at Carmel River Beach. The theoretical horizontal velocity spectra were computed from the wave spectra using the linear theory transfer function

$$S_{uc}(f) = \left[\frac{\sigma \cosh(k(h+z))}{\sinh(kh)}\right]^2 S_{\eta}(f) \qquad (2)$$

where

$S_{uc}(f)$ = calculated horizontal velocity power spectrum (m^2/sec),

$S_{\eta}(f)$ = measured wave height power spectrum (m^2-sec),

σ = angular frequency = $2\pi f$(sec^{-1}),

k = wave number (m^{-1}),

h = mean water depth (m),

z = depth of flow meter below the mean water depth (m).

Figures 8 and 9 are graphs of the measured and calculated spectral velocity values at Tower #1 for 4 March and 29 May. Additional spectra are contained in Appendix G. On the average at Del Monte Beach, the calculated horizontal velocity values underestimated the measured velocities by 79%. The same theoretical calculations for the data collected at Carmel River Beach underestimated the measured values by 86%.

A possible explanation for the low calculated values is that the wave profiles change during the shoaling and

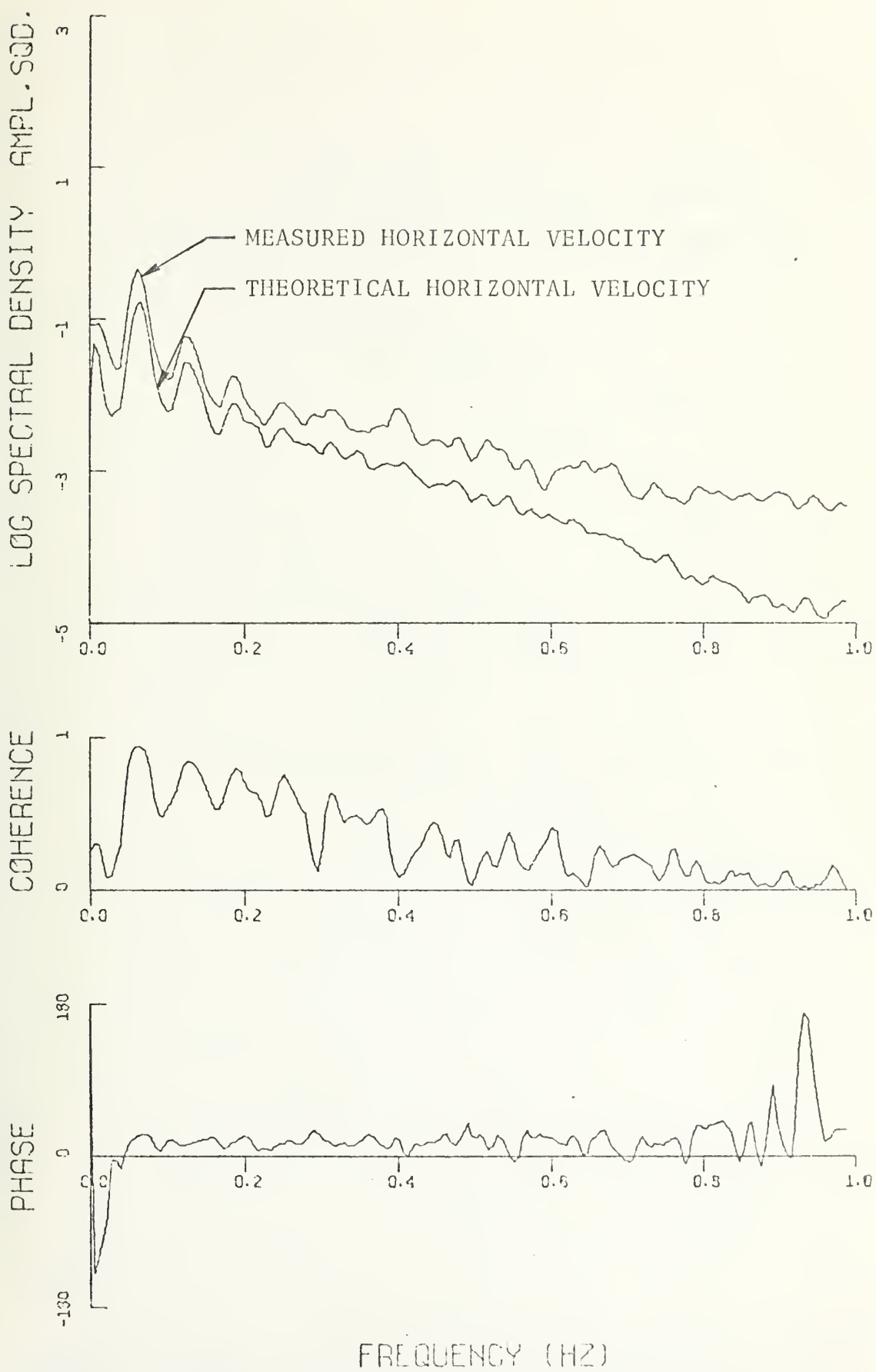

FIGURE 8. Power, Coherence and Phase Spectra for Flow Meter #1 and Wave Gauge #1 on 4 March 1975

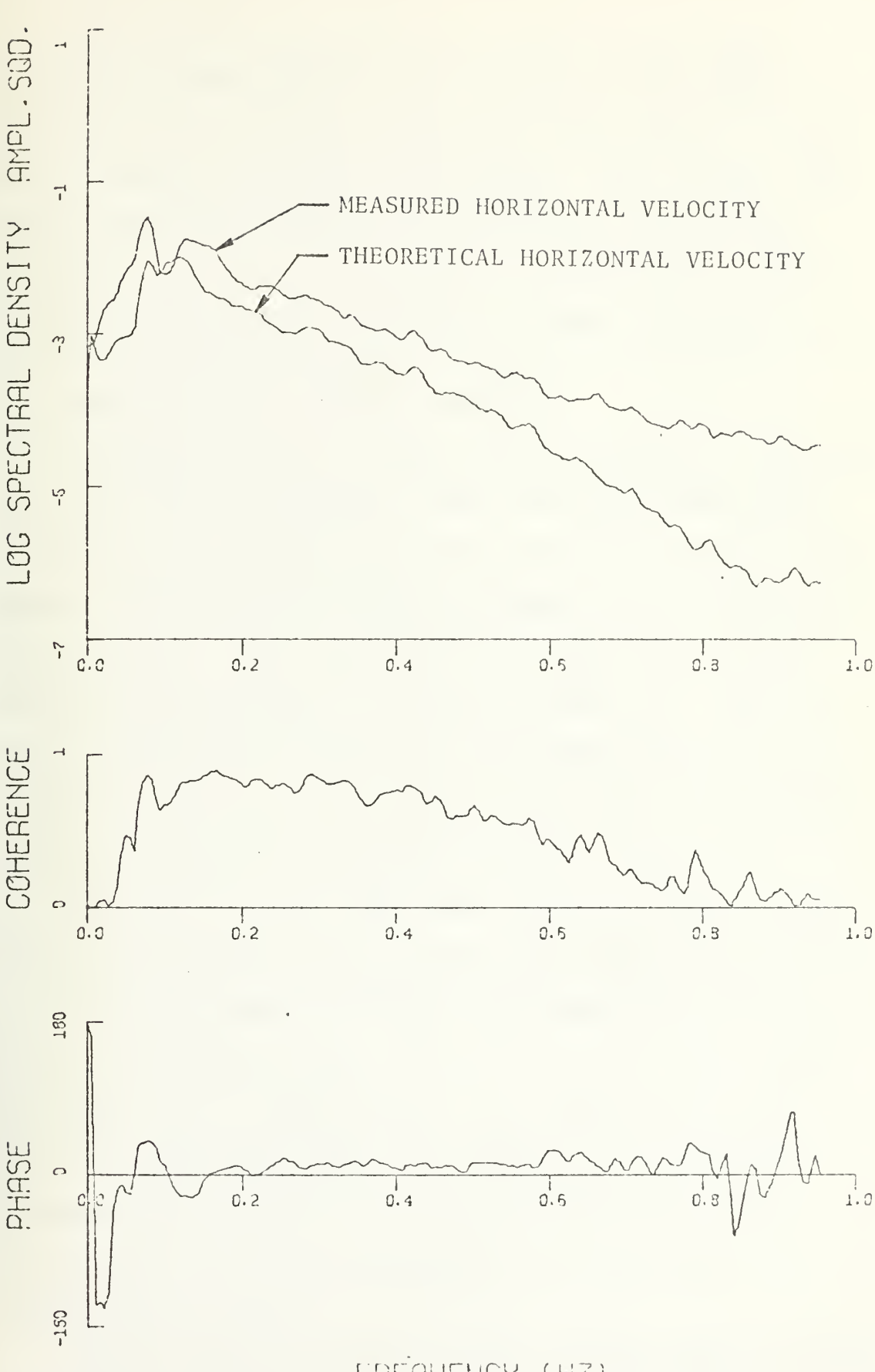

FIGURE 9. Power, Coherence and Phase Spectra for Flow Meter #1 and Wave Gauge #1 on 29 May 1975

breaking process, becoming more peaked at the crest, thus lessening the applicability of linear (Airy) theory which assumes sinusoidal wave shapes. Additionally, the wider separation between the measured and theoretical spectral values above 0.5 Hz may be explained by turbulence of the breaking waves in the higher frequency areas.

D. EXAMINATION OF SPECTRAL HARMONICS

An examination of the low frequency spectral components for each data set indicates that pronounced approximate harmonics are present in the data analyzed from Del Monte Beach. Such harmonics are not evident in the Carmel River Beach spectra. The frequencies and amplitudes of each analyzed spectral peak is listed in Table III. The frequency differences between spectral peaks and the ratios of the second, third and fourth peaks versus the primary peak are listed in Table IV.

Spectral analysis shows that definite second, third and fourth harmonics are present for 4 March and 5 March with few exceptions. Evidence of second and third harmonics is present in the analyzed data from Wage Gauges #1 and #2 on 6, 8 and 9 March. An examination of the spectral amplitudes shows that there is no consistent relationship between various components either for a given data set or when comparing like components of different data sets.

The maximum wave energies were concentrated at frequencies ranging from 0.061 Hz to 0.092 Hz corresponding to

TABLE III. FREQUENCIES AND AMPLITUDES AT SPECTRAL PEAKS

Date	Instrument	f_o	a_o	f_1	a_1	f_2	a_2	f_3	a_3
4 March	WG #1	.067	.0066	.128	.0011	.190	.00034	.251	.00017
	FM #1	.061	.1425	.128	.0183	.190	.00558	.251	.00253
	WG #2	.061	.0036	.123	.0005	.184	.00018	.246	.00010
	FM #2	.061	.0918	.123	.0146	.195	.00512	.246	.00286
5 March	WG #1	.067	.0019	.134	.0006	.190	.00021	.257	.00015
	FM #1	.067	.0474	.128	.0075	.195	.00245	.257	.00133
	WG #2	.067	.0026	.134	.0005	.190	.00024	.251	.00015
	FM #2	.067	.0636	.128	.0074	.206	.00195	.251	.00204
6 March	WG #1	.078	.0004	.156	.0001	.234	.00003	--	--
	FM #1	.078	.0304	.151	.0060	.251	.00244	--	--
	WG #2	.078	.0018	.156	.0002	.234	.00008	--	--
	FM #2	.078	.0224	.156	.0023	.257	.00112	--	--
	WG #3	.078	.0018	.167	.0001	.234	.00007	--	--
8 March	WG #1	.084	.0017	.168	.0003	.251	.00015	--	--
	FM #1	.084	.0334	.168	.0034	.251	.00130	--	--
	WG #2	.084	.0025	.159	.0003	.243	.00013	--	--
	FM #2	.075	.0421	.159	.0054	.251	.00228	--	--
9 March	WG #1	.092	.0016	.192	.0004	.277	.00019	--	--
	FM #1	.092	.0187	.192	.0034	.277	.00172	--	--
	WG #2	.092	.0009	.201	.0002	.310	.00007	--	--
	FM #2	.092	.0171	.167	.0050	.268	.00227	--	--
29 May	WG #1	.078	.0016	.122	.0018	.201	.00046	.290	.00029
	FM #1	.078	.0339	.128	.0173	.228	.00418	.279	.00321
	WG #2	.128	.0005	.223	.0001	.279	.00006	--	--

f = frequency (Hz) at spectral peaks

a = amplitude at spectral peaks

subscripts: 0 = primary, 1 = secondary, etc.

TABLE IV. HARMONIC FREQUENCIES AND SPECTRAL AMPLITUDE RATIOS

Date	Instrument	f_0	f_1-f_0	f_2-f_1	f_3-f_2	a_1/a_0	a_2/a_0	a_3/a_0
4 March	WG #1	.067	.061	.062	.061	.167	.052	.026
	FM #1	.061	.067	.062	.061	.128	.039	.017
	WG #2	.061	.062	.061	.062	.139	.050	.028
	FM #2	.061	.062	.072	.051	.159	.056	.031
5 March	WG #1	.067	.067	.056	.067	.315	.110	.079
	FM #1	.067	.061	.067	.062	.158	.052	.028
	WG #2	.067	.067	.056	.061	.192	.092	.058
	FM #2	.067	.061	.078	.045	.116	.030	.032
6 March	WG #1	.078	.078	.078	--	.250	.075	--
	FM #1	.078	.073	.100	--	.197	.080	--
	WG #2	.078	.078	.078	--	.111	.044	--
	FM #2	.078	.078	.101	--	.102	.050	--
	WG #3	.078	.089	.067	--	.056	.039	--
8 March	WG #1	.084	.084	.083	--	.176	.088	--
	FM #1	.084	.084	.083	--	.102	.039	--
	WG #2	.084	.075	.084	--	.120	.052	--
	FM #2	.075	.084	.092	--	.128	.054	--
9 March	WG #1	.092	.100	.085	--	.250	.119	--
	FM #1	.092	.100	.085	--	.182	.092	--
	WG #2	.092	.109	.109	--	.222	.078	--
	FM #2	.092	.075	.101	--	.292	.133	--
29 May	WG #1	.078	.044	.079	.089	1.120	.287	.181
	FM #1	.078	.050	.100	.051	.510	.123	.095
	WG #2	.128	.095	.156	--	.200	.120	--

f = frequency (Hz) at spectral peaks

a = amplitude at spectral peaks

Subscripts: 0 = primary, 1 = secondary, etc.

periods of 16.4 to 10.9 seconds, respectively, which agreed with visual observations. Additionally, prominent sub-harmonic peaks between 0.011 and 0.022 Hz are noted in the measured velocity spectra computed from Del Monte Beach data. This agrees with the work of Bub (1974), who observed a sub-harmonic at 0.011 Hz. Guzza and Davis (1974) state that in a theoretical analysis of edge waves excited by incoming waves, the prominent edge wave mode is the first sub-harmonic of the primary frequency. It is plausible, therefore, that the observed low frequency sub-harmonic peaks were caused by edge waves in the surf zone. Such sub-harmonics are not observed in the measured velocity spectra generated from Carmel River Beach data.

E. PHASE AND COHERENCE

The curling crests of the unstable breaking waves tend to lead the horizontal particle velocities in the body of the waves as can be seen in the phase measurements between waves and velocities. (See Table V.) The maximum phase difference would be expected at breaking. Data from Tower #1 on 4 March indicates that the theoretical horizontal velocity leads the measured horizontal velocity by about 20 degrees. Since most waves observed were breaking on Tower #1, a possible explanation for the 30 degree phase angle at Tower 2 is that the waves reorganized between the towers and broke a second time at Tower #2. Since this author's observations concentrated primarily on the initial

TABLE V. PHASE RELATIONSHIPS

Date	Instruments	Average Measured Phase Angle	Observed Position of Breaking Waves
4 March	WG #1 - FM #1	20° to 0.80 Hz	At Tower #1
	WG #2 - FM #2	30° to 0.55 Hz	
5 March	WG #1 - FM #1	5° to 0.61 Hz	At Tower #2
	WG #2 - FM #2	20° to 0.42 Hz	
6 March	WG #1 - FM #1	0° to 0.32 Hz	At Tower #3
	WG #2 - FM #2	0° to 0.35 Hz	
8 March	WG #1 - FM #1	5° to 0.37 Hz	Larger breakers outside Tower #1
	WG #2 - FM #2	10° to 0.39 Hz	Smaller breakers at Tower #2
9 March	WG #1 - FM #1	5° to 0.31 Hz	Larger breakers outside Tower #1
	WG #1 - FM #2	15° to 0.38 Hz	Smaller breakers at Tower #2
29 May	WG #1 - FM #1	10° to 0.58 Hz	At Tower #1

breaking position, the possible reorganization and second breaking were not observed. The phase angles on 5 March are 5 and 20 degrees at Towers #1 and #2, respectively. This agrees with observations and indicates that the breakers started to curl at Tower #1 and broke at Tower #2. The zero degree phase relationships on 6 March show that the waves had not started to break until shoreward of Tower #2. This agrees with the observation of waves breaking on Tower #3. The phase angles on 8 and 9 March indicate that the smaller breakers began to curl at Tower #1 and were near breaking at Tower #2. Again, this agrees with observations.

In contrast to the plunging-type breakers at Del Monte Beach, surging-spilling breakers were observed at Carmel River Beach. This was to be expected considering the beach slopes. A spilling breaker is characterized by turbulent water forming at the wave crest and eventually flowing down and covering the leading edge of the wave. Spilling begins at the crest when a small tongue of water moves faster than the wave form as a whole (Galvin, 1972). The measured phase angle at Carmel River Beach shows that the cascading crests led the horizontal particle velocities in the body of the wave by 10 degrees.

The values of coherence show varying degrees of linearity in the transfer functions between different spectra. Coherence between wave and horizontal velocity spectra at Tower #1 on 29 May is above 0.53 out to 0.58 Hz (See

Figure 9), above 0.68 out to 0.53 Hz on 8 March and above 0.60 out to 0.41 Hz on 9 March. (See Appendix G.) Other coherence calculations show a fair to poor degree of linearity, which is consistent with the observed strong non-linearities.

F. THEORETICAL AND CALCULATED PHASE SPECTRA

A theoretical phase spectrum was calculated for comparison with the measured wave spectrum from two wave gauges. The theoretical phase was computed from the relationship

$$\phi = \frac{\sigma x}{C_1} \tag{3}$$

where

ϕ = phase,

σ = angular frequency = $2\pi f$ (sec^{-1}),

x = distance between wave gauges (m),

C_1 = celerity = $(gh)^{1/2}$ (m/sec),

g = gravity (m/sec^2),

h = mean water depth (m).

Figure 10 shows typical examples of the theoretical and measured phases. The theoretical phases computed from Del Monte Beach data underpredict the actual phase relationships, whereas an overprediction is noted in the Carmel River Beach phases. The author then determined what value of celerity (C_2) would cause the theoretical and actual phases to agree out to the first zero crossing (where $\phi = 180° = \pi$)

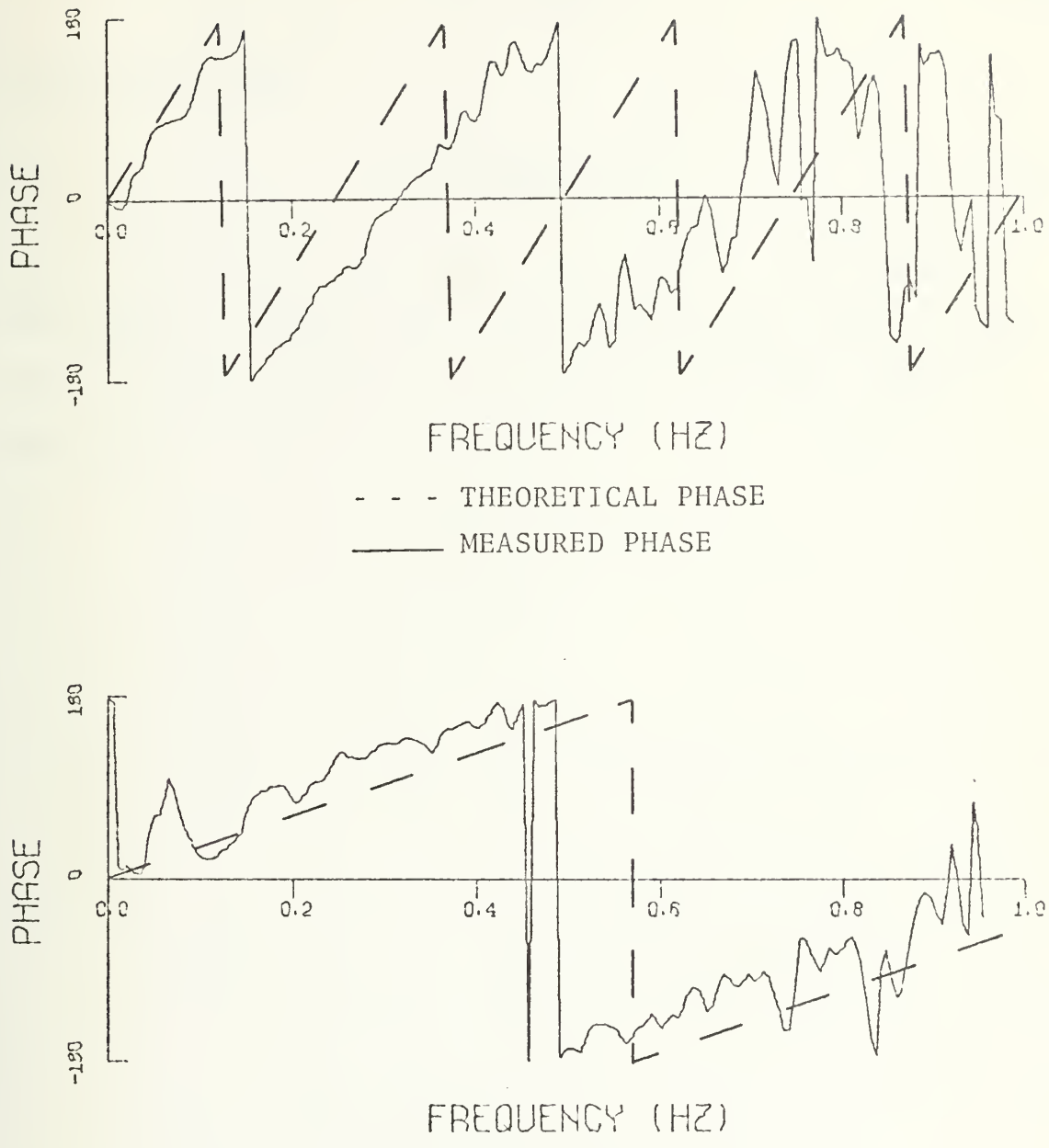

FIGURE 10. Examples of Theoretical and Measured Phases from Del Monte Beach (top) and Carmel River Beach

by first solving for C_2 from an iteration of equation (3)

$$C_2 = 2fx \tag{4}$$

and then solving

$$C_2 = (g(h+\alpha))^{1/2} \tag{5}$$

for α. The results are shown in Table VI. No evident relationship between α and other parameters, such as beach slope, mean water depth and standard deviation, could be determined.

TABLE VI. PARAMETERS CALCULATED FOR PHASE COMPARISONS

Date	Instruments	Beach Slope	h(meters)	x(meters)	f(Hz)	C_2(m/sec)	α(meters)
4 March	WG #1 - WG #2	14.3:1	0.85039	11.60	0.15625	3.625	0.4905
5 March	WG #1 - WG #2	17.3:1	1.40925	11.60	0.16741	3.884	0.1300
6 March	WG #1 - WG #2	25.8:1	1.45068	11.60	0.16741	3.884	0.0886
6 March	WG #2 - WG #3	37.2:1	1.10902	17.10	0.10045	3.435	0.0953
8 March	WG #1 - WG #2	23.7:1	0.90669	11.60	0.16765	3.889	0.6370
9 March	WG #1 - WG #2	30.5:1	0.84584	11.60	0.17603	4.084	0.8560
29 May	WG #1 - WG #2	7.2:1	1.67881	3.54	0.49107	3.477	-0.4453

V. CONCLUSIONS

Breaking waves in the surf zone can be characterized as being highly non-linear. Qualitative observations of wave and velocity profiles show secondary waves indicative of non-linear waves. The probability density functions calculated for the flow velocity records compared better with the Gram-Charlier distribution than with the Gaussian distribution when tested using the chi-square goodness-of-fit test. However, seven of the thirteen wave records more closely approximated the Gaussian distribution. This is a result of the truncated form of the Gram-Charlier probability density function used in calculations, and points out the importance of including higher order moments in describing wave phenomena in very shallow water.

The values of the horizontal power spectral components calculated from wave spectra using linear theory indicate a qualitative, but not a quantitative, relationship. Comparing the results of Bub (1974), Thornton and Richardson (1974) and this author, it is evident that increased breaker heights result in larger estimation errors. Additional investigation is warranted to determine if specific breaker heights and/or types result in specific underestimation values. If so, linear theory may be applied to achieve a reasonably accurate determination of flow velocities. The coherence values between waves and

horizontal velocity decrease as breaker height increases, indicating that the wave motion becomes more non-linear and more turbulent under this condition.

The theoretical phase calculations based on the linear theory approximation for celerity did not accurately predict the observed phases in this research. The values of α, determined so as to force the theoretical phases to agree with the observed values at the first zero crossing, show no consistency.

Use of electromagnetic flow meters and the improved capacitance wave gauges and instrument towers permits the gathering of accurate continuous data with sturdy and reliable equipment.

APPENDIX A

BEACH PROFILES AT DEL MONTE BEACH 4-10 MARCH 1975

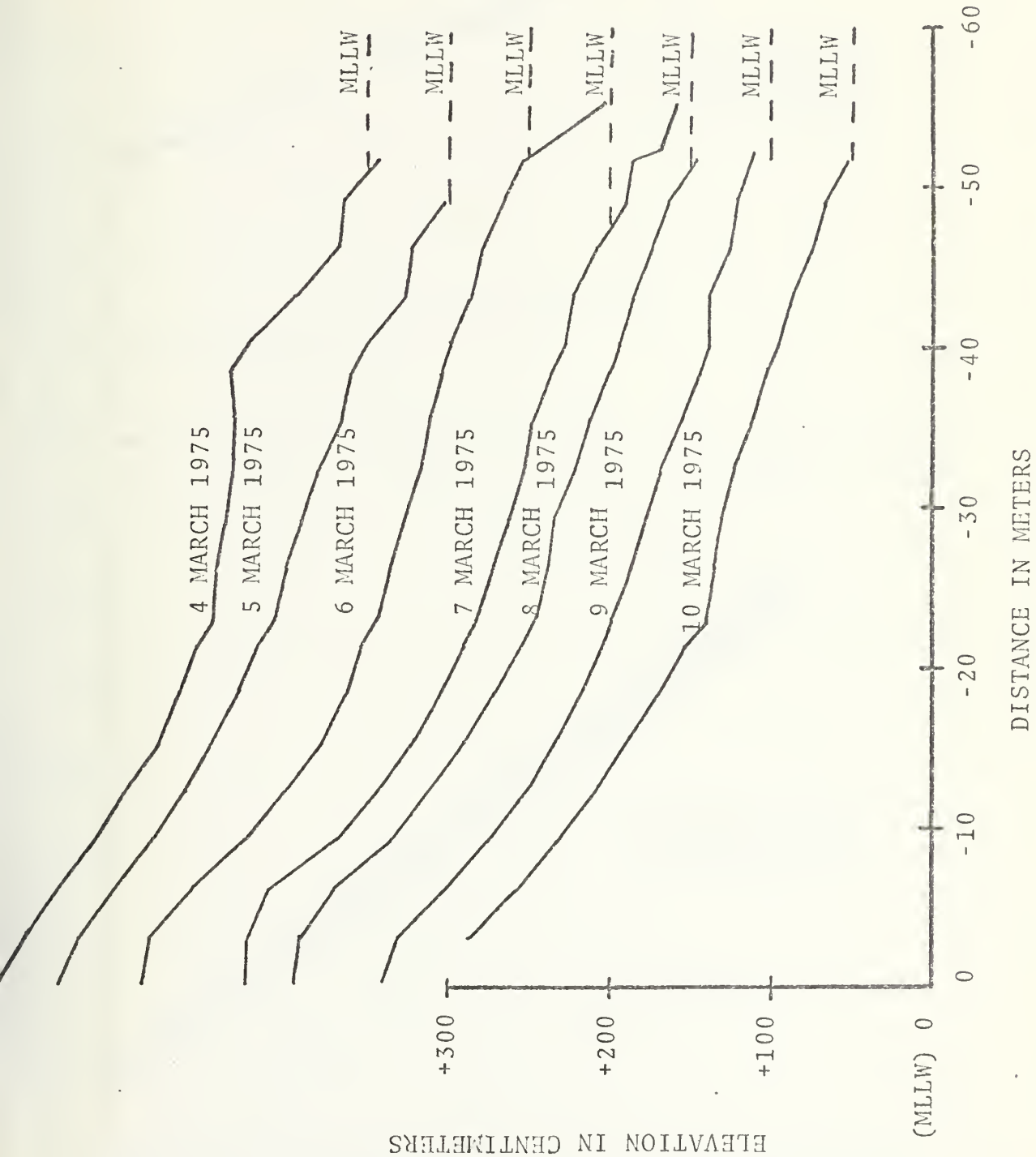

APPENDIX B

CAPACITANCE WAVE GAUGE CALIBRATIONS

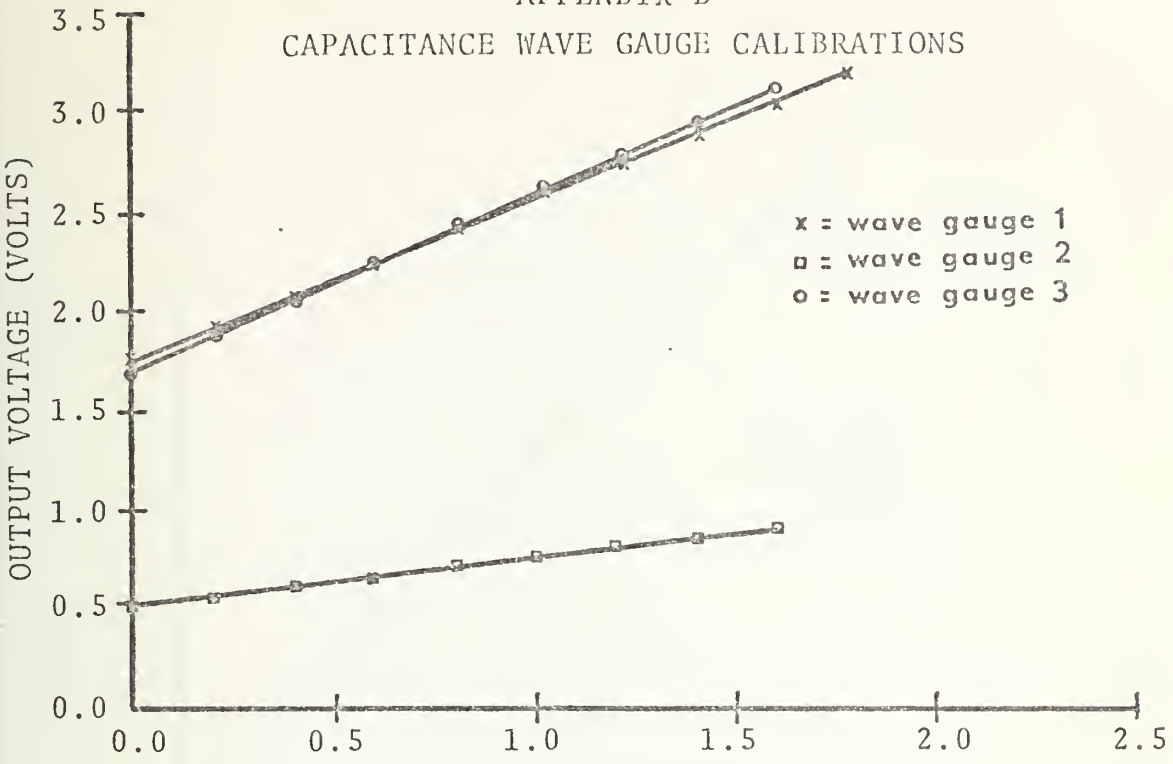

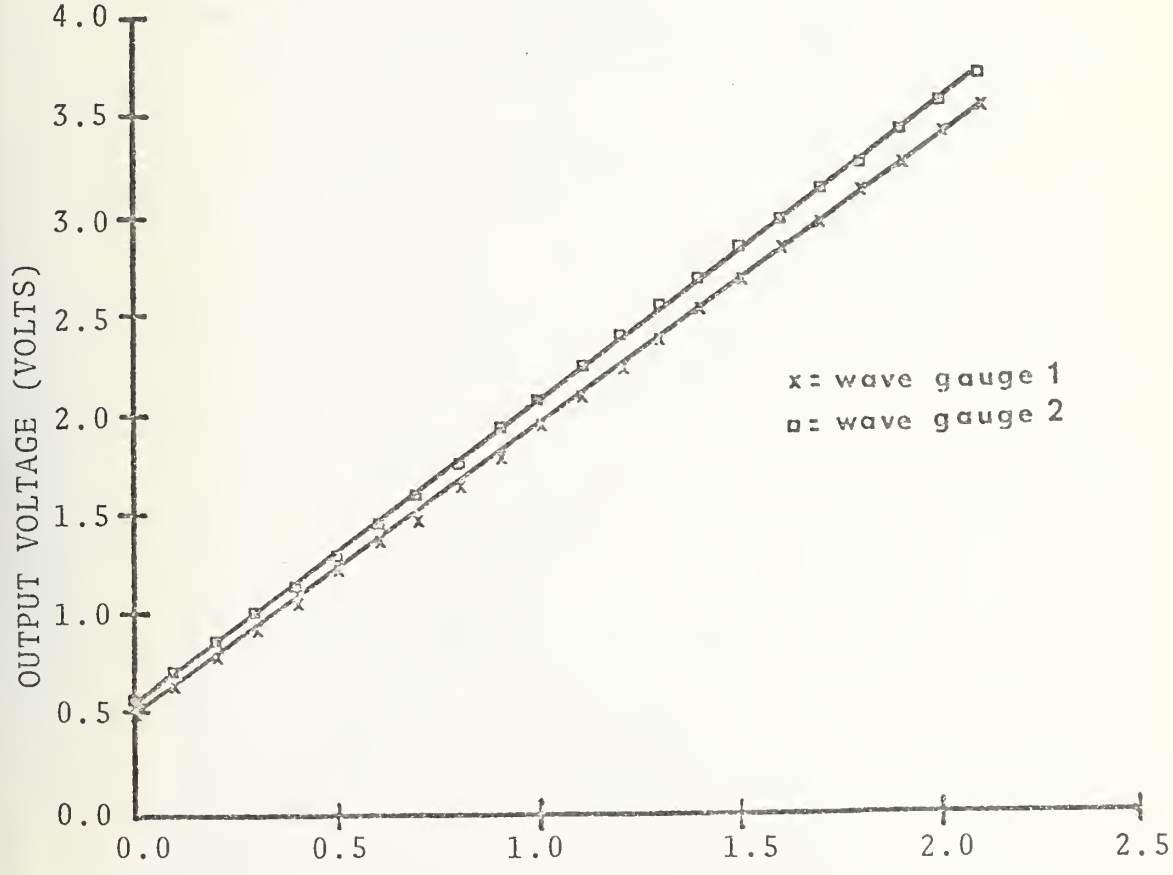

APPENDIX C

FLOW METER CALIBRATIONS

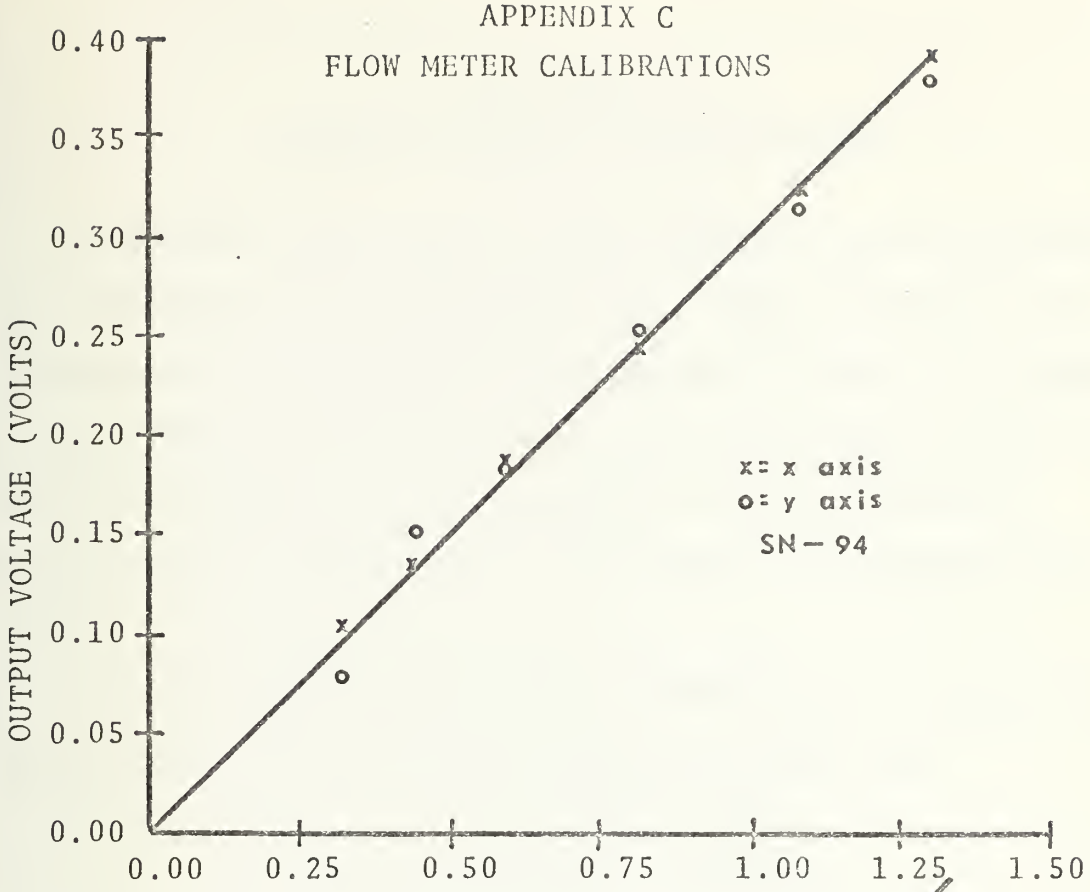

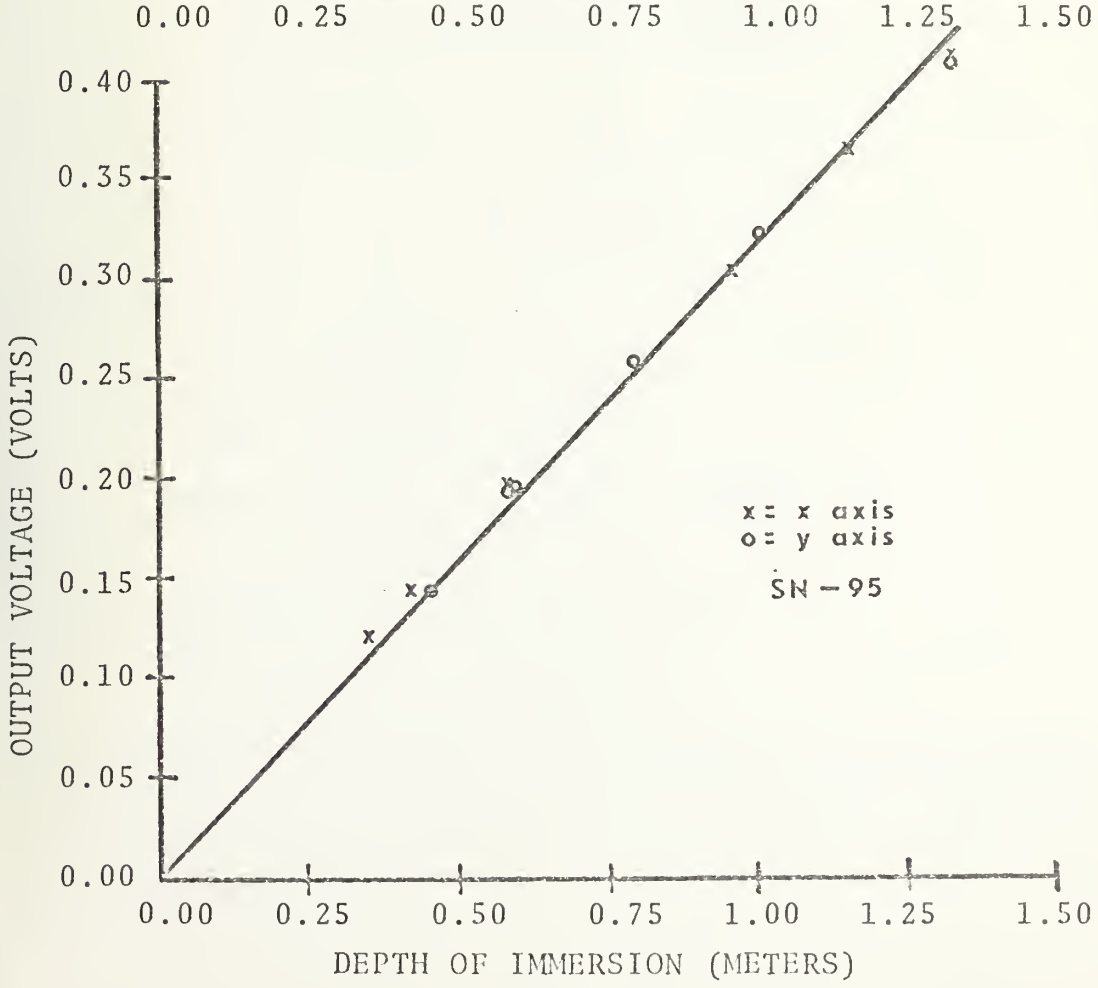

APPENDIX D

ANALYSIS DETAILS AND FLOW CHART

A complete flow chart of data acquisition and analysis is presented on the following page. The parameters used during spectral analysis were chosen to balance the longest record that the computer could reasonably analyze with the best resolution over the frequency range of interest. Additionally, consideration was given to the computer run time.

In order to determine the optimum Nyquist frequency for data analysis the following equations were used:

$$\Delta t = (VDT)(NSKIP)(NCHAN) \tag{1}$$

and

$$f_N = \frac{1}{2(\Delta t)} \tag{2}$$

where

Δt = sampling interval,

VDT = sampling rate,

NSKIP = number of samples skipped in initial data array,

NCHAN = number of channels,

f_N = Nyquist frequency.

By varying the parameters of equation (1) various Nyquist frequencies were obtained and used during preliminary IBM 360 computer analysis.

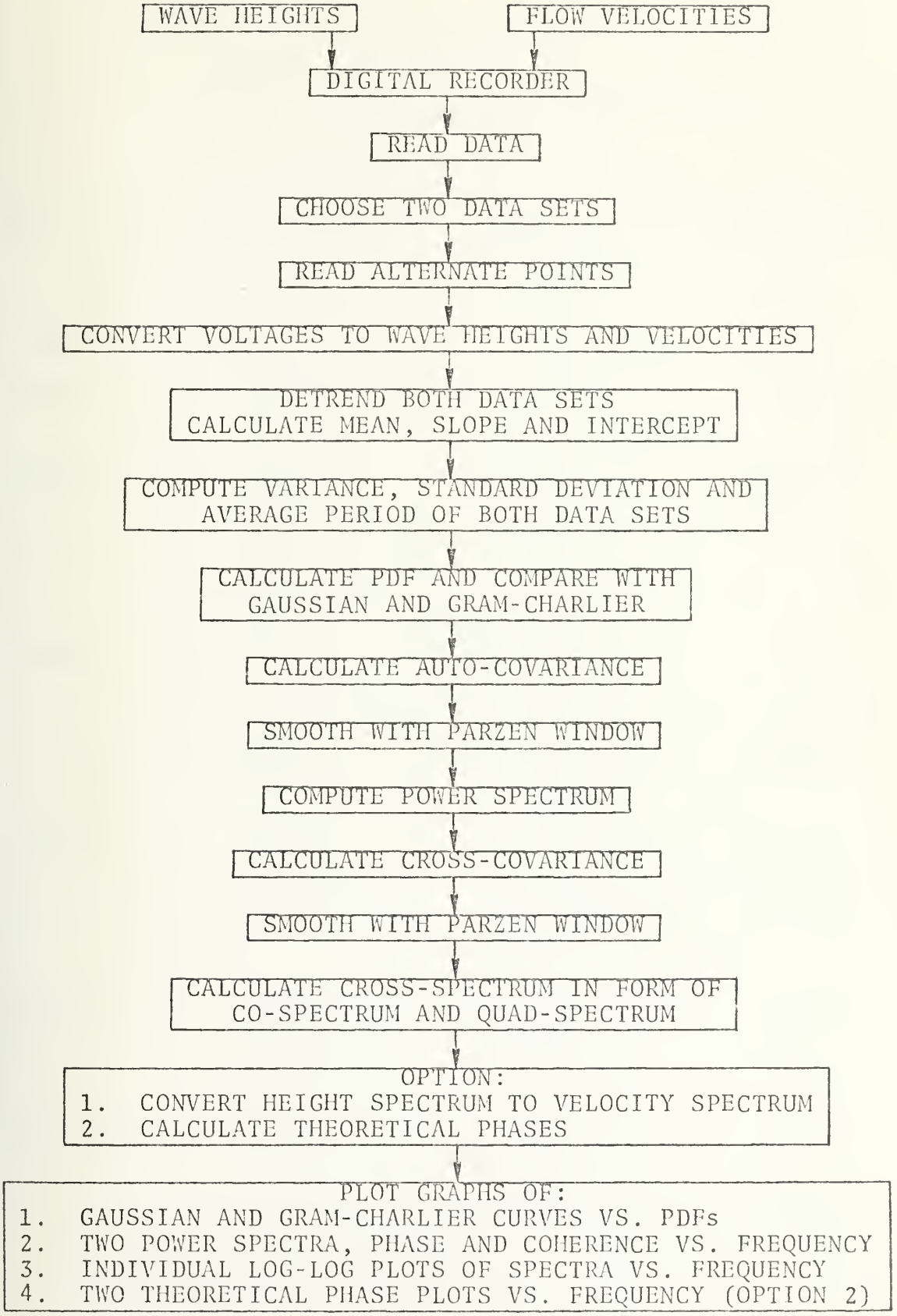
WAVE HEIGHTS
FLOW VELOCITIES
DIGITAL RECORDER
READ DATA
CHOOSE TWO DATA SETS
READ ALTERNATE POINTS
CONVERT VOLTAGES TO WAVE HEIGHTS AND VELOCITIES
DETREND BOTH DATA SETS
CALCULATE MEAN, SLOPE AND INTERCEPT
COMPUTE VARIANCE, STANDARD DEVIATION AND
AVERAGE PERIOD OF BOTH DATA SETS
CALCULATE PDF AND COMPARE WITH
GAUSSIAN AND GRAM-CHARLIER
CALCULATE AUTO-COVARIANCE
SMOOTH WITH PARZEN WINDOW
COMPUTE POWER SPECTRUM
CALCULATE CROSS-COVARIANCE
SMOOTH WITH PARZEN WINDOW
CALCULATE CROSS-SPECTRUM IN FORM OF
CO-SPECTRUM AND QUAD-SPECTRUM
OPTION:
1. CONVERT HEIGHT SPECTRUM TO VELOCITY SPECTRUM
2. CALCULATE THEORETICAL PHASES
PLOT GRAPHS OF:
1. GAUSSIAN AND GRAM-CHARLIER CURVES VS. PDFs
2. TWO POWER SPECTRA, PHASE AND COHERENCE VS. FREQUENCY
3. INDIVIDUAL LOG-LOG PLOTS OF SPECTRA VS. FREQUENCY
4. TWO THEORETICAL PHASE PLOTS VS. FREQUENCY (OPTION 2)

APPENDIX E

CALIBRATION FACTORS

Date	Instrument	CALA* (meters)	CALM** (meters/volt)
4 March	WG #1	-1.312	1.23
and	WG #2	-1.870	4.19
5 March	WG #3	-1.800	1.14
6 March	WG #1	-1.422	1.23
	WG #2	-1.620	4.19
	WG #3	-1.800	1.14
8 March	WG #1	-1.332	1.23
	WG #2	-1.570	4.19
	WG #3	-1.810	1.14
9 March	WG #1	-1.492	1.23
	WG #2	-1.510	4.19
	WG #3	-1.830	1.14
29 May	WG #1	-0.028	0.69
	WG #2	-0.370	0.66
All dates	FM #1	0.0	3.05
	FM #2	0.0	3.21

* Calibration Additive Factor

** Calibration Multiplicative Factor

APPENDIX F

PROBABILITY DENSITY FUNCTIONS VS.
GRAM-CHARLIER FREQUENCY DISTRIBUTIONS

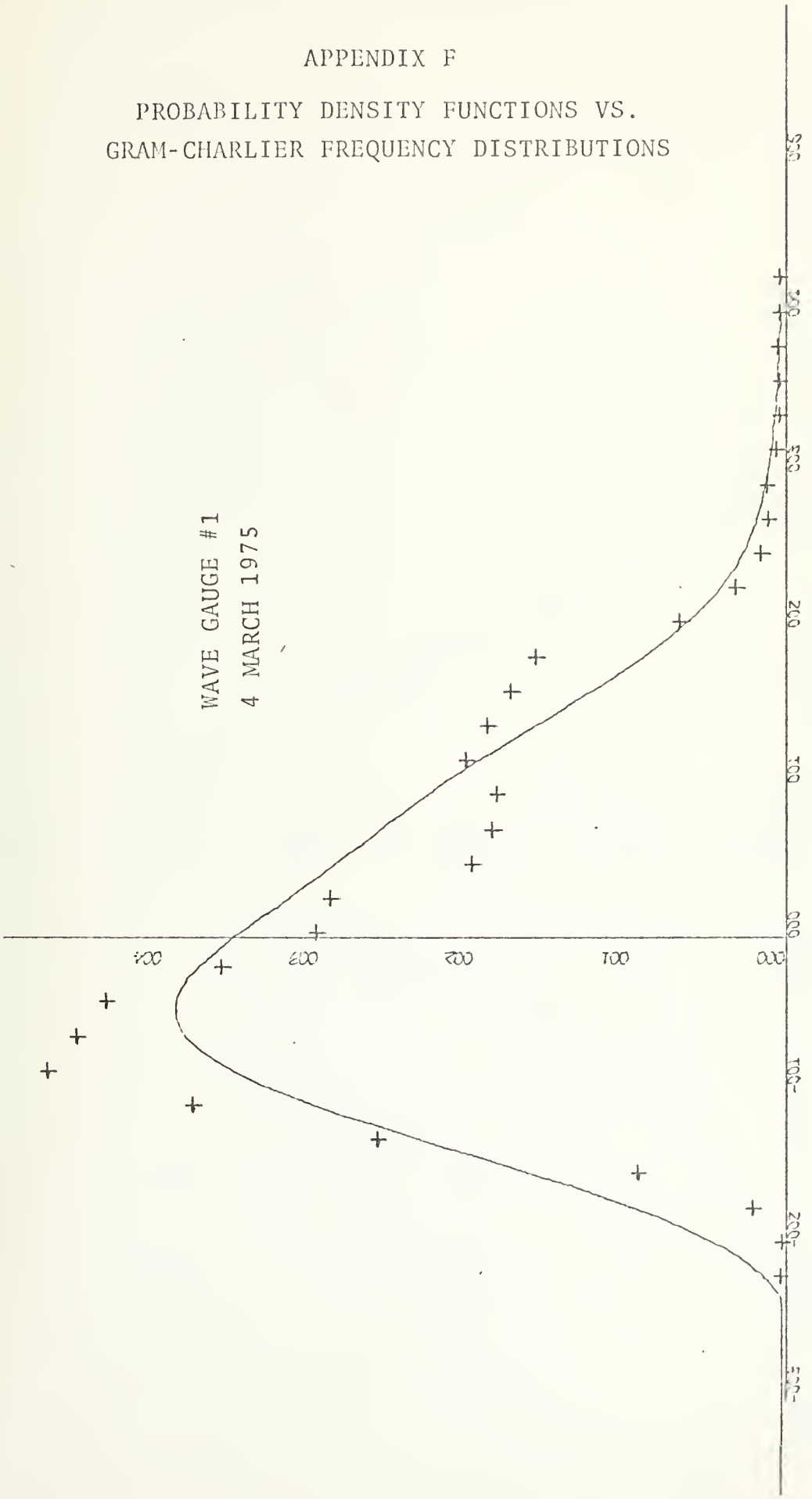

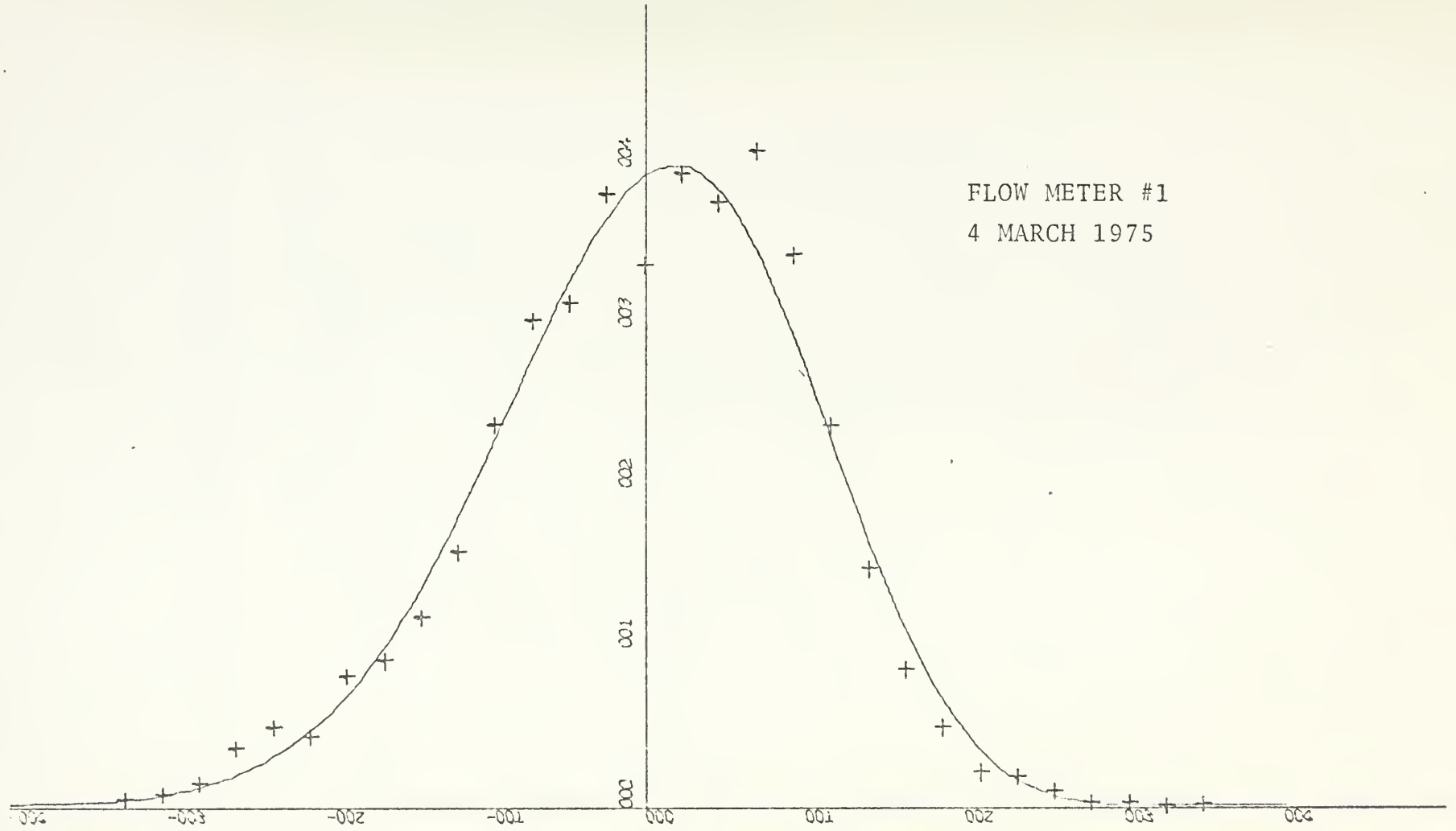
FLOW METER #1
4 MARCH 1975

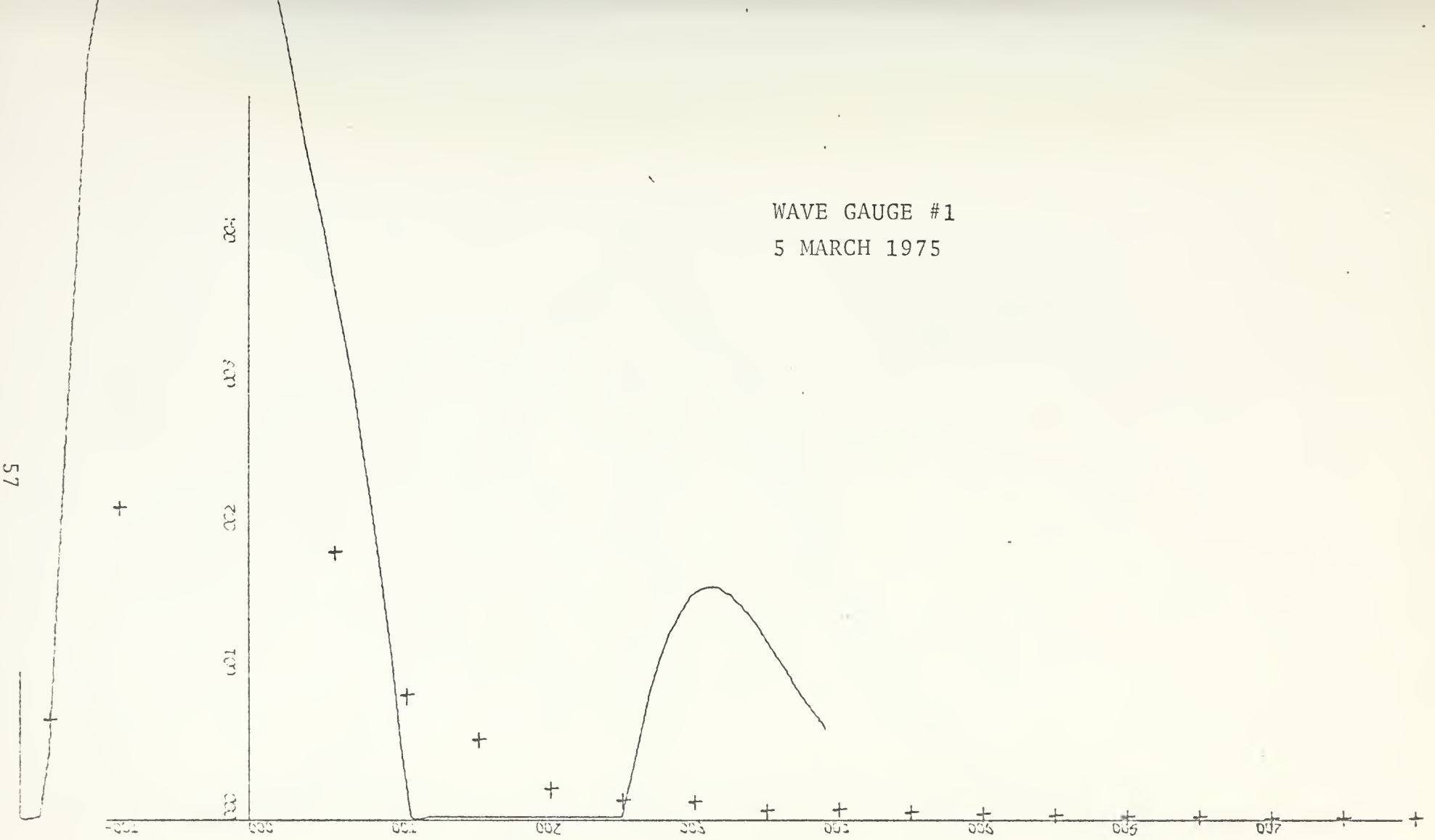
WAVE GAUGE #1
5 MARCH 1975

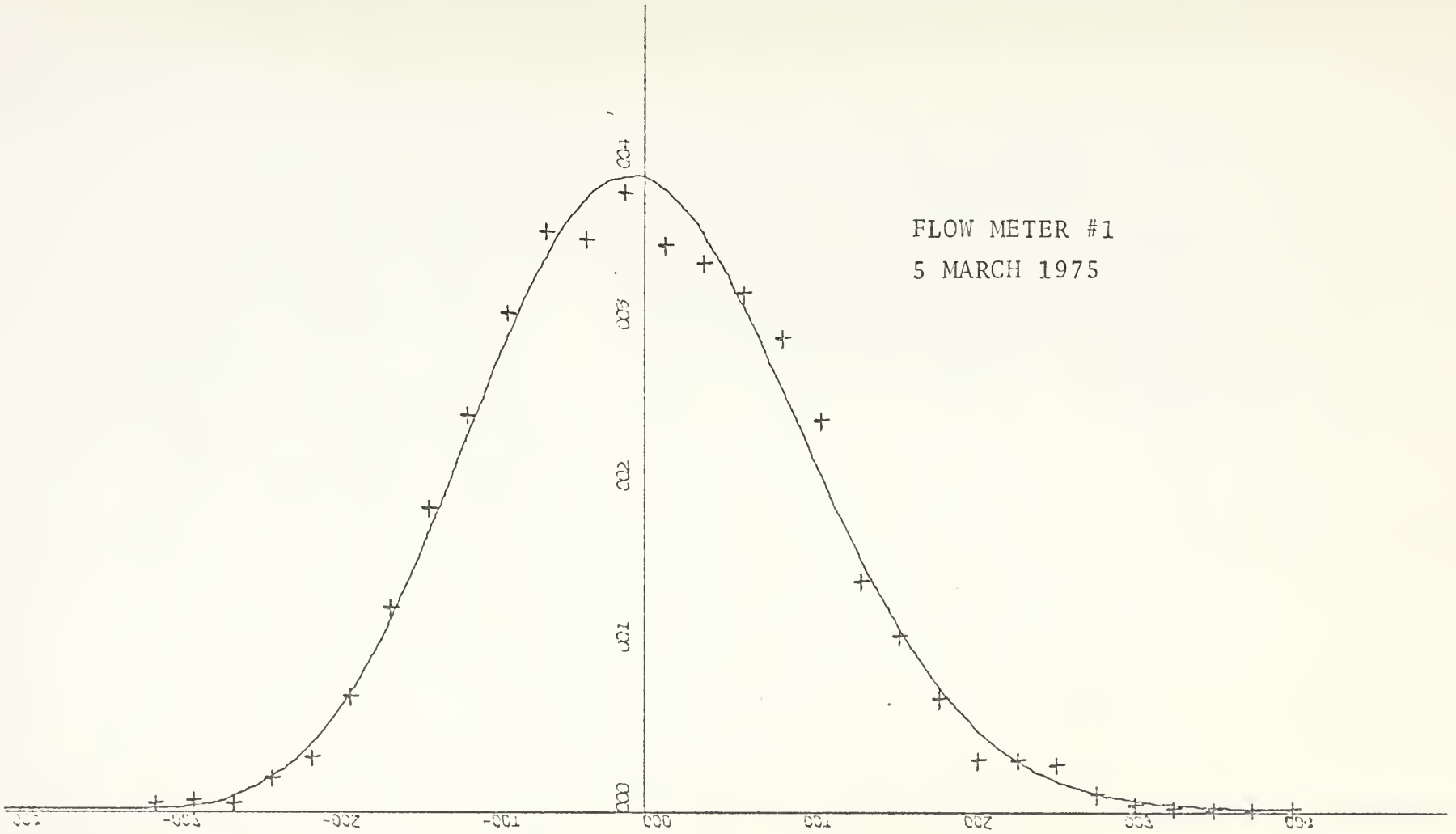
FLOW METER #1
5 MARCH 1975

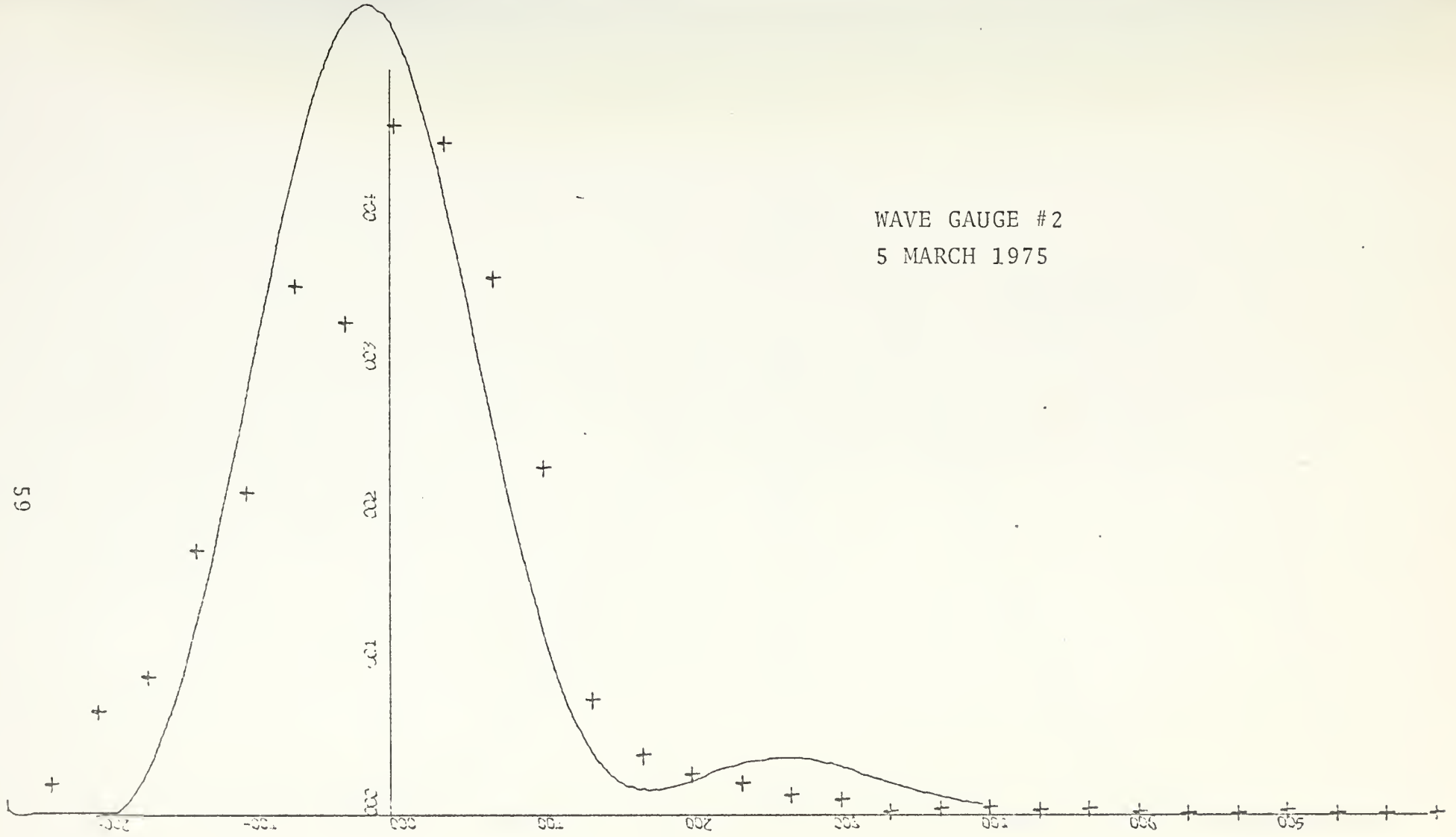
WAVE GAUGE #2
5 MARCH 1975
59

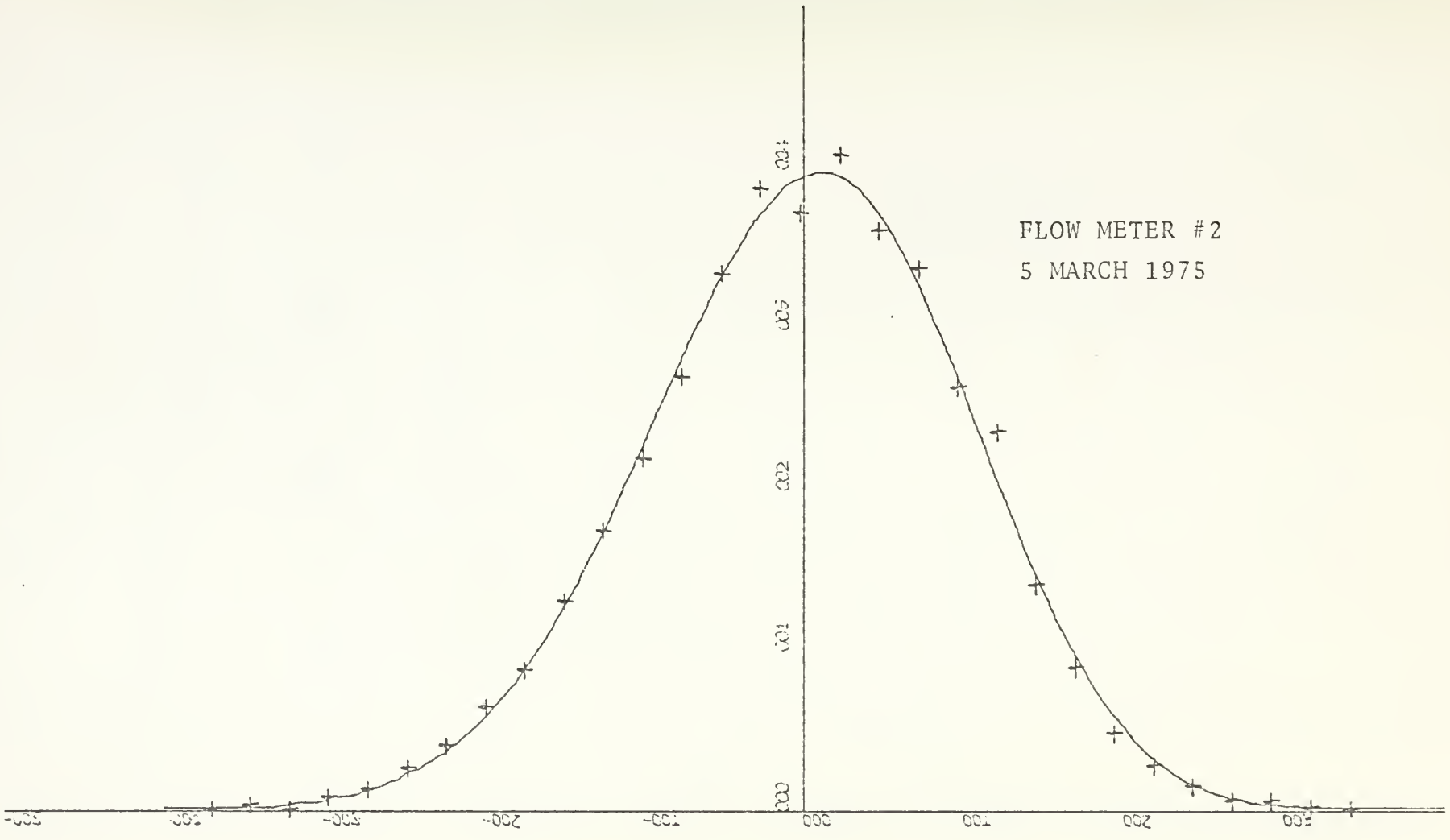
FLOW METER #2
5 MARCH 1975

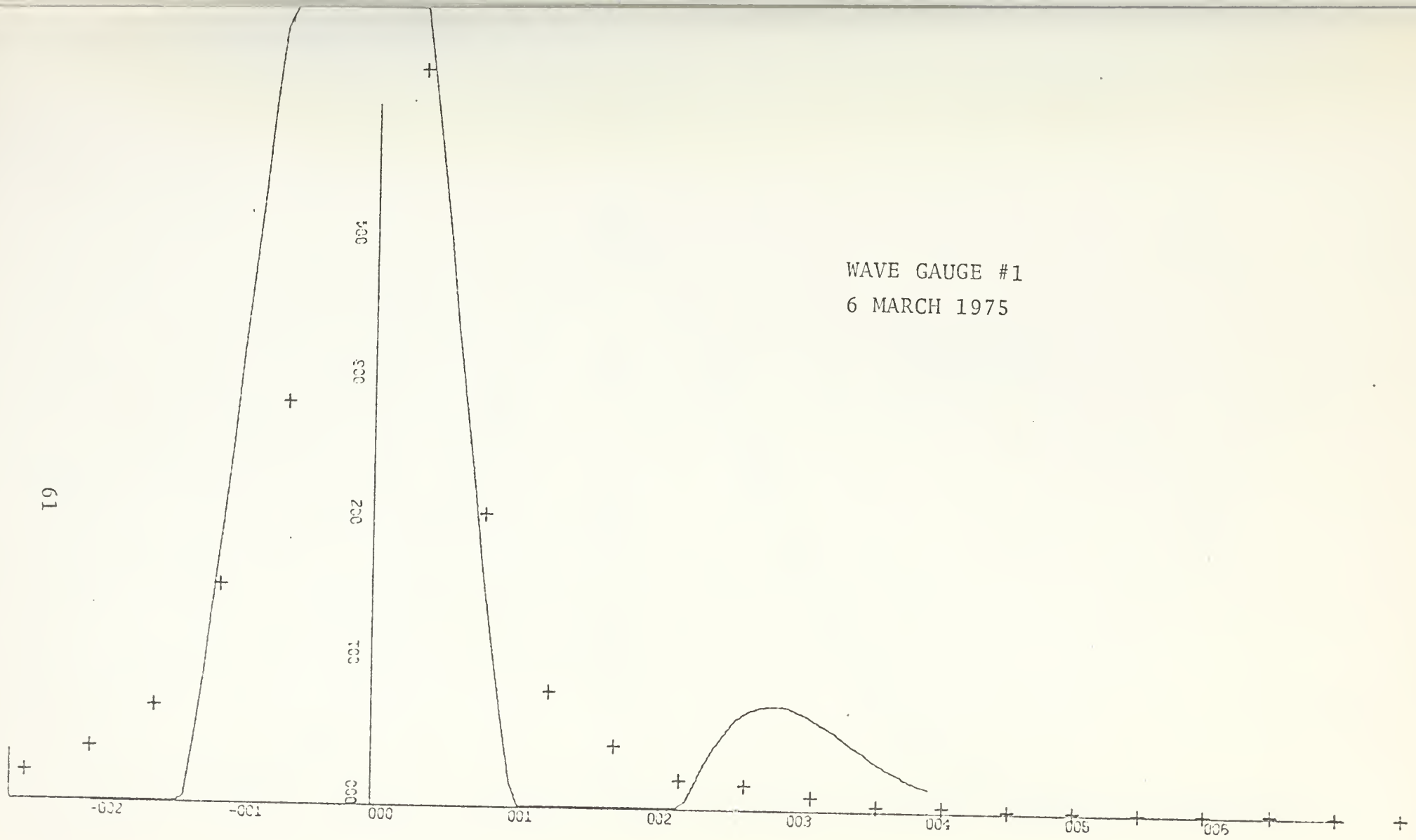
WAVE GAUGE #1
6 MARCH 1975
004
003
002
001
000
-002
-001
000
001
002
003
004
005
006

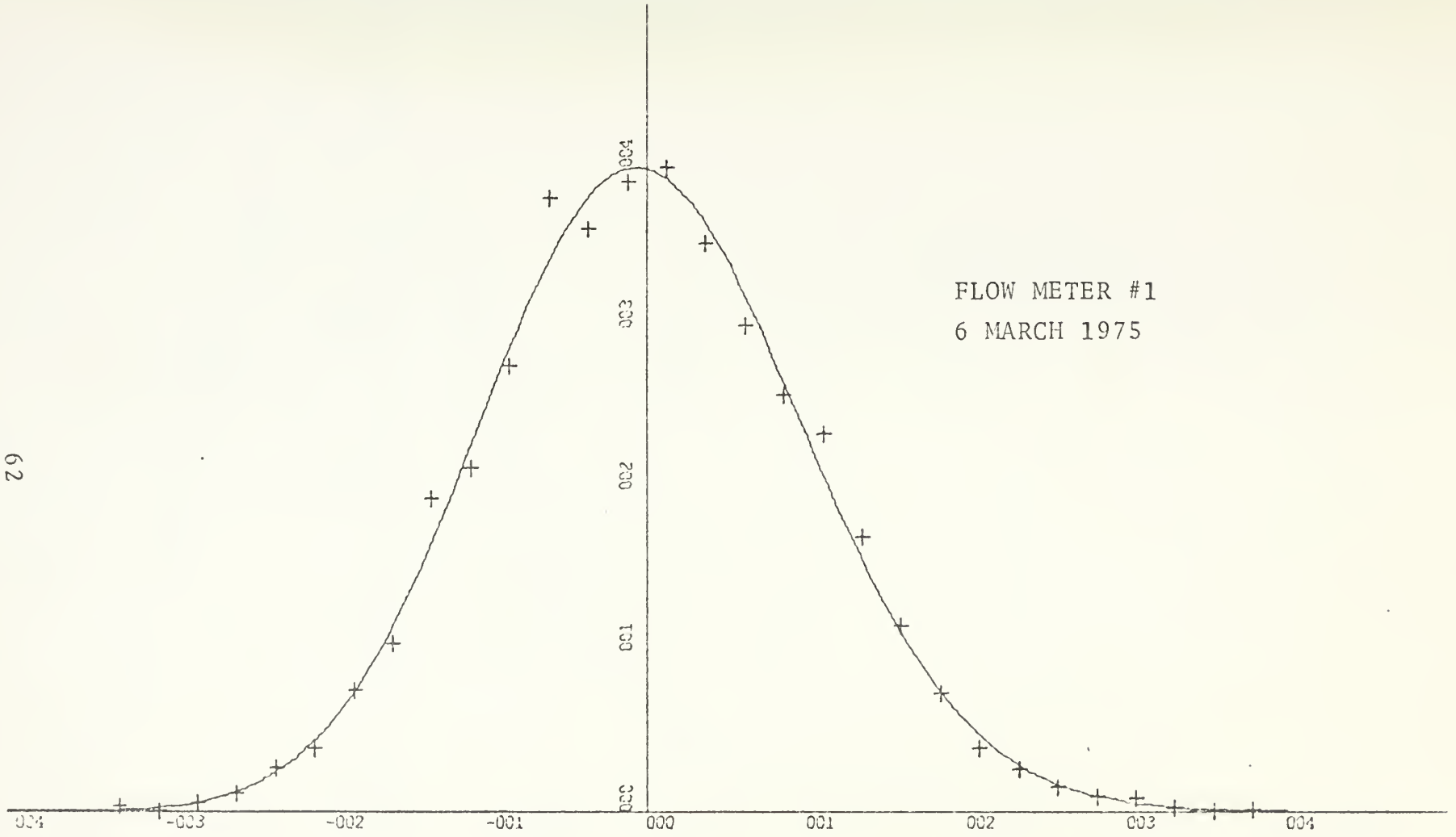
FLOW METER #1
6 MARCH 1975
004
003
002
001
000
-004
-003
-002
-001
000
001
002
003
004

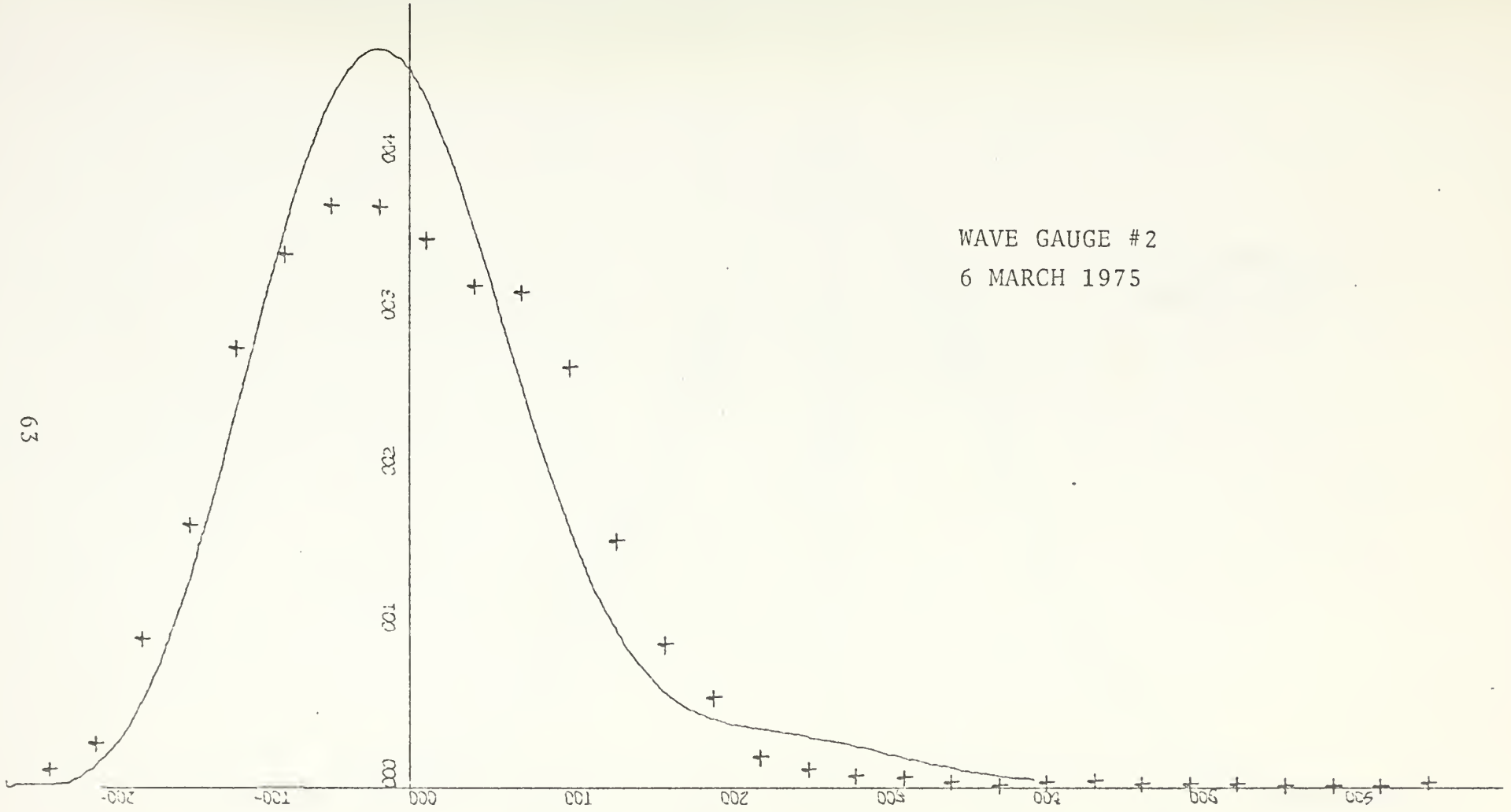
WAVE GAUGE #2
6 MARCH 1975
.004
.003
.002
.001
.000
-.002
-.001
.000
.001
.002
.003
.004
.005
.006
.007

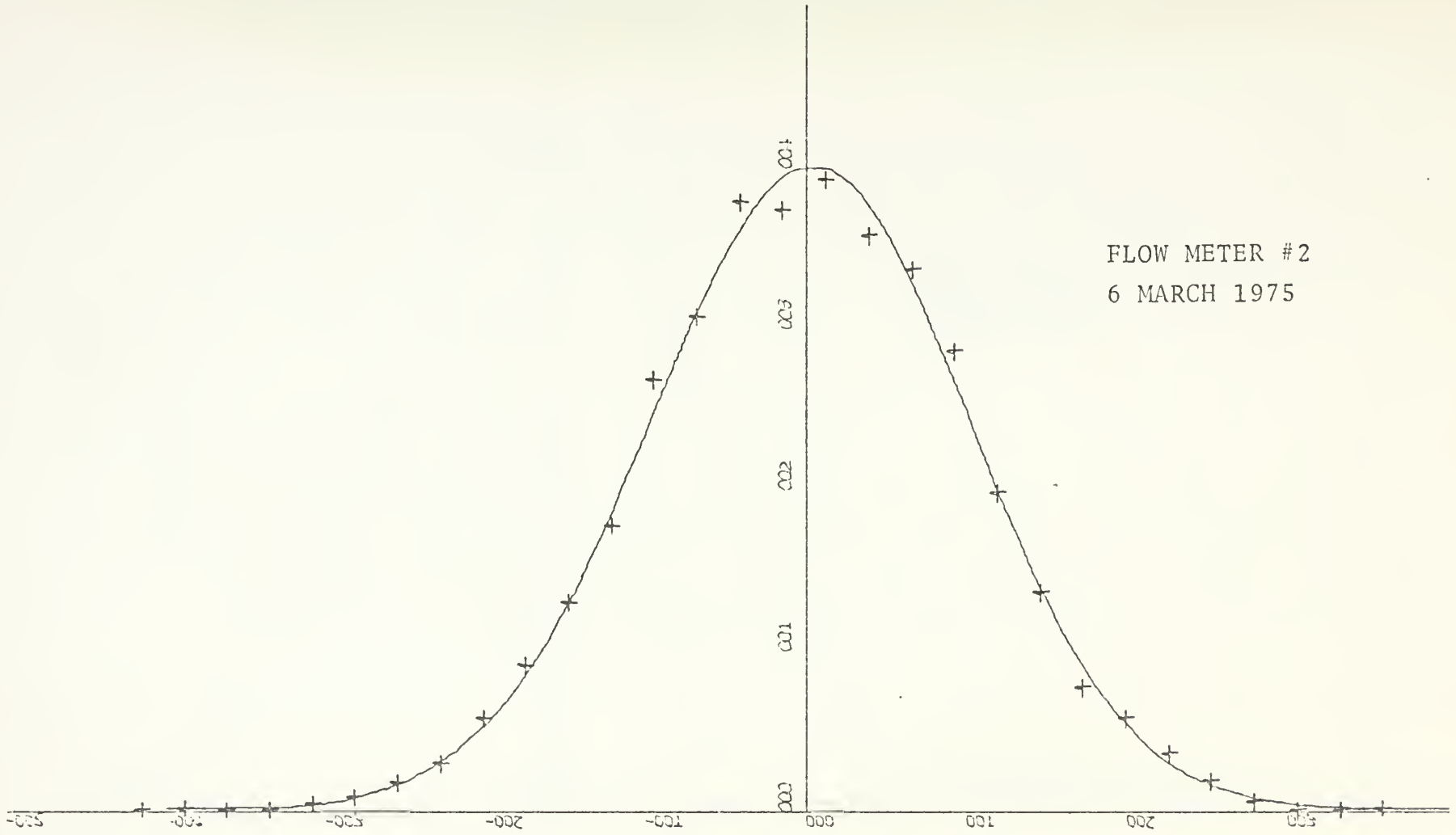
FLOW METER #2
6 MARCH 1975

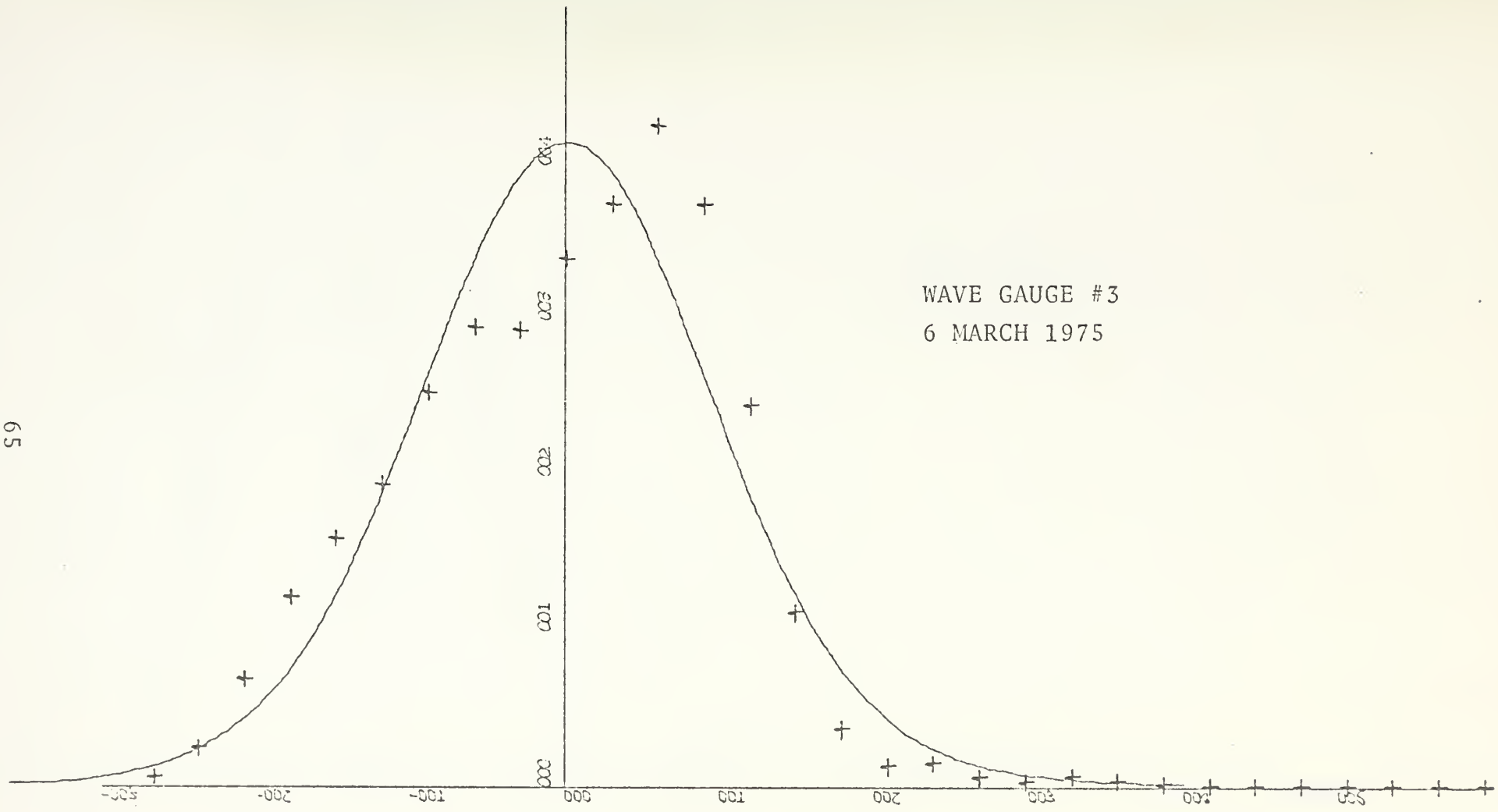
WAVE GAUGE #3
6 MARCH 1975

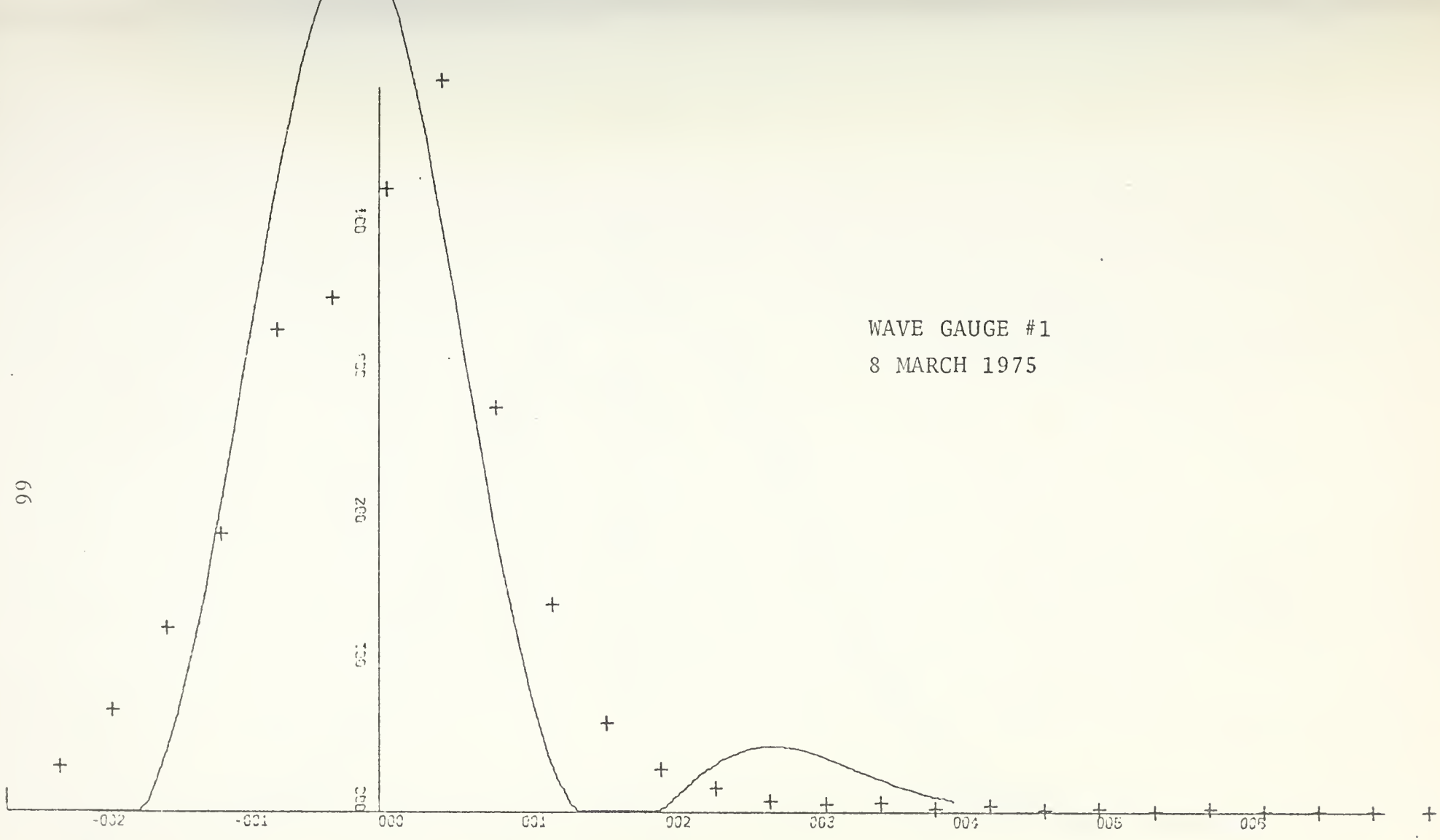
WAVE GAUGE #1
8 MARCH 1975
99
-002
-001
000
001
002
003
004
005
006

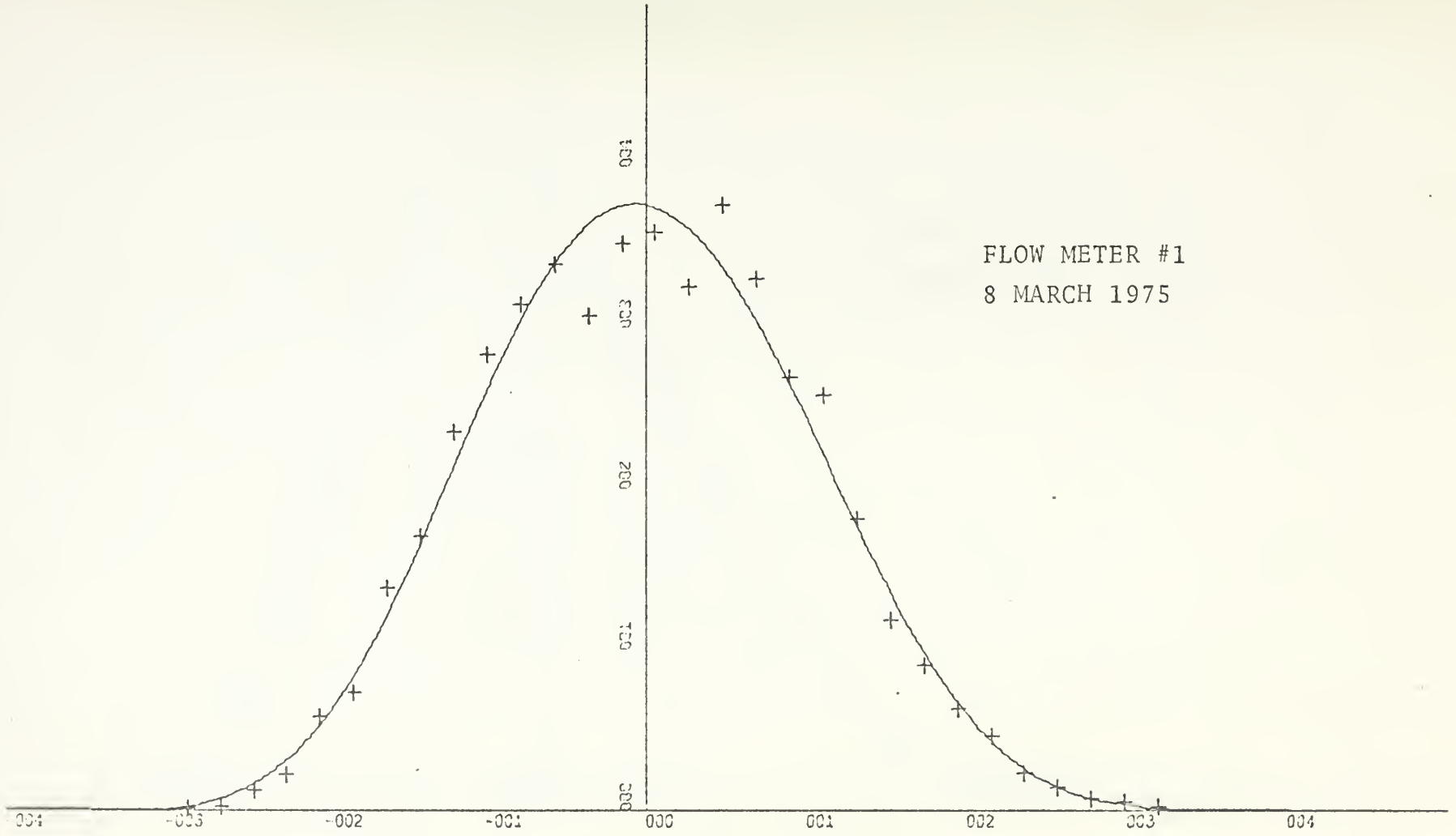
FLOW METER #1
8 MARCH 1975
004
003
002
001
000
-004
-003
-002
-001
000
001
002
003
004

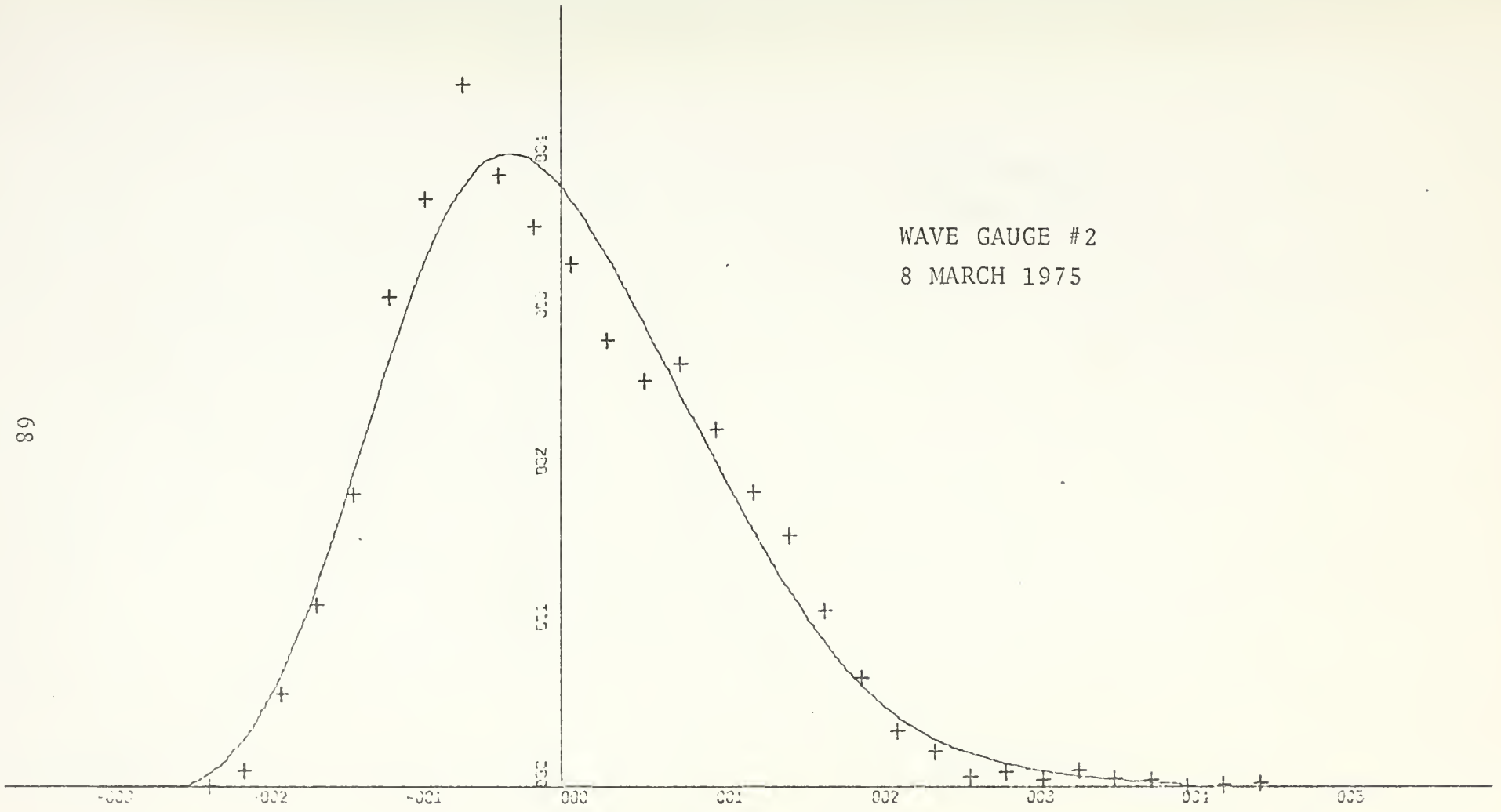
WAVE GAUGE #2
8 MARCH 1975

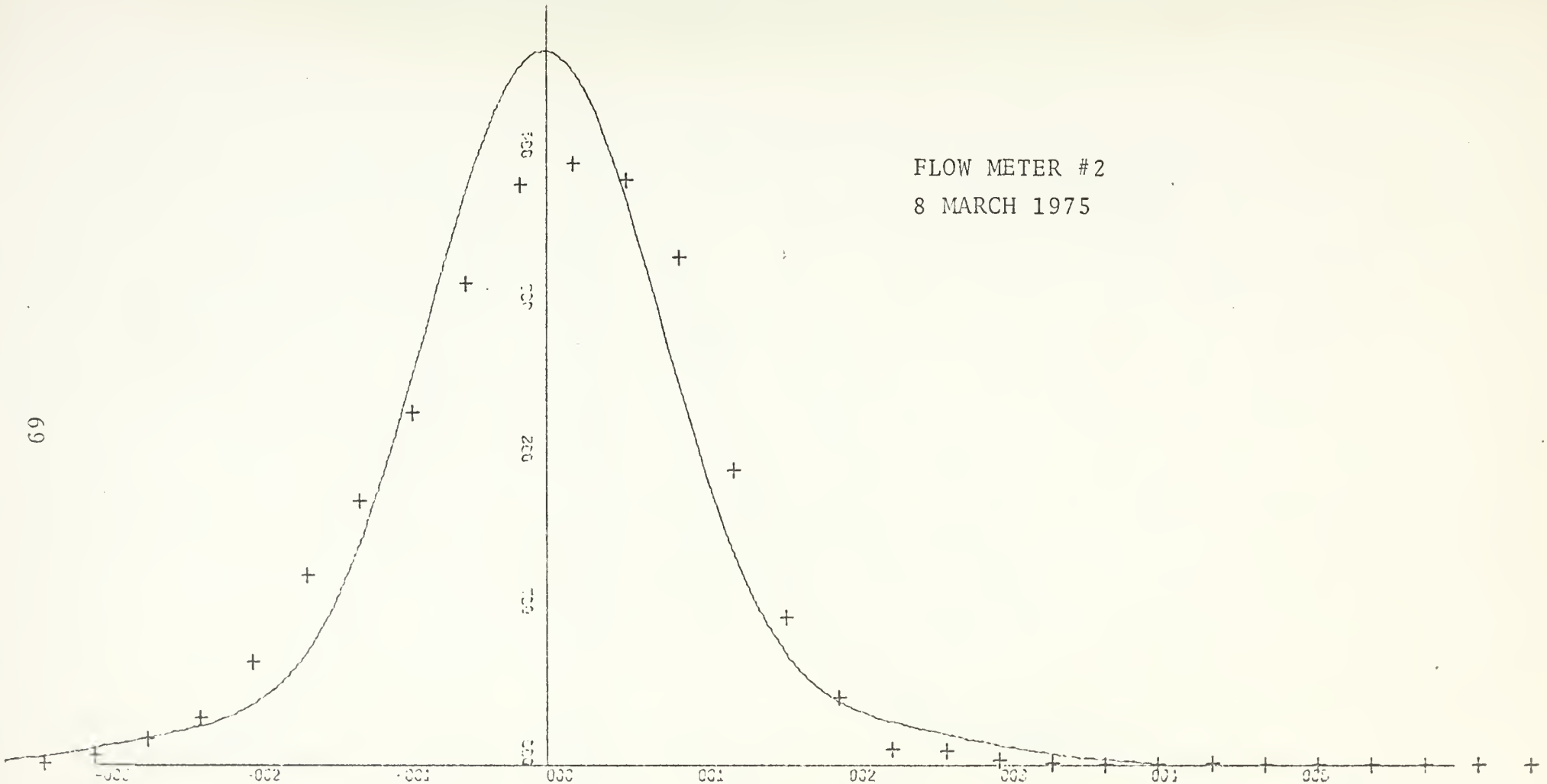
FLOW METER #2
8 MARCH 1975

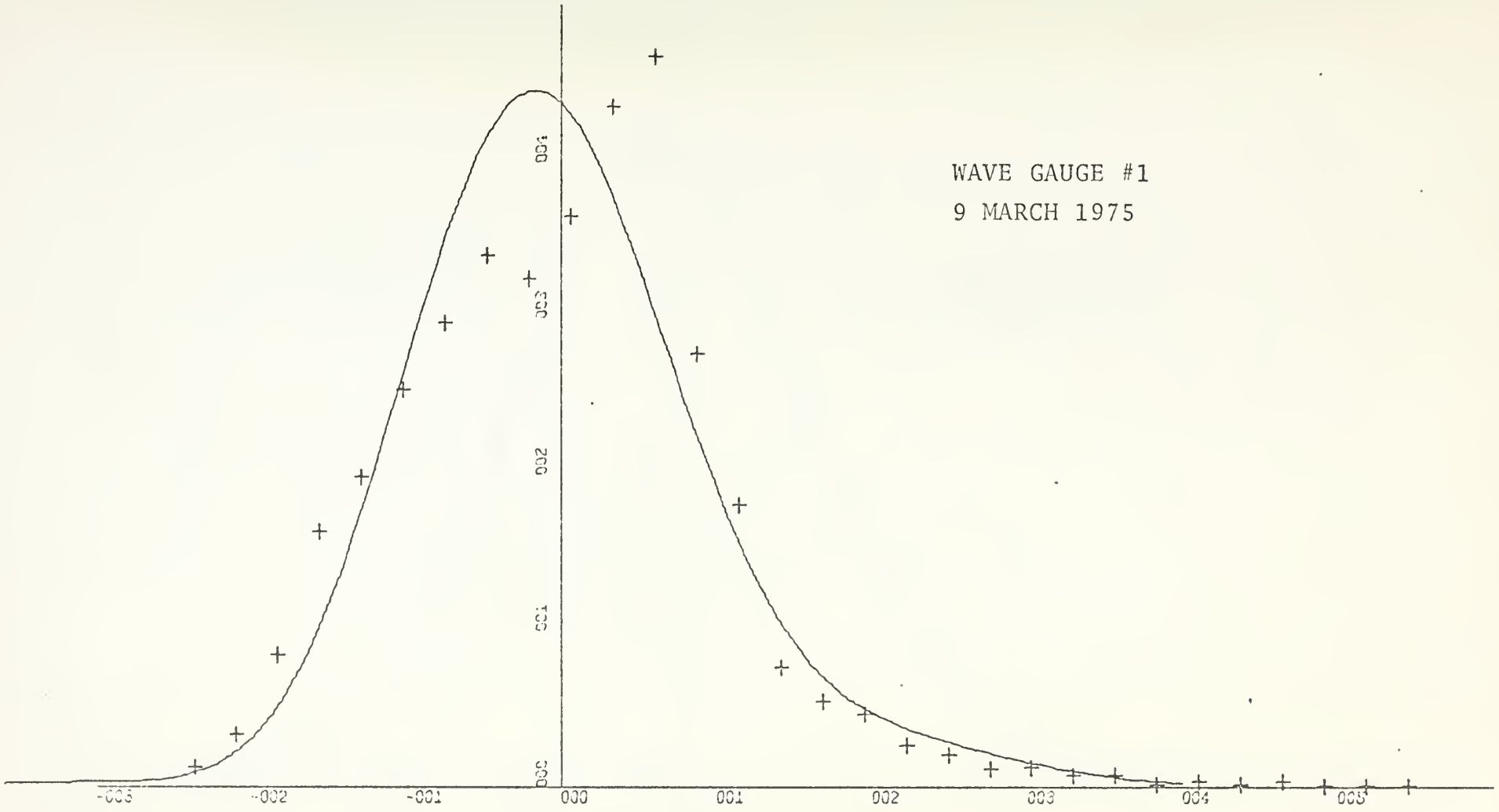
WAVE GAUGE #1
9 MARCH 1975
-003
-002
-001
000
001
002
003
004
005

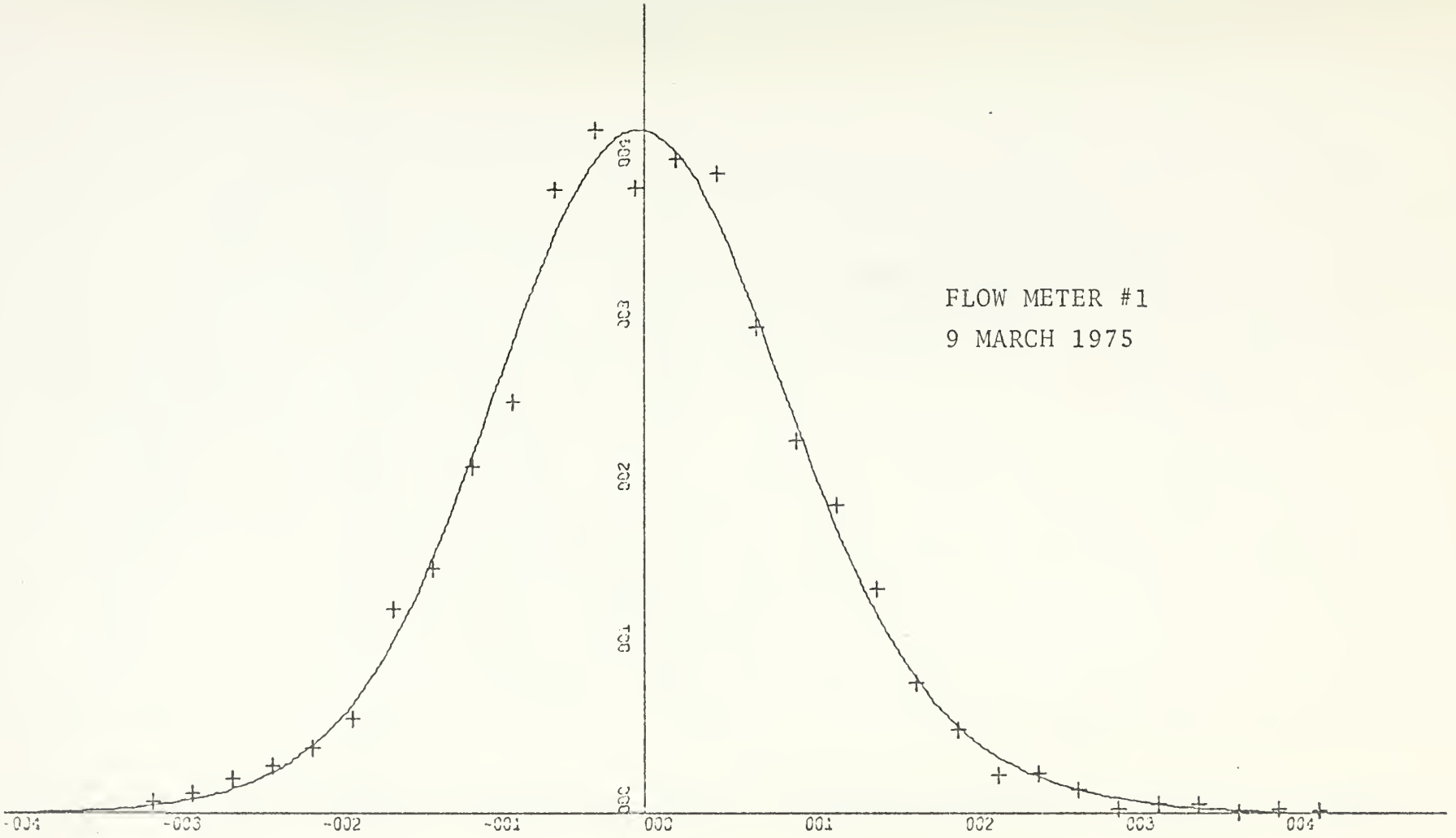
FLOW METER #1
9 MARCH 1975
-004
-003
-002
-001
000
001
002
003
004

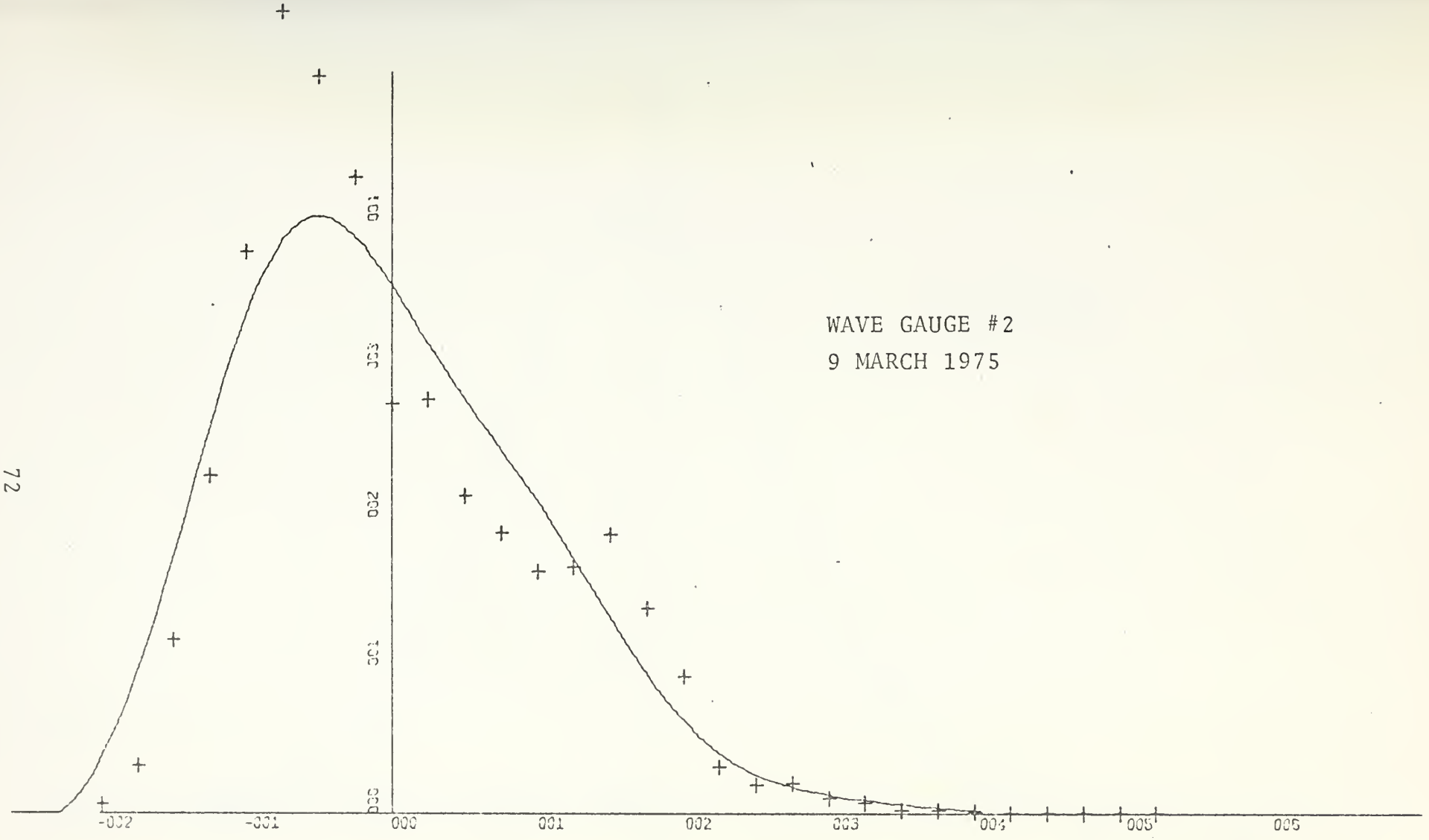
WAVE GAUGE #2
9 MARCH 1975
-002
-001
000
001
002
003
004
005
006

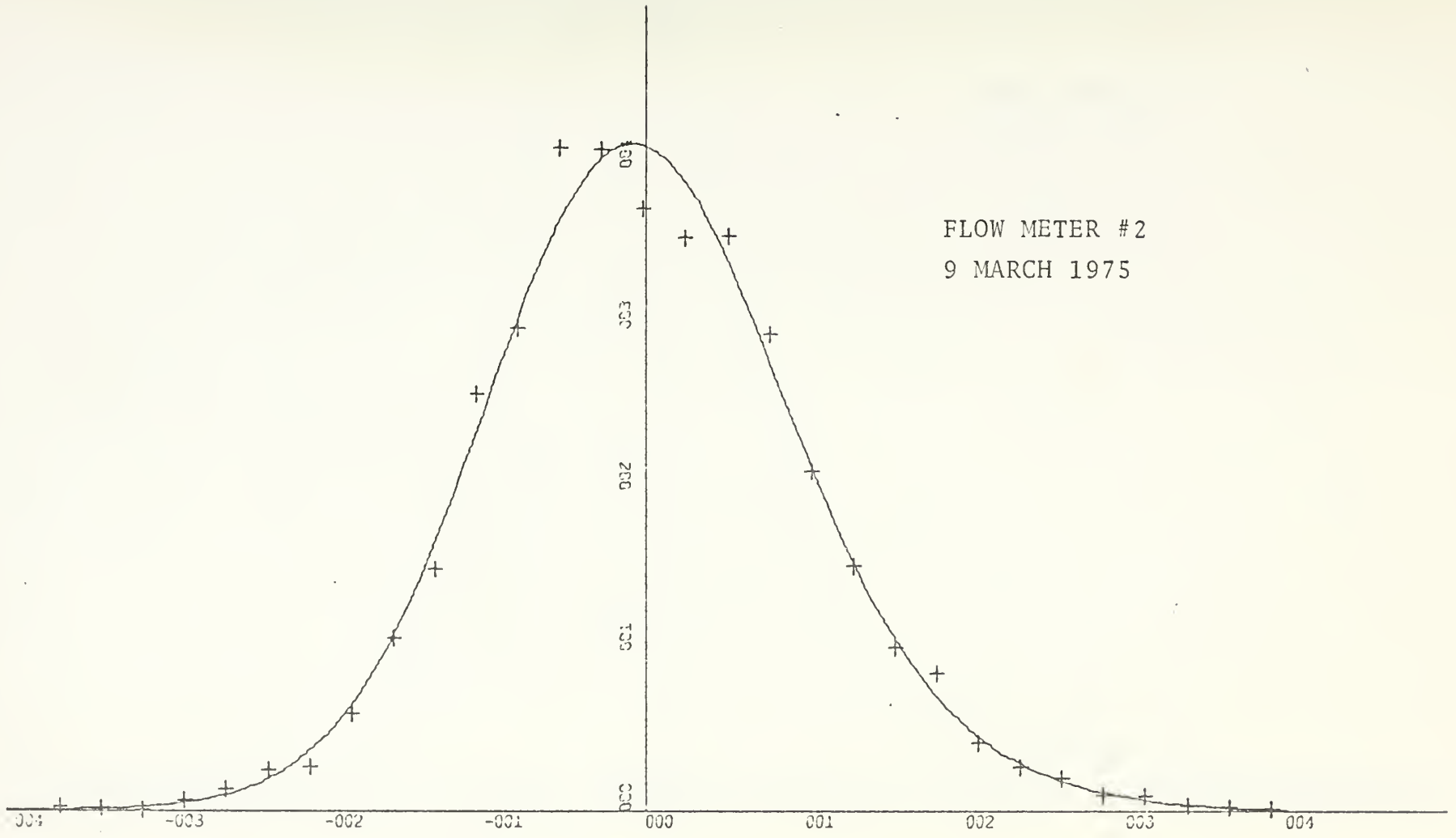
FLOW METER #2
9 MARCH 1975
-003
-002
-001
000
001
002
003
004

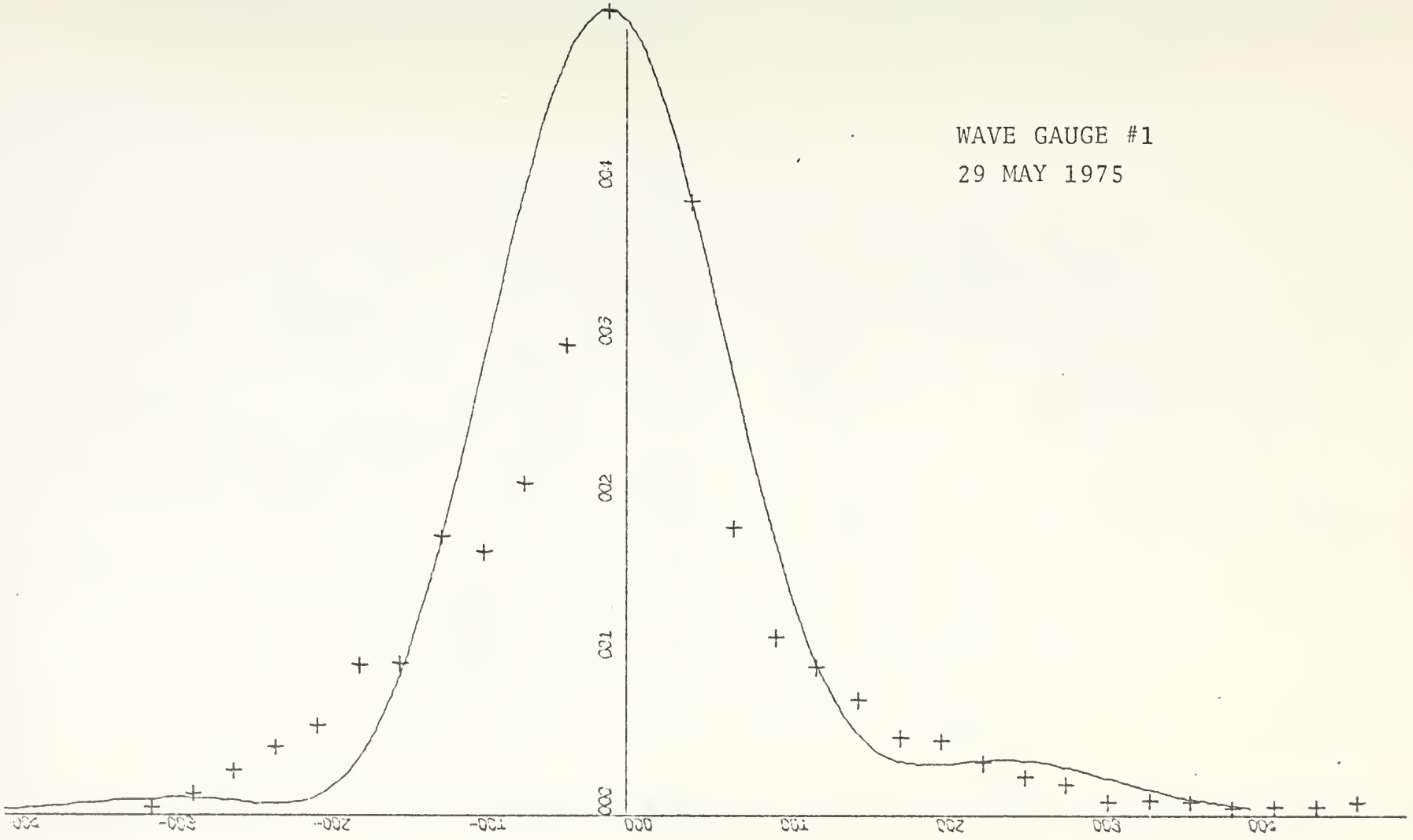
WAVE GAUGE #1
29 MAY 1975

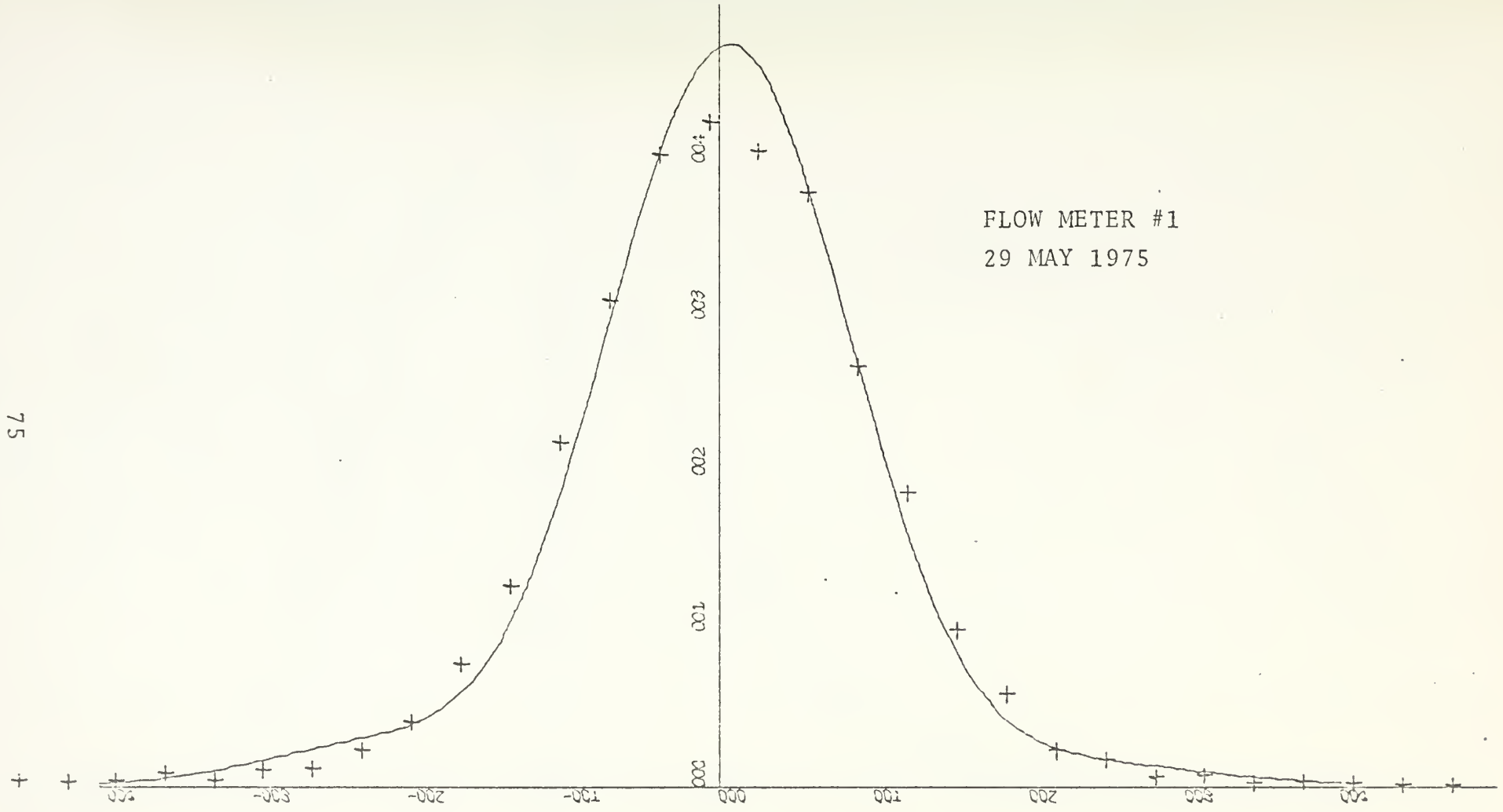
FLOW METER #1
29 MAY 1975

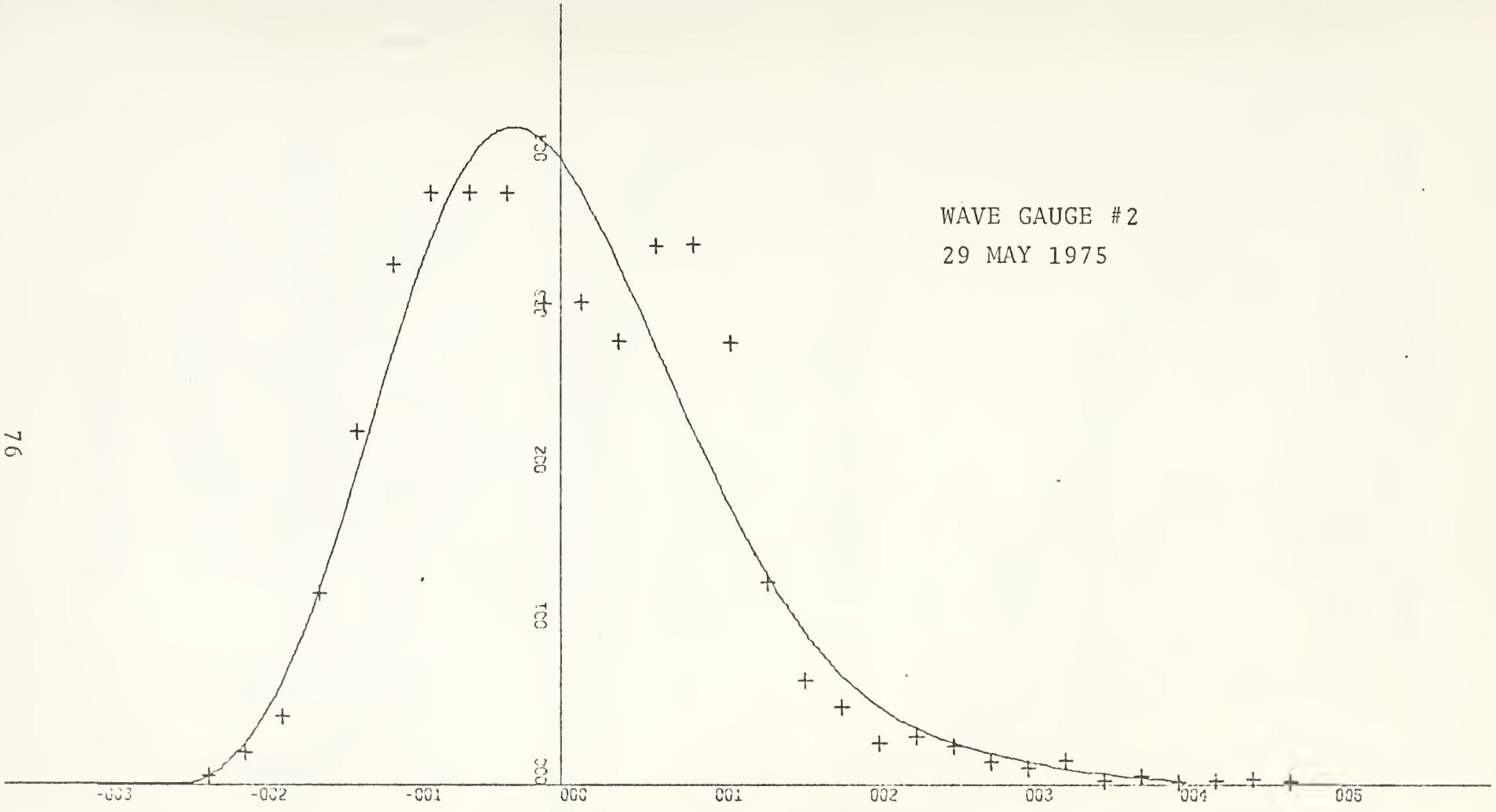
WAVE GAUGE #2
29 MAY 1975
-003
-002
-001
000
001
002
003
004
005

APPENDIX G

POWER, COHERENCE AND PHASE SPECTRA

FLOW METER #2 - WAVE GAUGE #2

4 MARCH 1975

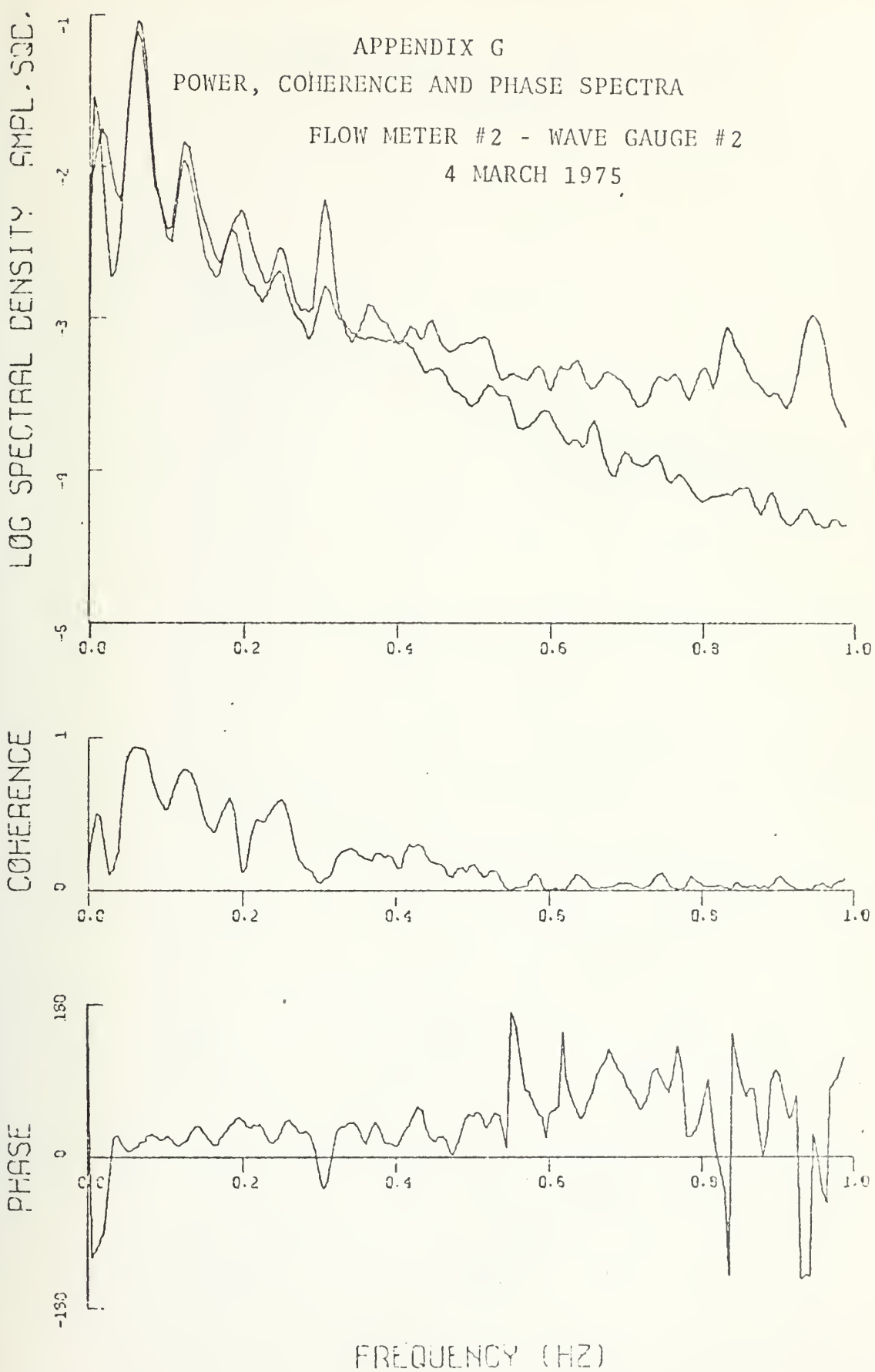

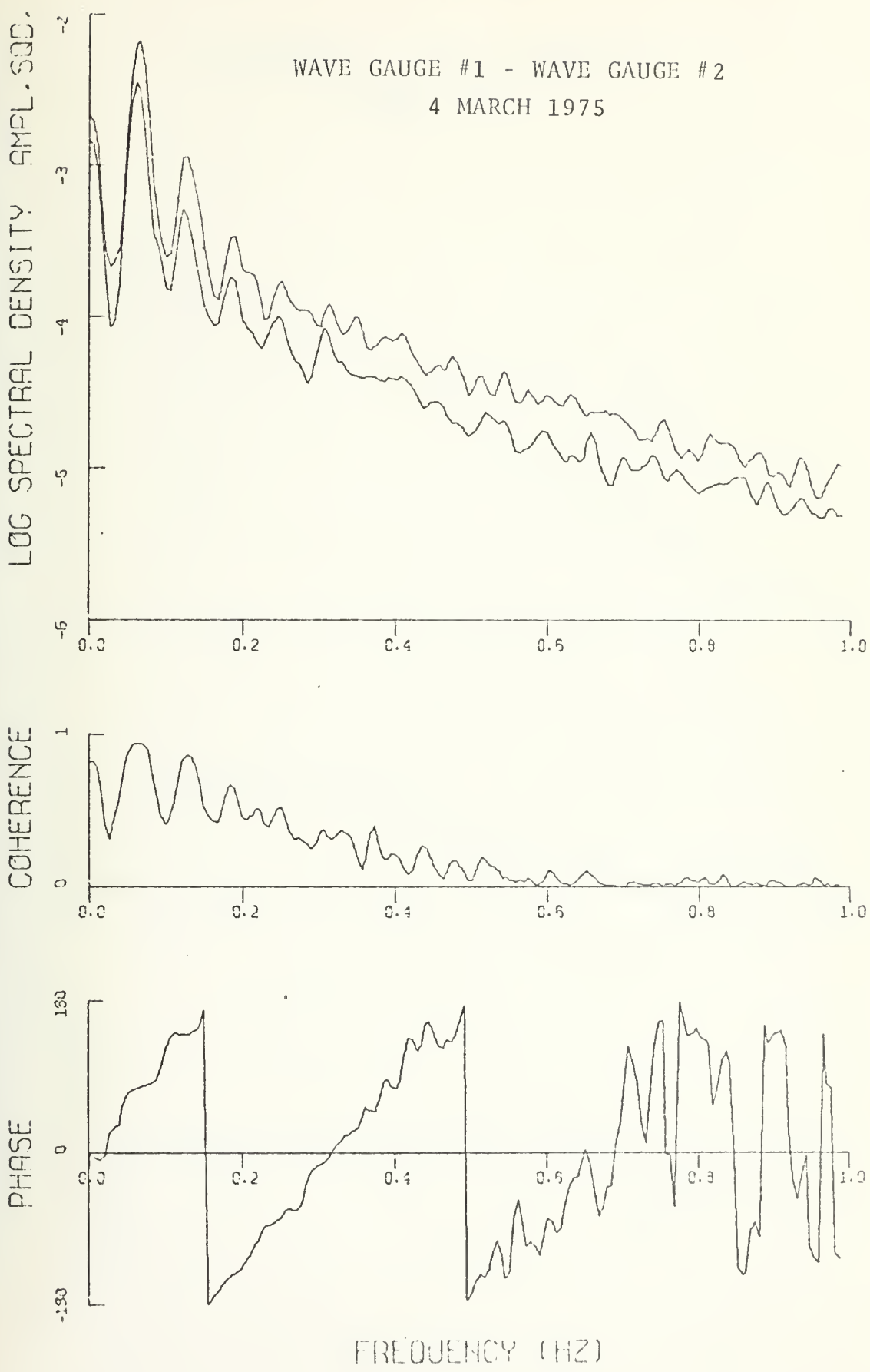
WAVE GAUGE #1 - WAVE GAUGE #2
4 MARCH 1975
LOG SPECTRAL DENSITY AMPL. SQD.
-2
-3
-4
-5
-6
0.0
0.2
0.4
0.6
0.8
1.0
COHERENCE
1
0
PHASE
180
0
-180
FREQUENCY (HZ)

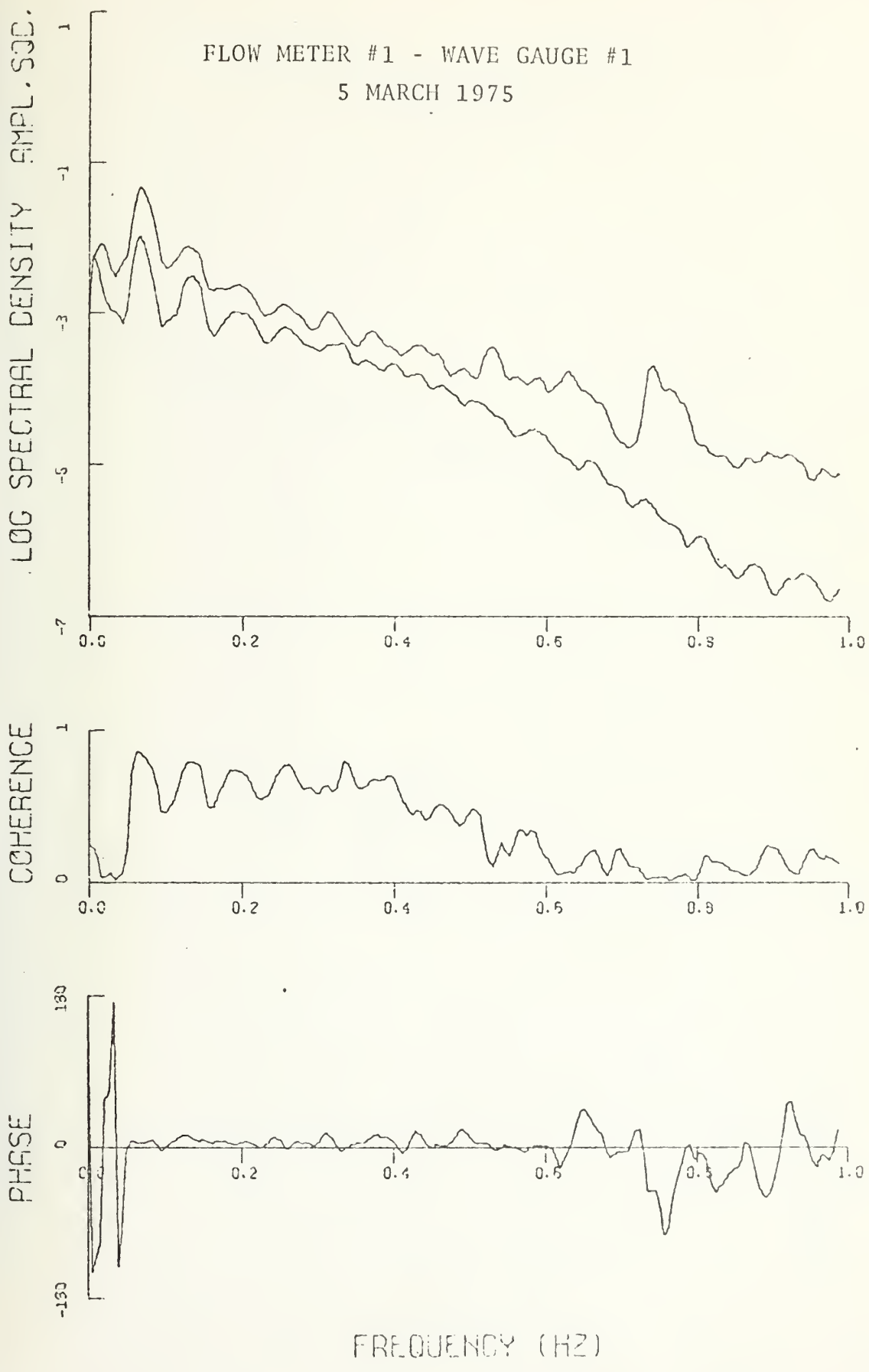
FLOW METER #1 - WAVE GAUGE #1
5 MARCH 1975
LOG SPECTRAL DENSITY AMPL.SQD.
1
-1
-3
-5
-7
0.0
0.2
0.4
0.6
0.8
1.0
COHERENCE
1
0
0.0
0.2
0.4
0.6
0.8
1.0
PHASE
180
0
-180
0.0
0.2
0.4
0.6
0.8
1.0
FREQUENCY (HZ)

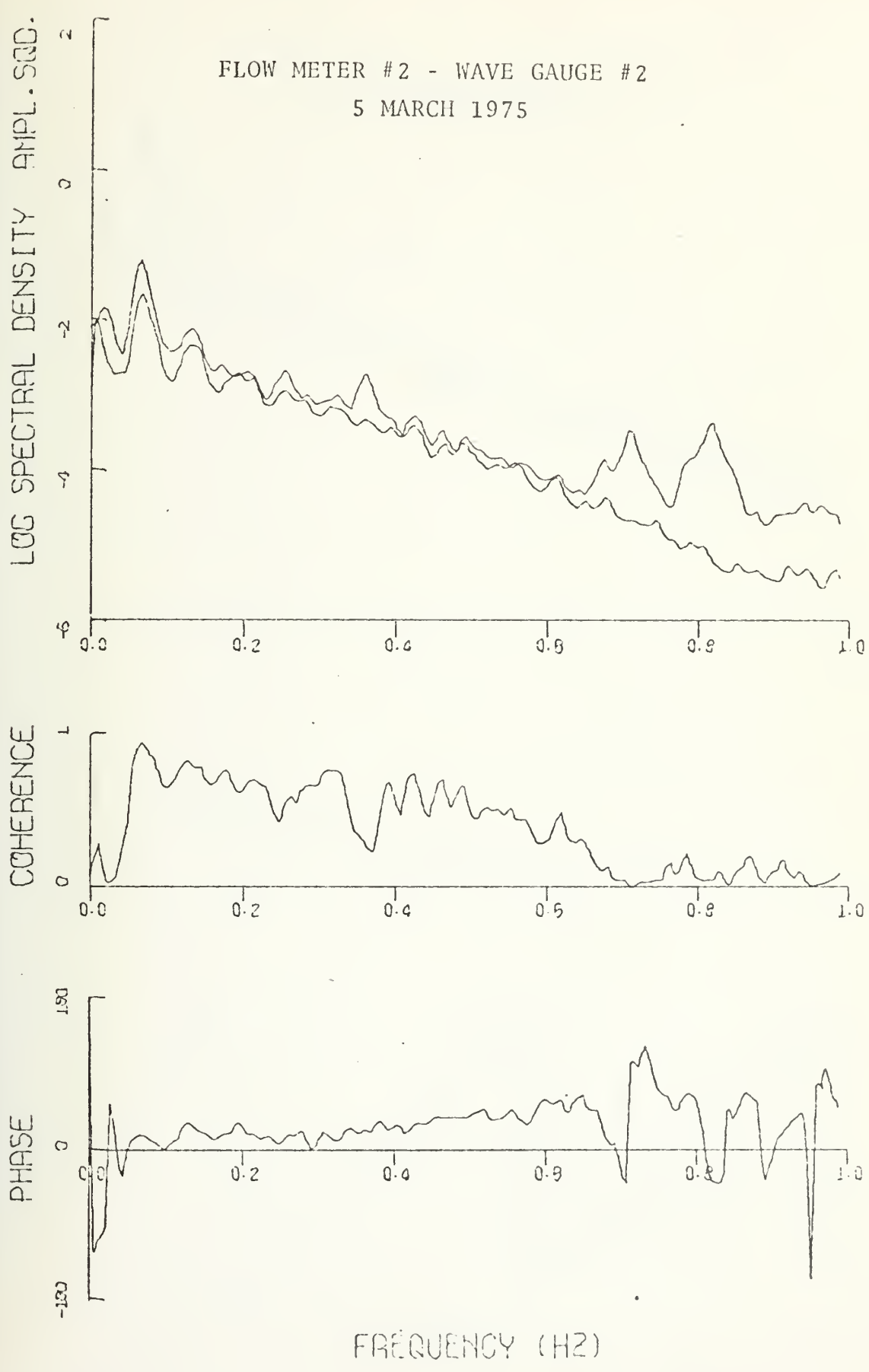
FLOW METER #2 - WAVE GAUGE #2
5 MARCH 1975
LOG SPECTRAL DENSITY AMPL. SQD.
2
0
-2
-4
-6
0.0
0.2
0.4
0.6
0.8
1.0
COHERENCE
1
0
0.0
0.2
0.4
0.6
0.8
1.0
PHASE
180
0
-180
0.0
0.2
0.4
0.6
0.8
1.0
FREQUENCY (HZ)

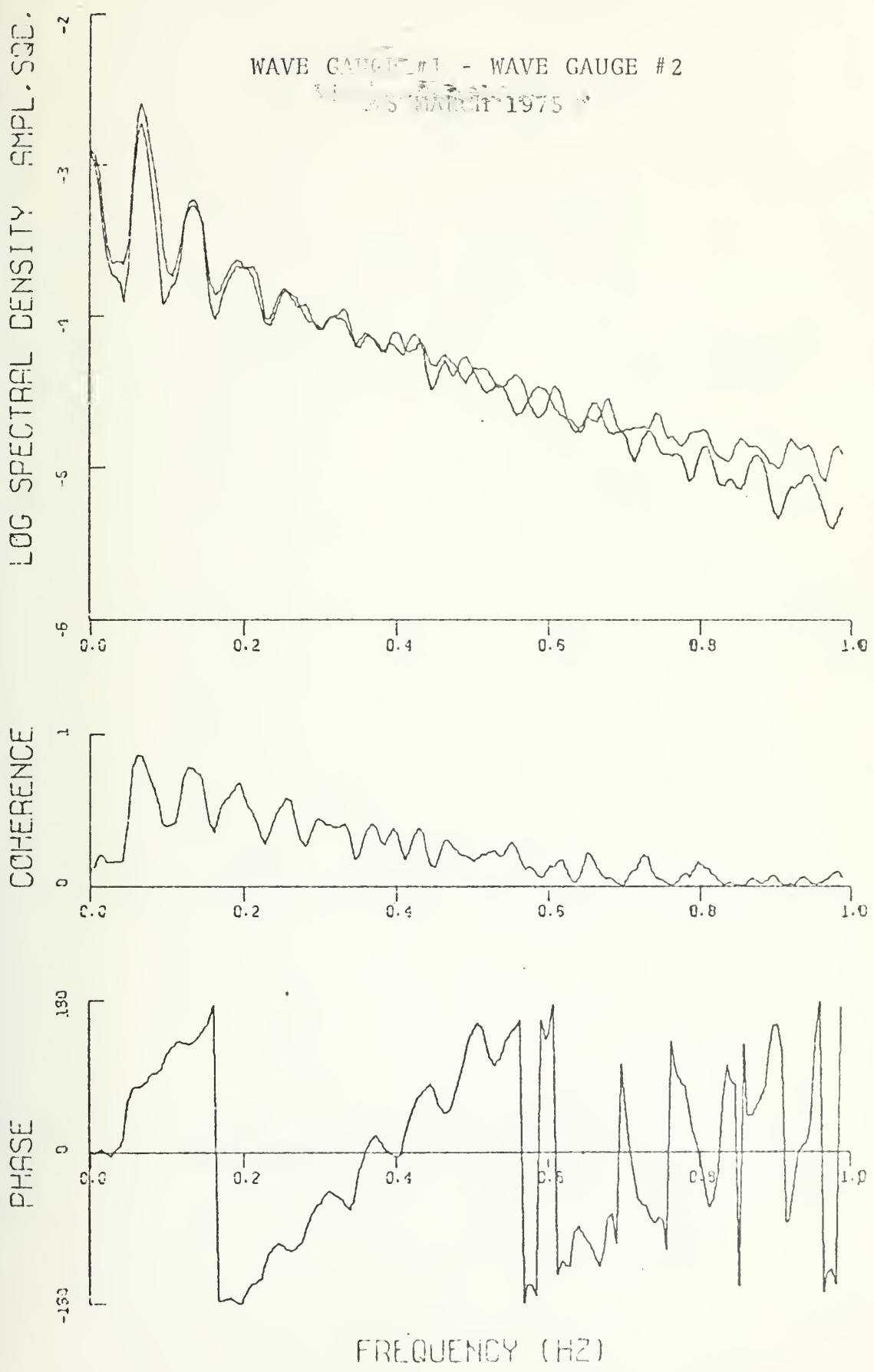
WAVE GAUGE #1 - WAVE GAUGE #2
LOG SPECTRAL DENSITY AMPL.SQD.
-2
-3
-4
-5
-6
0.0
0.2
0.4
0.6
0.8
1.0
COHERENCE
1
0
PHASE
180
0
-180
FREQUENCY (HZ)

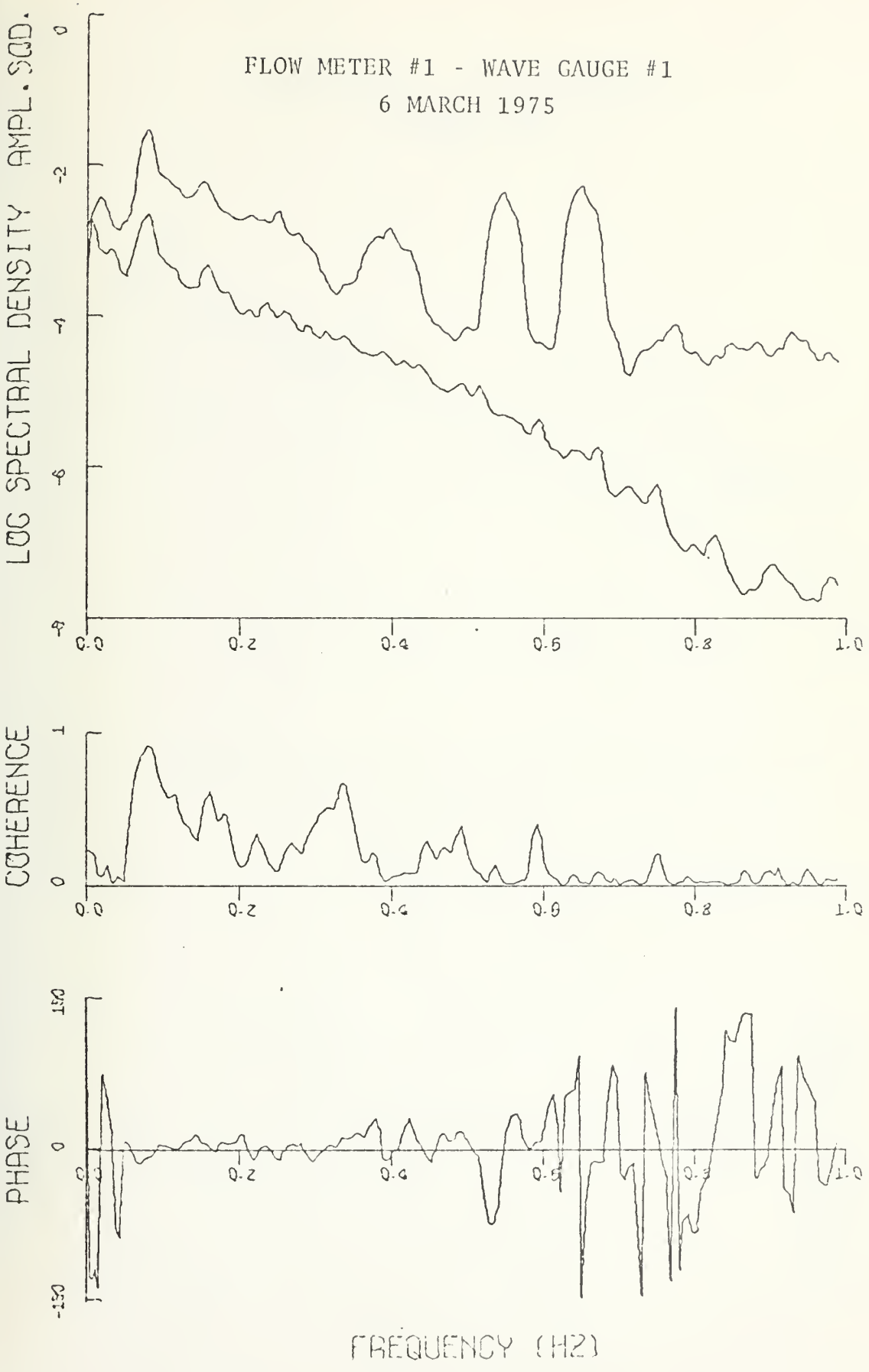
FLOW METER #1 - WAVE GAUGE #1
6 MARCH 1975
LOG SPECTRAL DENSITY AMPL.SQD.
0
-2
-4
-6
-8
0.0
0.2
0.4
0.6
0.8
1.0
COHERENCE
1
0
PHASE
150
0
-150
FREQUENCY (HZ)

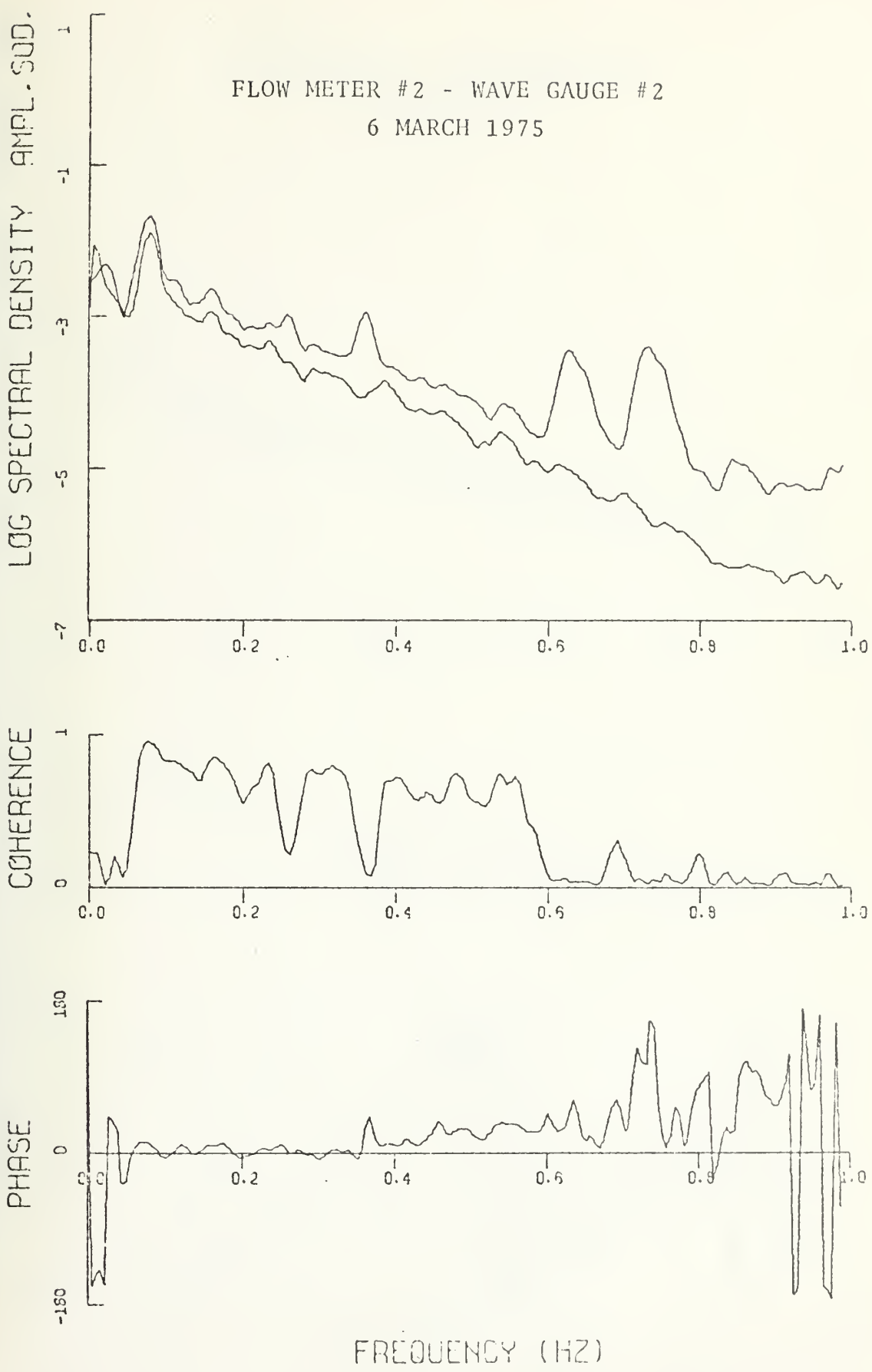
FLOW METER #2 - WAVE GAUGE #2
6 MARCH 1975
LOG SPECTRAL DENSITY AMPL.-SQD.
1
-1
-3
-5
-7
0.0
0.2
0.4
0.6
0.8
1.0
COHERENCE
1
0
0.0
0.2
0.4
0.6
0.8
1.0
PHASE
180
0
-180
0.0
0.2
0.4
0.6
0.8
1.0
FREQUENCY (HZ)

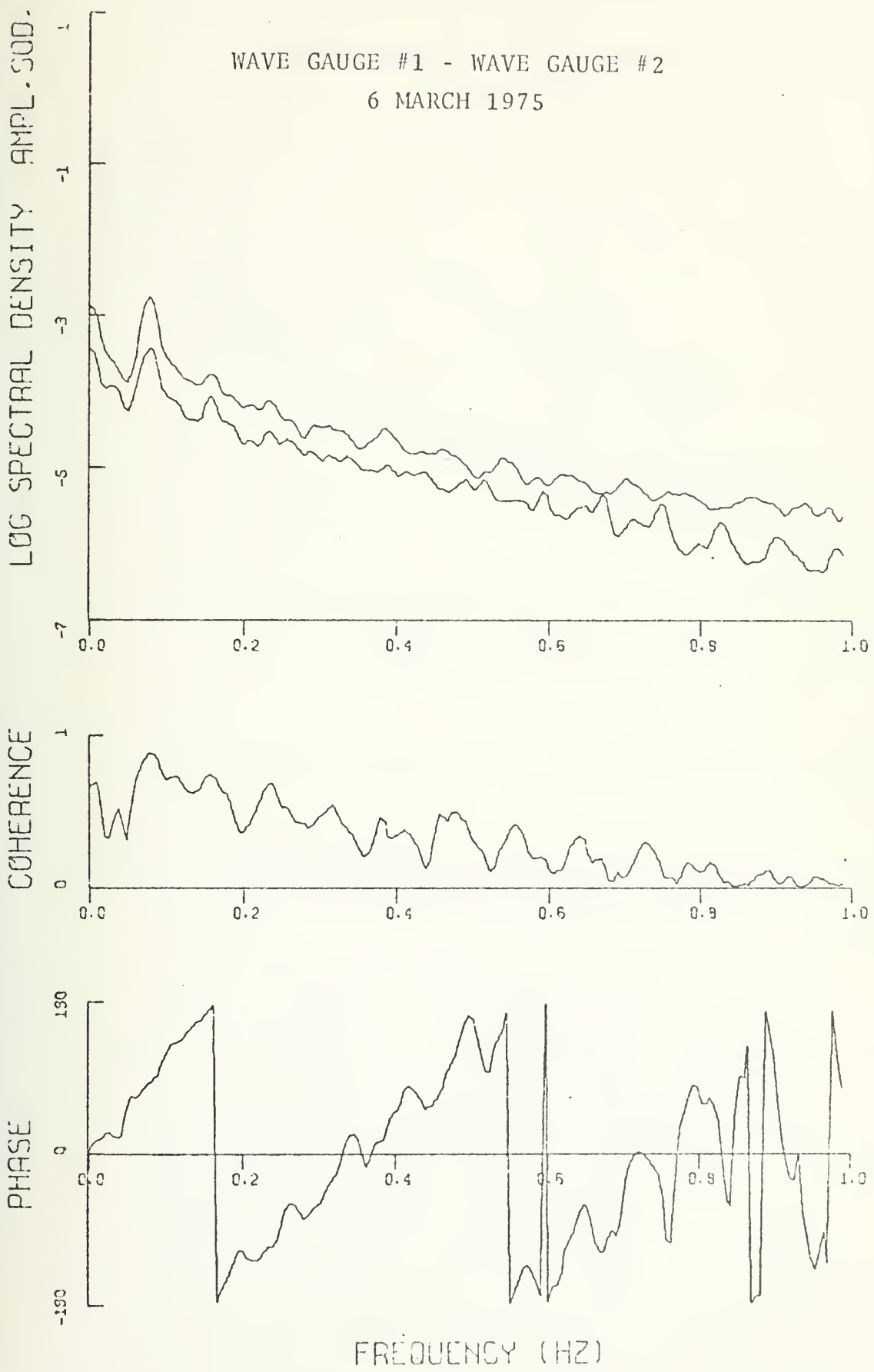
WAVE GAUGE #1 - WAVE GAUGE #2
6 MARCH 1975
LOG SPECTRAL DENSITY AMPL. SQD.
1
-1
-3
-5
-7
0.0
0.2
0.4
0.6
0.8
1.0
COHERENCE
1
0
0.0
0.2
0.4
0.6
0.8
1.0
PHASE
180
0
-180
0.0
0.2
0.4
0.6
0.8
1.0
FREQUENCY (HZ)

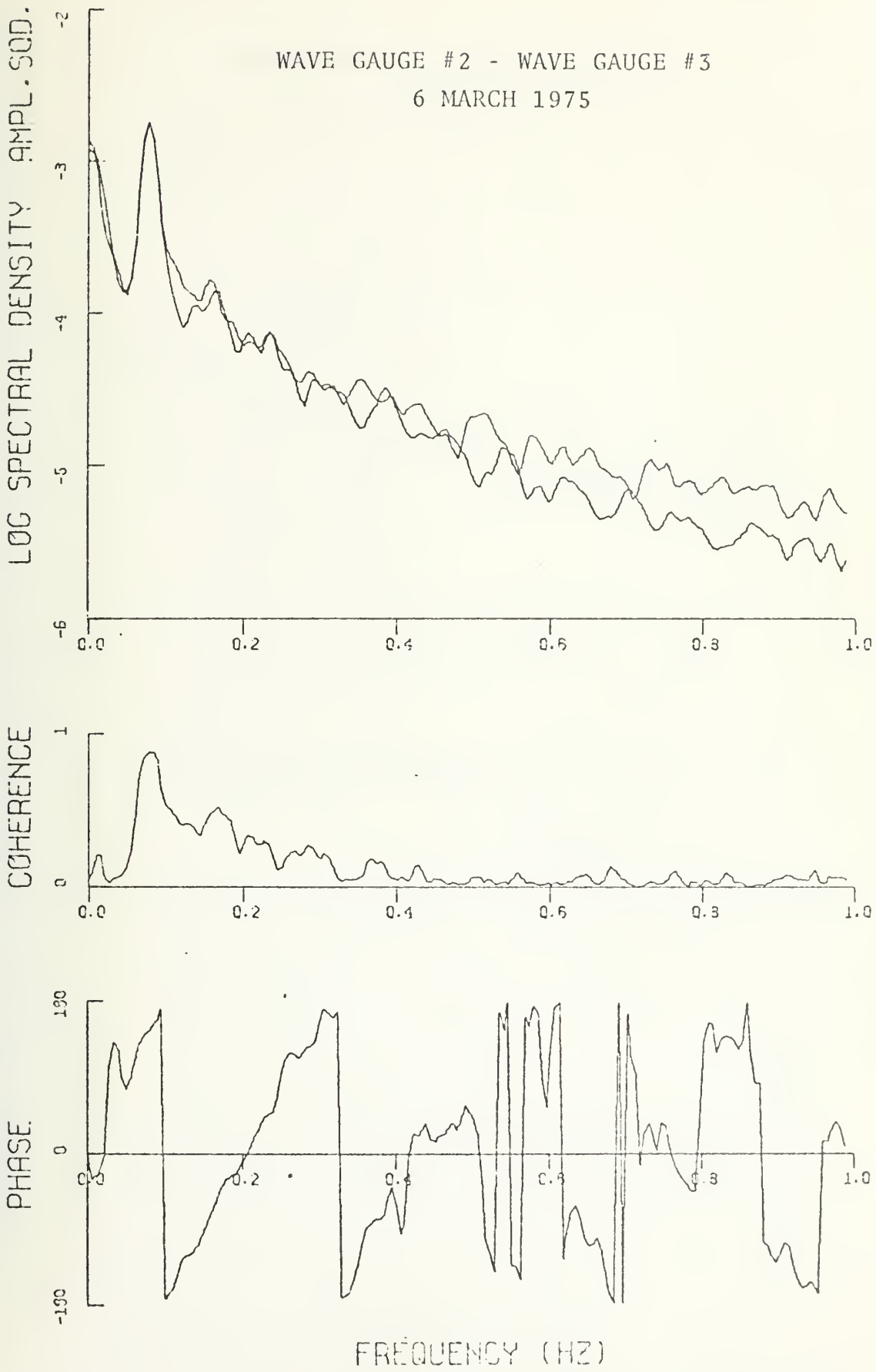
WAVE GAUGE #2 - WAVE GAUGE #3
6 MARCH 1975
LOG SPECTRAL DENSITY AMPL. SQD.
-2
-3
-4
-5
-6
0.0
0.2
0.4
0.6
0.8
1.0
COHERENCE
1
0
PHASE
180
0
-180
FREQUENCY (HZ)

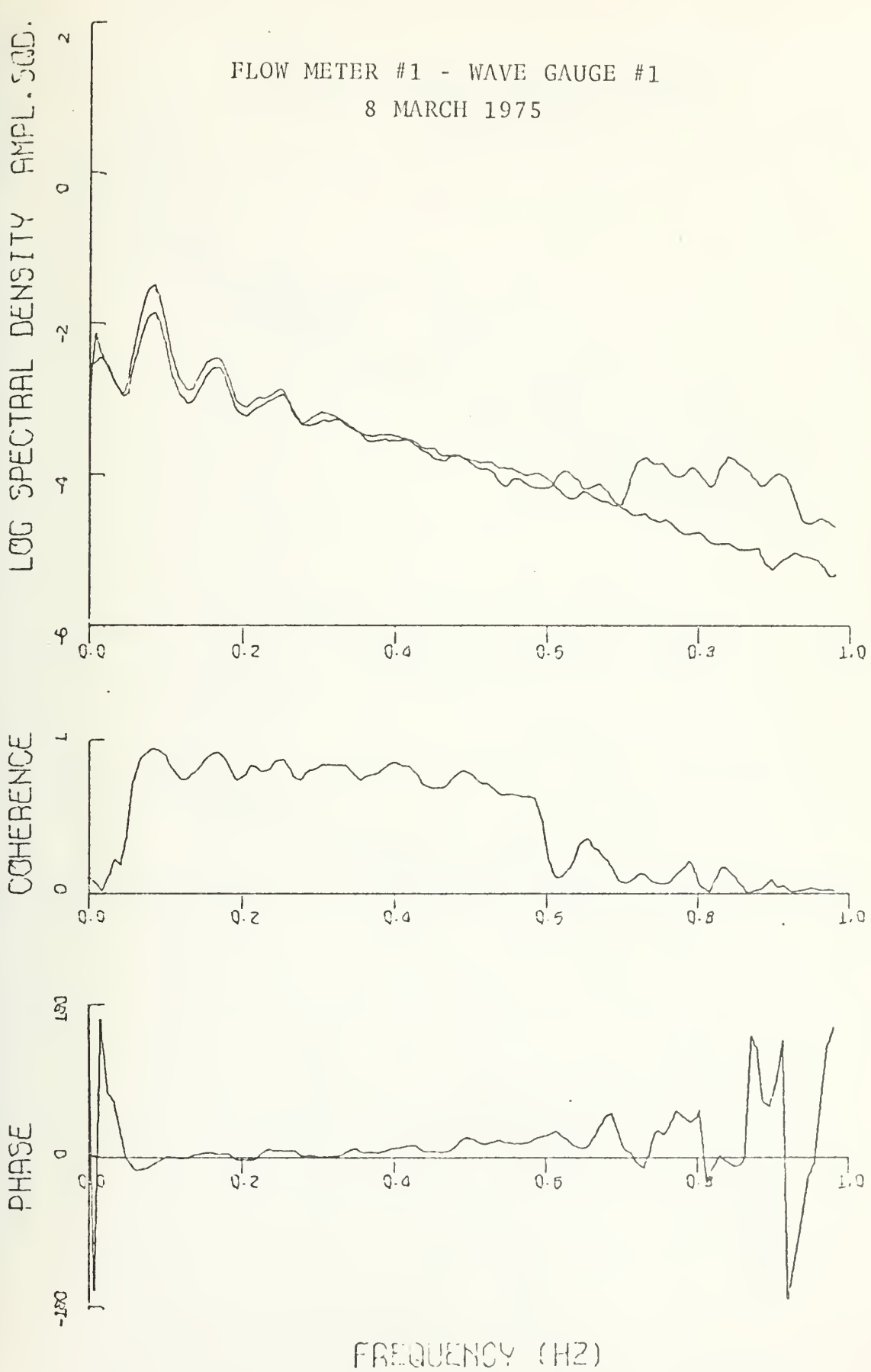
FLOW METER #1 - WAVE GAUGE #1
8 MARCH 1975
LOG SPECTRAL DENSITY AMPL. SQD.
2
0
-2
-4
-6
0.0
0.2
0.4
0.6
0.8
1.0
COHERENCE
1
0
PHASE
180
0
-180
FREQUENCY (HZ)

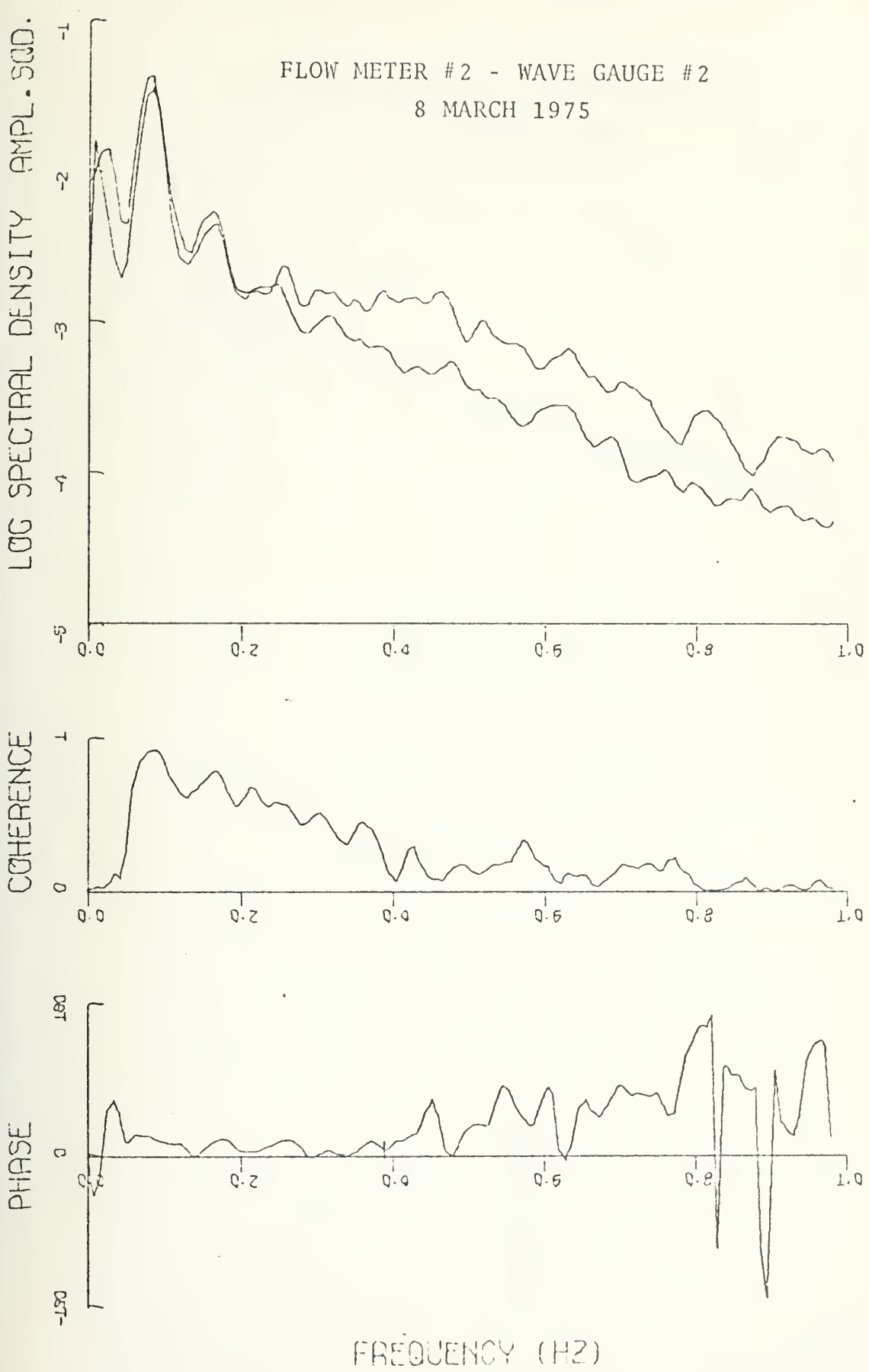
FLOW METER #2 - WAVE GAUGE #2
8 MARCH 1975
LOG SPECTRAL DENSITY AMPL. SQD.
-1
-2
-3
-4
-5
0.0
0.2
0.4
0.6
0.8
1.0
COHERENCE
1
0
PHASE
180
0
-180
FREQUENCY (HZ)

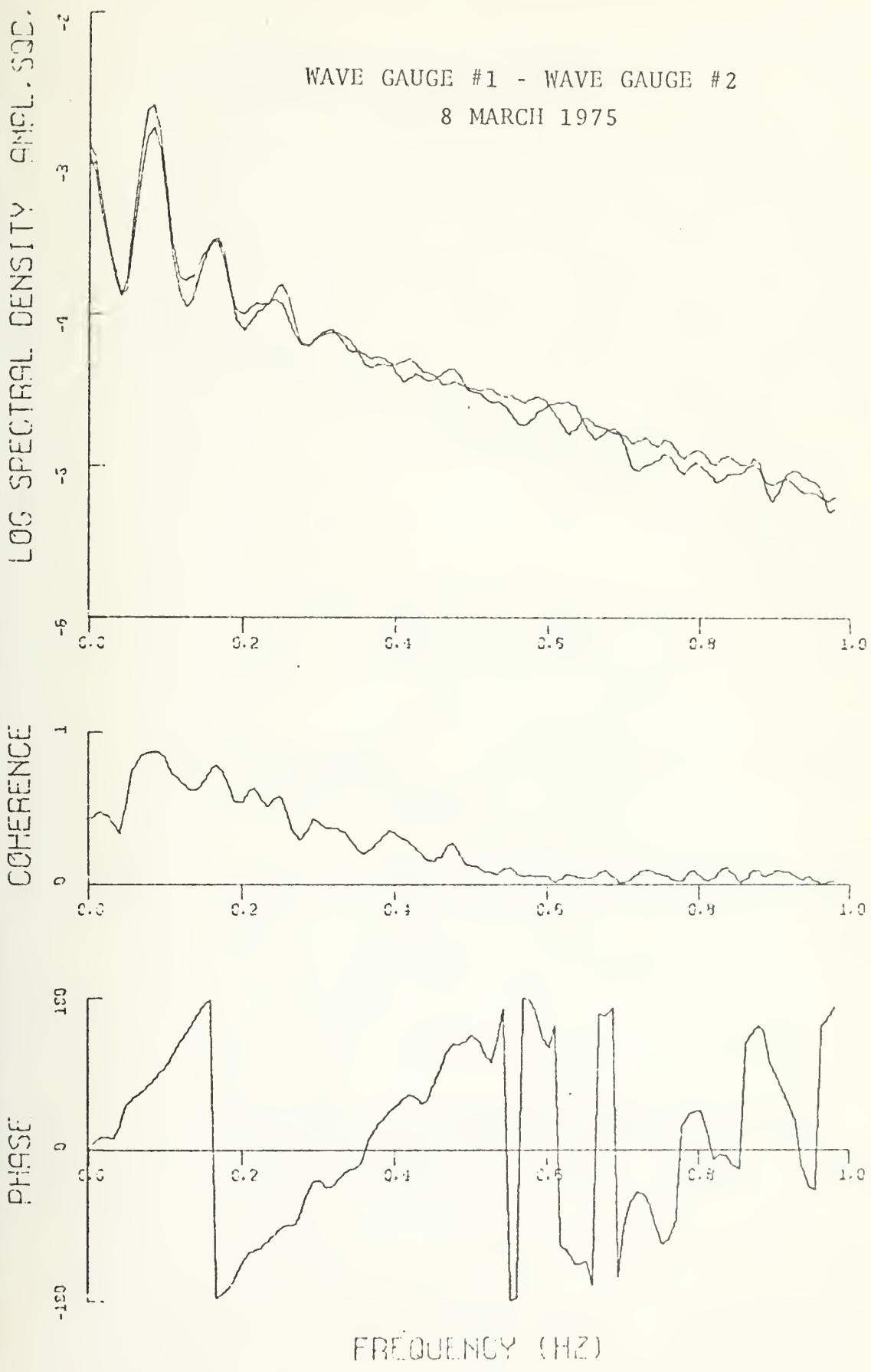
WAVE GAUGE #1 - WAVE GAUGE #2
8 MARCH 1975
LOG SPECTRAL DENSITY (M**2 SEC.
-2
-3
-4
-5
-6
0.0
0.2
0.4
0.6
0.8
1.0
COHERENCE
1
0
PHASE
180
0
-180
FREQUENCY (HZ)

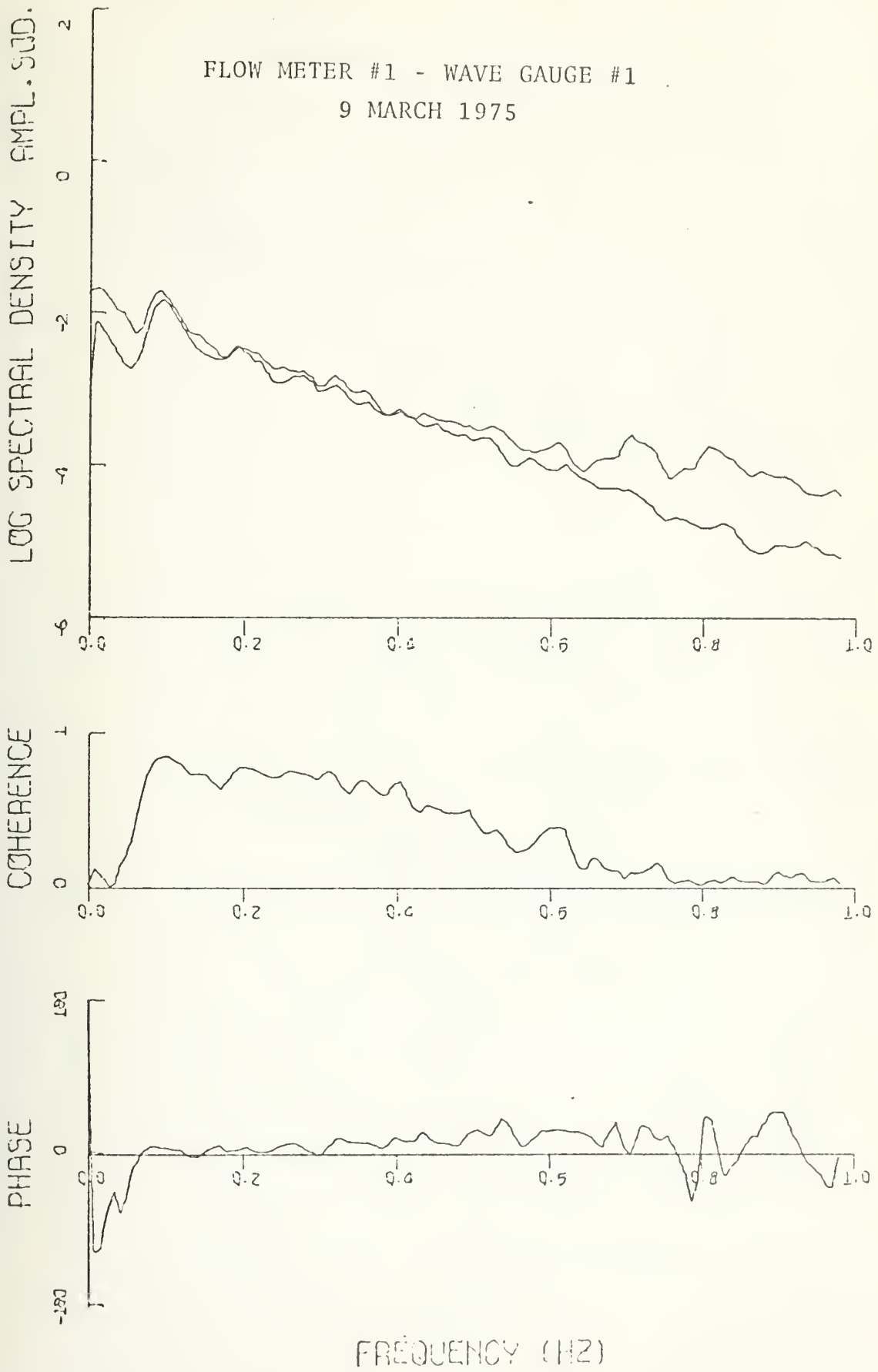
FLOW METER #1 - WAVE GAUGE #1
9 MARCH 1975
LOG SPECTRAL DENSITY AMPL. SQD.
2
0
-2
-4
-6
0.0
0.2
0.4
0.6
0.8
1.0
COHERENCE
1
0
0.0
0.2
0.4
0.6
0.8
1.0
PHASE
180
0
-180
0.0
0.2
0.4
0.5
0.8
1.0
FREQUENCY (HZ)

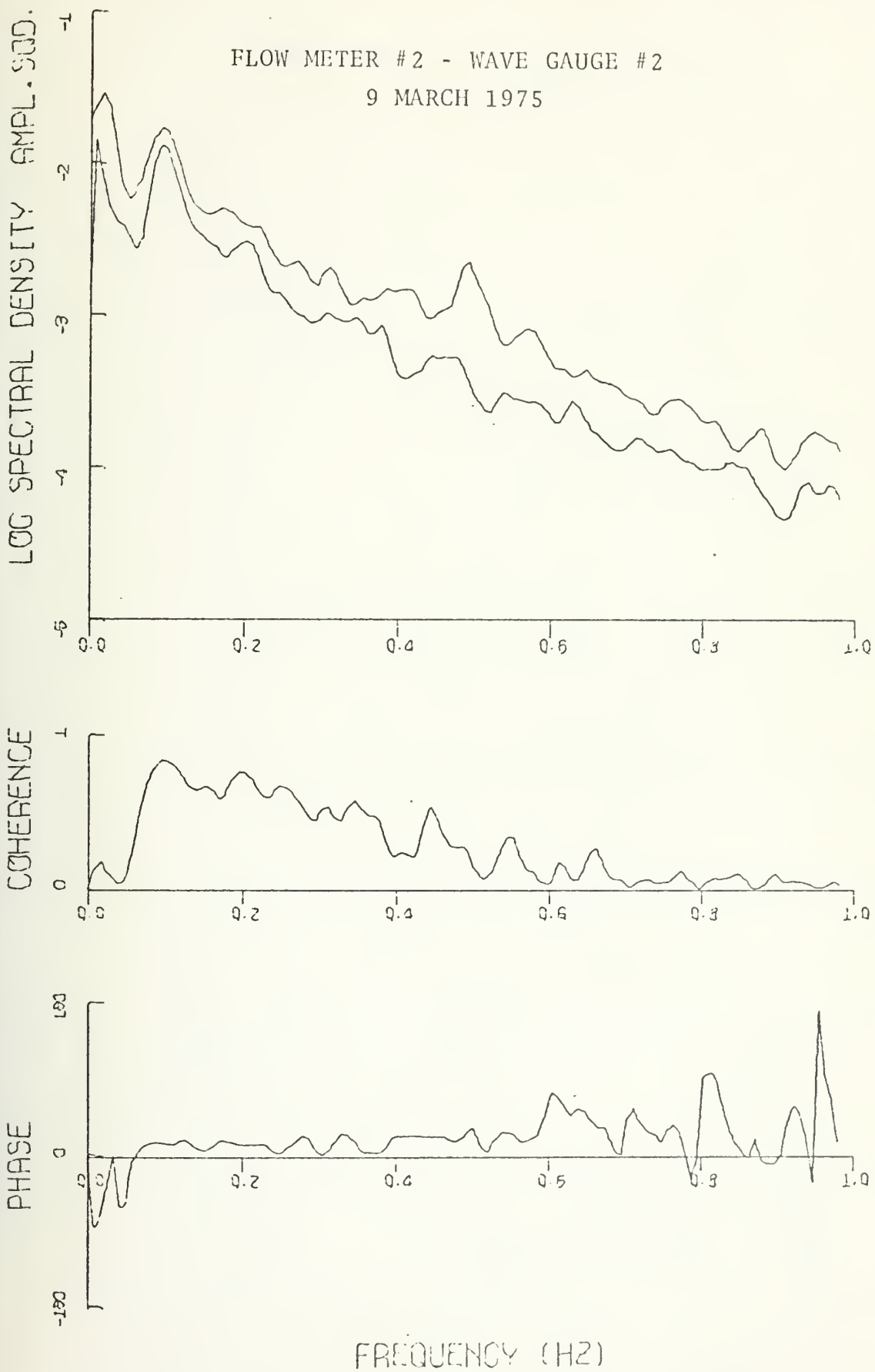
FLOW METER #2 - WAVE GAUGE #2
9 MARCH 1975
LOG SPECTRAL DENSITY AMPL. SQD.
-1
-2
-3
-4
-5
0.0
0.2
0.4
0.6
0.8
1.0
COHERENCE
1
0
PHASE
180
0
-180
FREQUENCY (HZ)

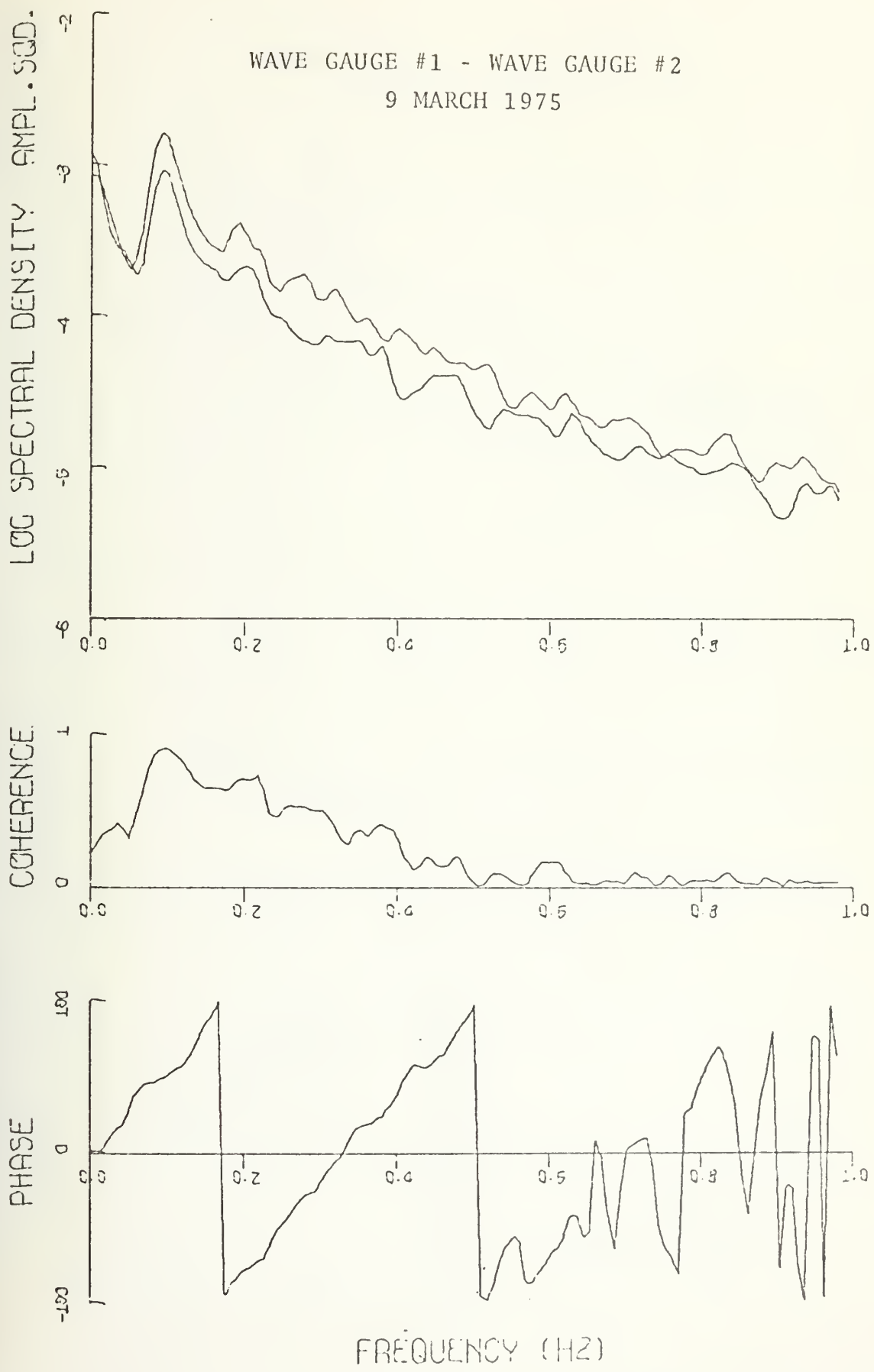
WAVE GAUGE #1 - WAVE GAUGE #2
9 MARCH 1975
LOG SPECTRAL DENSITY AMPL.SQD.
-2
-3
-4
-5
-6
0.0
0.2
0.4
0.6
0.8
1.0
COHERENCE
1
0
PHASE
180
0
-180
FREQUENCY (HZ)

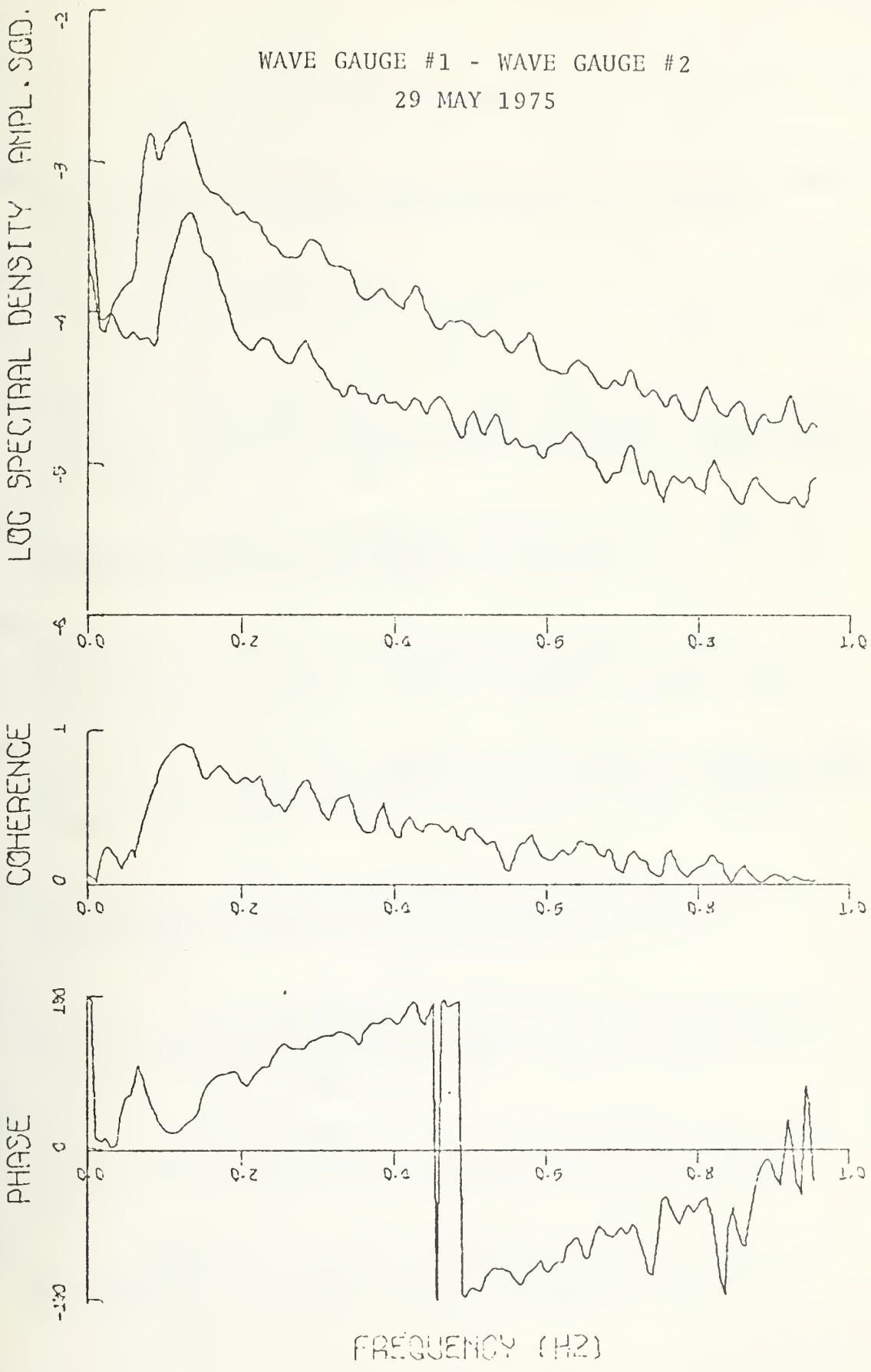
WAVE GAUGE #1 - WAVE GAUGE #2
29 MAY 1975
LOG SPECTRAL DENSITY AMPL. SQD.
-2
-3
-4
-5
-6
0.0
0.2
0.4
0.6
0.8
1.0
COHERENCE
1
0
PHASE
180
0
-180
FREQUENCY (HZ)

BIBLIOGRAPHY

Adeyemo, M. D., "Velocity Fields in the Wave Breaker Zone," Proceedings of the Twelfth Conference on Coastal Engineering, v. 1, p. 435-460, ASCE, 1970.

Bascom, W., Waves and Beaches, Doubleday and Co., Inc., 1964.

Bub, F. L., Surf Zone Wave Kinematics, M. S. Thesis, Naval Postgraduate School, Monterey, California, 1974.

Führböter, A., and Büsching, F., "Wave Measuring Instrumentation for Field Investigations on Breakers," Proceedings of the International Symposium on Ocean Wave Measurement and Analysis, ASCE, 1974.

Galvin, C. J., "Wave Breaking in Shallow Water," Waves on Beaches and Resulting Sediment Transport, p. 413-456, Academic Press, Inc., 1972.

Gaughan, M. K., and Komar, P. D., "The Theory of Wave Propagation in Water of Gradually Varying Depth and the Prediction of Breaker Type and Height," Journal of Geophysical Research, v. 80, p. 2991-2996, 20 July 1975.

Inman, D. L., and Nasu, N., Orbital Velocity Associated with Wave Action near the Breaker Zone, Technical Memorandum No. 79, U. S. Army Corps of Engineers, Beach Erosion Board, March 1956.

Iverson, H. W., "Waves and Breakers in Shoaling Water," Proceedings of the Third Conference on Coastal Engineering, Council on Wave Research, p. 1-12, ASCE, 1952.

McGoldrick, L. F., A System for the Generation and Measurement of Capillary-Gravity Waves, Technical Report No. 3, University of Chicago, Department of the Geophysical Sciences, August 1969.

Miller, R. L., and Ziegler, J. M., "The Internal Velocity Field in Breaking Waves," Proceedings of the Ninth Conference on Coastal Engineering, p. 103-122, ASCE, 1964.

Steer, R., Kinematics of Water Particle Motion within the Surf Zone, M. S. Thesis, Naval Postgraduate School, Monterey, California, 1972.

Thornton, E. B., "A Field Investigation of Sand Transport in the Surf Zone," Proceedings of the Eleventh Conference on Coastal Engineering, p. 335-351, ASCE, 1968.

Thornton, E. B., and Krapohl, R. F., "Water Particle Velocities Measured under Ocean Waves," Journal of Geophysical Research, v. 79, p. 847-852, 20 February 1974.

Thornton, E. B., and Richardson, D. P., The Kinematics of Water Particle Velocities of Breaking Waves within the Surf Zone, Technical Report NPS-58TM74011A, Naval Postgraduate School, Monterey, California, January 1974.

Walker, J. R., Estimation of Ocean Wave-Induced Particle Velocities from the Time History of a Bottom Mounted Pressure Transducer, M. S. Thesis, University of Hawaii, 1969.

Wood, W. L., A Wave and Current Investigation in the Nearshore Zone, Department of Natural Science, Michigan State University, E. Lansing, 1973.

INITIAL DISTRIBUTION LIST

		No. Copies
1.	Defense Documentation Center Cameron Station Alexandria, Virginia 22314	2
2.	Library, Code 0212 Naval Postgraduate School Monterey, California 93940	2
3.	Department Chairman, Code 58 Department of Oceanography Naval Postgraduate School Monterey, California 93940	3
4.	Assoc Professor E. B. Thornton, Code 58 Tm Department of Oceanography Naval Postgraduate School Monterey, California 93940	5
5.	LCDR James J. Galvin, USN 77 Highland Road Somerville, Massachusetts 02144	3
6.	Oceanographer of the Navy Hoffman II 200 Stovall Street Alexandria, Virginia 22332	1
7.	Office of Naval Research Code 480 Arlington, Virginia 22217	1
8.	Dr. Robert E. Stevenson Scientific Liaison Office, ONR Scripps Institution of Oceanography La Jolla, California 92037	1
9.	Library, Code 3330 Naval Oceanographic Office Washington, D. C. 20373	1
10.	SIO Library University of California, San Diego P. O. Box 2367 La Jolla, California 92037	1

11.	Department of Oceanography Library University of Washington Seattle, Washington 98105	1
12.	Department of Oceanography Library Oregon State University Corvallis, Oregon 97331	1
13.	Commanding Officer Fleet Numerical Weather Central Monterey, California 93940	1
14.	Commanding Officer Environmental Prediction Research Facility Monterey, California 93940	1
15.	Department of the Navy Commander Oceanographic System, Pacific Box 1390 FPO San Francisco 96610	1
16.	Commander, Naval Weather Service Command Naval Weather Service Headquarters Washington Navy Yard Washington, D. C. 20390	1
17.	Coastal Studies Institute Louisiana State University Baton Rouge, Louisiana 70803	1
18.	School of Marine and Atmospheric Science University of Miami Miami, Florida 33149	1
19.	Mr. John F. Borchardt Gilbert Associates, Inc. P. O. Box 1498 Reading, Pennsylvania 19603	1
20.	LT Frank L. Bub, USN Fleet Weather Central COMNAVMARIANIS, Box 2 FPO San Francisco 96630	1

Thesis
G142 Galvin
c.1 Kinematics of surf.
zone breaking waves:
measurement and analysis.